6. APPENDIX

6.1 REVIEW OF PREVIOUS INFORMATION

6.1.1 Tilburg Fair Holland 1995 (EWP/95/20)

This work was undertaken at the request of HSE. The aim of the study was to provide ergonomics advice regarding any problems with rides that were being considered for the Glasgow Christmas Fair. Four rides were selected for assessment; the Sky Tower, Spin Ball, Evolution and Crazy Jump. No acceleration data was recorded for the Crazy Jump. The report does include an assessment of the passenger restraint, which concluded that the current design makes it unsuitable for children. This was due to the large distance between the restraint bar and the seat pan that could potentially allow a passenger to slip under the restraint bar and be ejected from the ride. This may also be an issue for adults who cannot brace their feet against the foot rest. The report recommends a minimum height restriction of 1.4 meters (corresponding to a 5^{th} PCTL 12 year old).

6.1.2 Jump and Smile (La Sauterelle) – Nottingham 2000 (ERG/00/12)

This report details a joint visit to Nottingham Market Square to undertake an ergonomics assessment of the La Sauterelle fairground ride (Figure 27) following concerns regarding the effectiveness of the passenger containment system. The ride was manufactured by Safeco. No acceleration data was collected. It does include a qualitative assessment of the passenger containment system. The dimensions of the relevant containment system components and their associated body dimensions are given in Table . Analysis of the ride dimensions and associated body parts suggest that the fit of the restraint may not sufficiently contain large proportions of the potential ride passengers.

The ride has no means for passengers to brace against the rides forces using their legs and feet. There is a foot plate (step) below the seat pan, but this is designed to enable passengers to step into the car. The gaps between seat pan and lap bar and seat back and lap bar suggest that smaller passengers gain little support from these structures. As a result bracing and containment relies mainly on the hand rail and seat back rather than containment of the lap bar to contain them. This, in conjunction with the dynamics of the ride, has the potential for passengers to move voluntarily and involuntarily into a position where they could be ejected by the ride forces. The main recommendation arising from this report was that the passenger containment system should be reviewed by a competent person and improvements made to increase the effectiveness of the lap bar system and to improve the potential for passenger bracing against the ride forces.

Figure 27 La Sauterelle

Table 18 Relevant containment system components and their associated body dimensions

Dimension	Measurement (mm)	Body dimension (mm)	Passenger range	Data (mm)	Mismatch (mm)
Backrest height	500	Seated shoulder height	Large	658	-158
Seat pan height	560 to 660	Popliteal height	Small	415	-145 to -245
Seat pan depth	410	Buttock to popliteal	Small	416	6
Backrest width	1100 (3 seats)	Bideltoid	Large	(486 x 3) =1458	-358
Side support height	370	Seated shoulder height	Large	658	-288
Side support depth	410	Buttock to popliteal	Large	544	-134
Backrest to lap bar	420	Abdominal depth	Small to large	200 to 325	-220 to 95
Seat pan to lap bar	160	Thigh thickness	Small to large	127 to 176	-33 to -16
Seat back to hand rail	472	Forward reach	Small to large	628 to 834	156 to 362
Diameter handrail	25	Grip diameter	Small	44	19

6.1.3 Crazy Frog – 2004 – Scotland (Glasgow / St Andrews) ERG/04/02 and ERG/04/20

This work was undertaken in response to an incident in 2003, when a female member of the public (IP) sustained an injury whilst on a Jumping Frogs ride (Figure 28). The objectives of this study were:

1. To record g-forces exerted on passengers by the Jumping Frogs ride;
2. To determine the likelihood of spinal (or any other) injury due to the ride forces or ride environment;
3. To provide recommendations on ways to reduce the risk of injury from exposure to ride forces

Two visits were made in order to measure the ride g-forces. In order to take measurements of the ride motion an Entran® +/-25g, tri-axial accelerometer was attached to the seat. This accelerometer was orientated such that its coordinate system was as indicated in Table . The data was recorded onto a data logger (HSL proprietary equipment: 'e-fairlog') at 40Hz and downloaded onto a laptop computer using HSL proprietary software and the results were then passed through a Butterworth 10 Hz low pass filter in accordance with BS EN 13814:2004.

1. Performed a low-pass software filter (Butterworth 10Hz) to remove noise.

2. Imported data file into Excel and identified any z-axis data points that exceeded 2g and –0.1g

3. Identified peak values and match these with types of ride motion. From the initial tests at St Andrews, 2 key types of ride motion were identified. These types of motion, described below, can be alternated between cars to create different overall patterns of motion:

    a. Low-frequency high-amplitude 'wave' motion;
    b. High-frequency low-amplitude 'bouncing' motion.

4. Calculated the typical jerk (rate of onset / change of g) values for periods of the main motion types.

Two main types of ride motion were identified and examined; Low-frequency (1.2 Hz) wave type motions and higher-frequency (0.6Hz) bouncing motions. The g-forces found ranged between approximately 2.8 and 3.3g (peak) for the wave motions and approximately 2.6 and 4.1g (peak) for the bouncing motions. The g forces recorded during the visits are shown in (Figure 29 to Figure 34). The g-forces, as single case events, are not believed to present a significant risk of injury to the majority of the population. However, the repetitive nature of the accelerations may present a risk of injury to some people primarily because of individual differences (i.e. lower than normal bone density, previously cumulated bone fatigue, damaged intervertebral discs). There is also some suggestion that rapid onsets of g may give insufficient time for muscular damping systems to react fully effectively, and that consecutive accelerations may therefore result in greater than expected applied stress to the vertebrae.

Table 19 Descriptions of g-force accelerations and their perceived effects on fairground ride occupants (E-Fairlog coordinate system)

Axis	***Direction of g-force***		***Description of g-force accelerations on the ride***	***Perceived effect of g-force on passenger (i.e. ride 'sensation')***
X	Fore / aft	Positive (+*g*X)	Ride accelerating in a backward direction, in relation to the seat orientation	**Occupant feeling like they are being forced forwards, away from the seat back**
		Negative (-*g*X)	Ride accelerating in a forward direction, in relation to the seat orientation	**Occupant feeling like they are being forced backwards, into the seat back**
Y	Side to side	Positive (+*g*Y)	Ride accelerating to the right hand side in relation to the seat orientation	**Occupant feeling like they are being forced to their left hand side, in relation to the seat**
		Negative (-*g*Y)	Ride accelerating to the left hand side in relation to the seat orientation	**Occupant feeling like they are being forced to their right hand side, in relation to the seat**
Z	Up / down	Positive (+*g*Z)	Ride accelerating upward in relation to the seat orientation	**Occupant feeling like they are being forced downwards, into their seat**
		Negative (-*g*Z)	Ride accelerating downward in relation to the seat orientation	**Occupant feeling like they are being forced upwards (i.e. weightless), out of their seat**

N.B. The coordinate system used in previous reports differs from that specified in BS EN 13814:2004 (in the direction of the Z axis). This is due to the historical development of the HSL g-force measuring system predating the Standard, and for consistency in HSL reports.

Trunk posture is another important factor in determining the stress which vertebrae will experience under a particular g-force. Studies indicate that trunk flexion postures (i.e. head nodding forwards, bending the trunk forwards) will lead to localised increases in the compression forces acting on the vertebrae (particularly at the front/anterior edges). Rate of onset levels (rate of onset of g) were determined from the data. The maximum rate of onset levels were significantly lower than those referred to in the studies identified in the literature. It is therefore not possible to say whether the rate of onset levels could be a risk factor on this particular ride. However, in view of the lack of research on repeated rate of onset exposure at the levels measured, it may be useful to assume for the time being that they could be a contributing risk factor and take steps to reduce exposure to them.

Figure 28 Safeco Crazy Frogs 11th August 2003 at St Andrews street fair

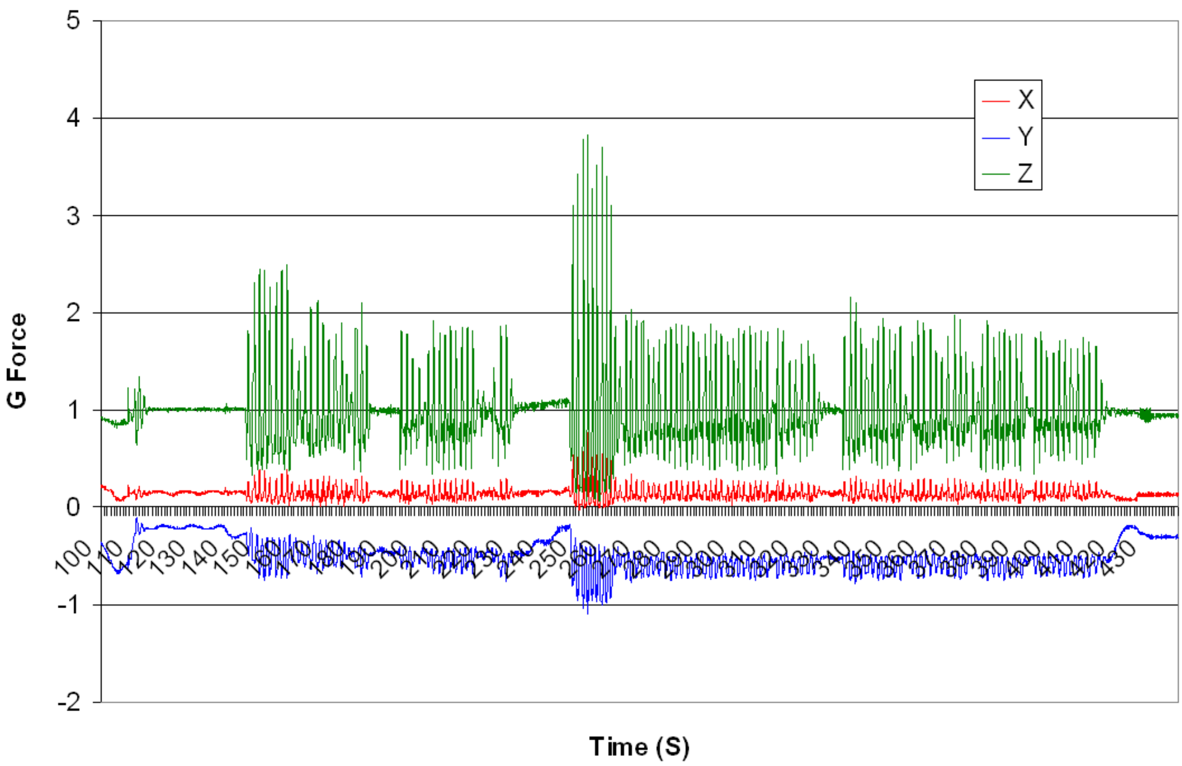

Figure 29 St Andrews Test 1

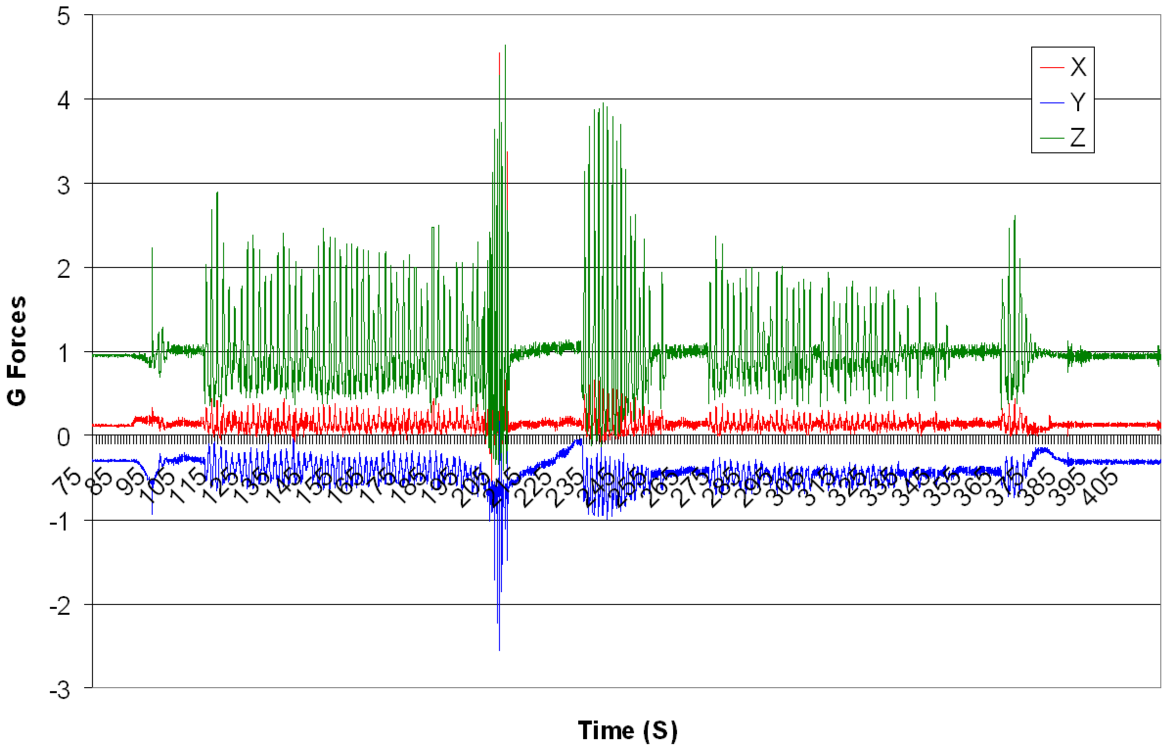

Figure 30 St Andrews Test 2

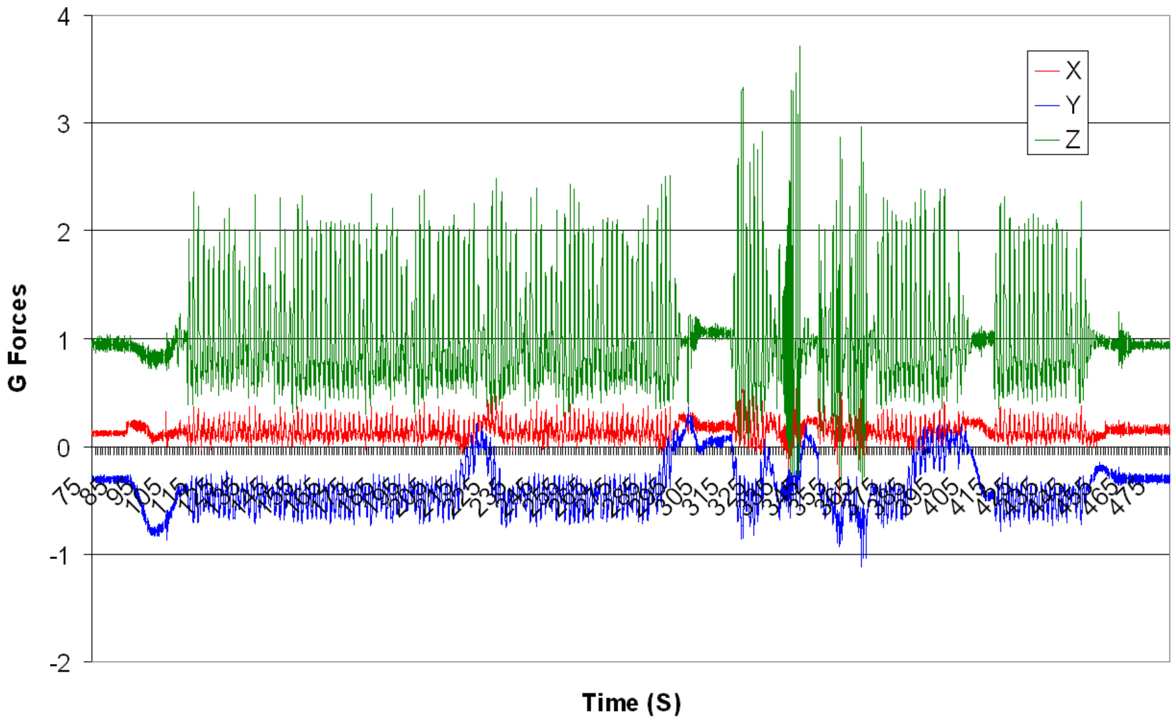

Figure 31 St Andrews Test 3

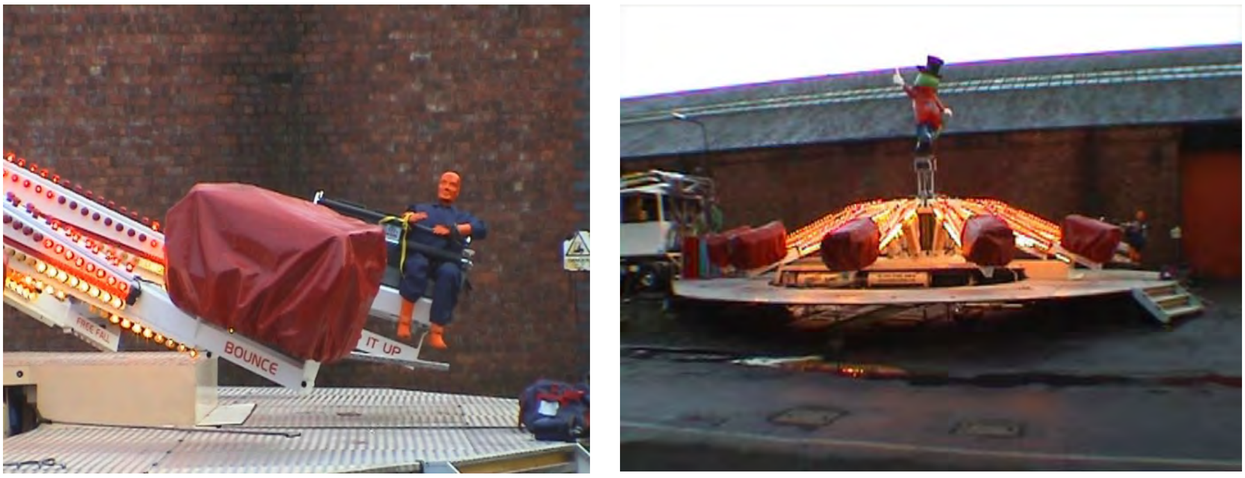

Figure 32 9th December 2003 at Horne's Yard in Glasgow

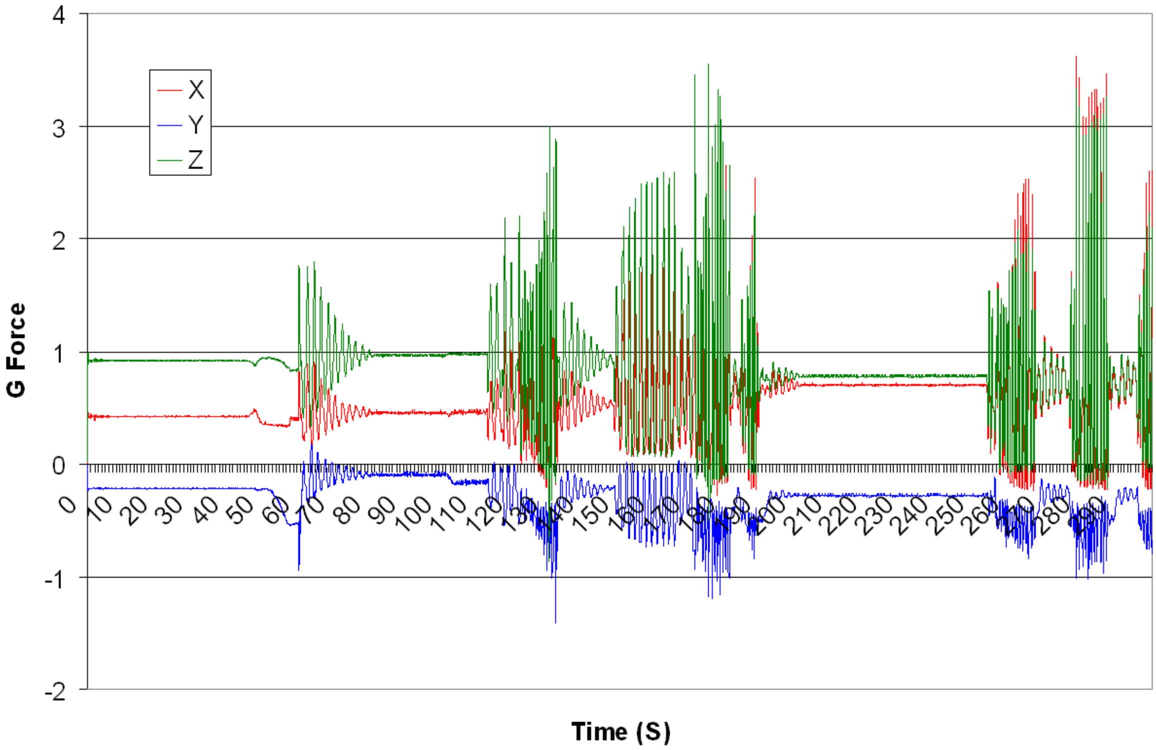

Figure 33 Glasgow Test 1

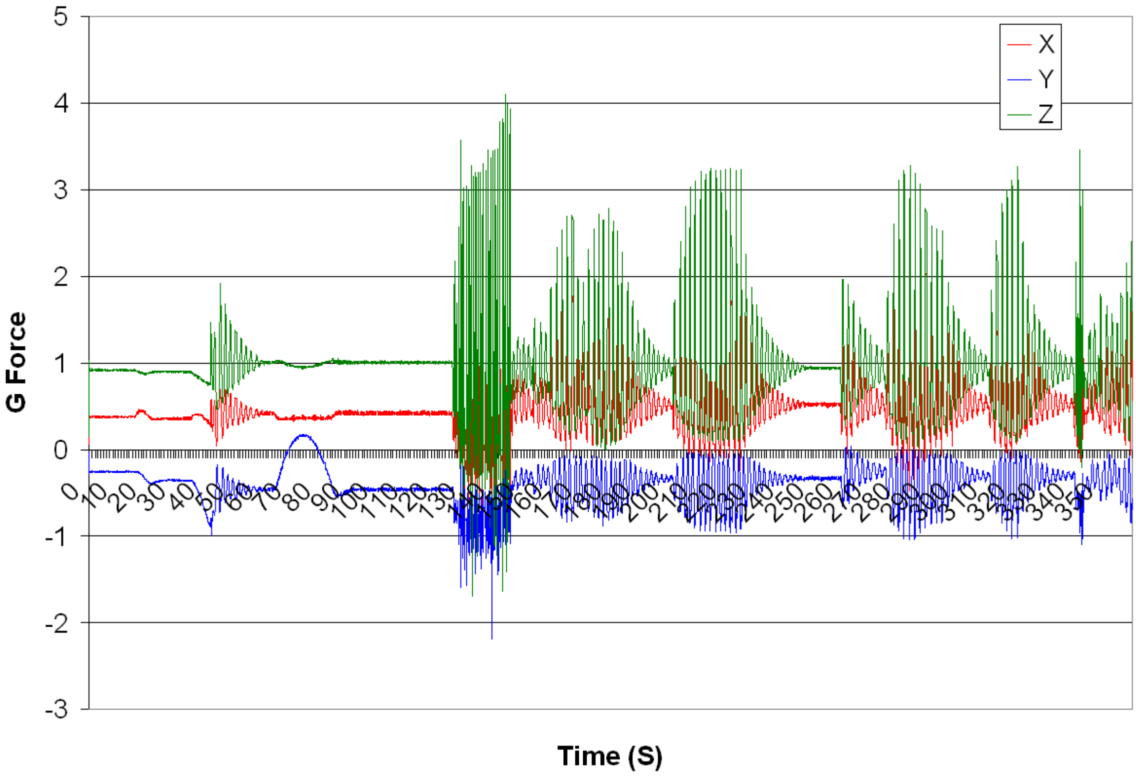

Figure 34 Glasgow Test 2

The following conclusions were reached as a result of this study:

- Steps should be taken to warn or try to filter out potential passengers from 'at risk' groups. This could involve a combination of effective signage, verbal information and observation by the operator(s).
- The high-frequency bouncing motion should be used as sparingly as possible, and in particular should be avoided while the ride is running in reverse.
- Changes to the containment/restrain system could be made to lead passengers to adopt less risky postures (such as bending forwards) during upwards accelerations (e.g. over shoulder restraints or chest belts).

6.1.4 Crazy Frog – Cambridge, 2009

This work was undertaken in response to an incident in 2009, when a member of the public sustained an injury whilst on a Jumping Frogs ride. Measurements of the amusement device accelerations and passenger containment dimensions were taken during a site visit to the Cambridge Midsummer Fair (Figure 35). This work was undertaken on behalf of Mr Edmund Milnes (HSE Specialist Inspector), who produced an incident report based on the data provided in Figure 36. HSL carried out no further analysis and no HSL report was produced.

Figure 35 Safeco Crazy Frogs – Cambridge, 2009

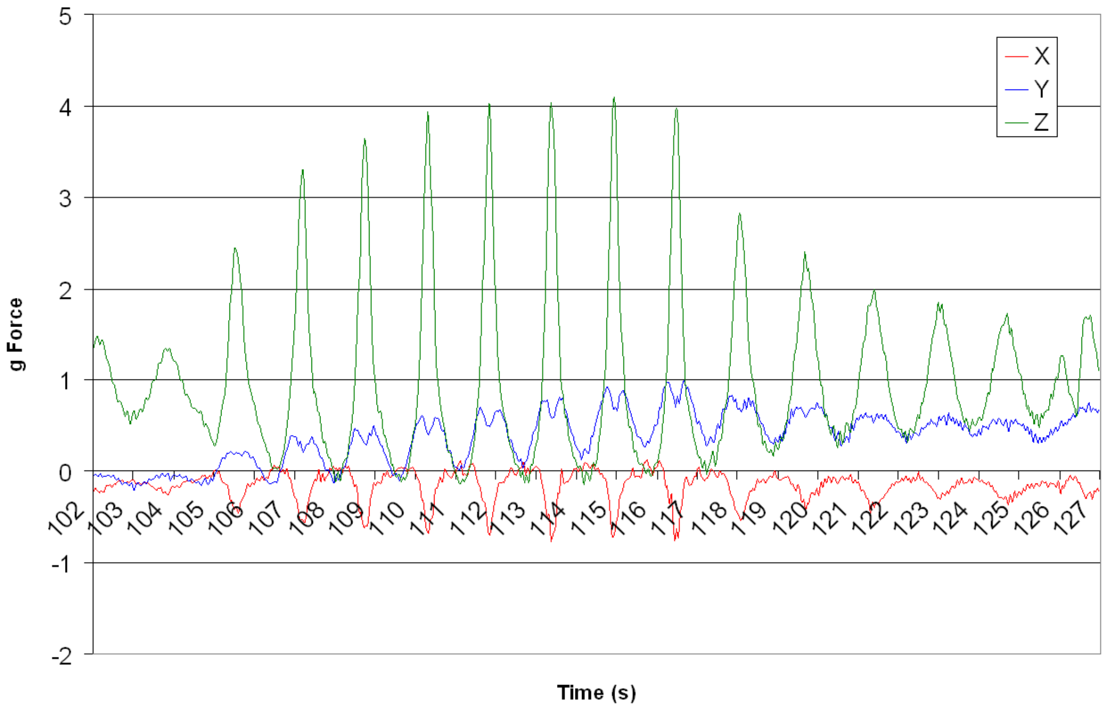

Figure 36 Safeco Crazy Frogs – Cambridge, 2009 25 s ride cycle

6.1.5 Evidence of seat-to-head acceleration exposure causing injury on amusement devices

Milnes's (6;7) measurements on a Safeco Crazy Frogs were made in a car in a partially loaded state (single average weight adult occupant dummy, approx. 70 kg) with a pneumatic pressure setting of 6.6 kgf/cm^2, and with the accelerometer mounted within the test dummy abdomen. Milnes's measurements will therefore be influenced by the dynamic response of the test dummy which is unknown, but which it is understood is not intended to accurately replicate the dynamic response of the human body in this situation. The test dummy used was an Occupant Protection Assessment Test (OPAT) dummy. When designed in 1972, the mannequin was intended to be representative of a 50th percentile adult male in size (1680 mm stature) and weight (70.6 kg). It was designed to provide human-like behaviour when used to evaluate lap-shoulder belt systems. The mannequin features a human-like clavicle and floating scapula design, and its rib cage mimics the shape of the human. However, it is somewhat limited in its ability to simulate the behaviour of a person, as its neck and back are rigid structures and unable to rotate or bend forwards, backwards, or sideways.

The operating pressure was set to account for the response of the other (unloaded) arms operating during the measurement period. This is likely to have reduced the measured acceleration recorded in the car due to the pressure being somewhat lower than it could be for a loaded condition.

Milnes (7) sets out to link the levels of measured acceleration on the ride to an injured person's (IP) probability of injury through estimating the compression forces generated within the IP when riding, and comparing this with reported compressive strength data for vertebrae.

Milnes (7) cites a study by Ruff (31) who is reported to have calculated that the L1 vertebrae typically supports approximately 50% of the body weight. It is not known whether this relates to a seated subject or not. Milnes (7) uses this relationship to estimate the mass supported above the injured persons L1 vertebrae as approximately 37 kg.

Using the simple force = mass x acceleration model to estimate force within the IP's spine (ignoring any biodynamic response of the human body), with the mass of 37 kg and acceleration of 4.1 G, the peak forces within IP's spine were estimated to be around 1500 N.

Assuming that the ride caused the IP's injury, and that the IP's vertebral ultimate compressive strength (UCS) was reduced through repetitive exposure, Milnes (7) used the information from Brinkmann (32) regarding repetitive loading to revise the range of UCS strength of the IP's vertebra. Milnes (7) produced estimates for the 10 bounces which constituted the highest accelerations recorded, revising the UCS value for the IP's vertebra upwards to 2258 N. This was within the range reported in the scientific studies for any fracture type and being approximately 9th percentile (including data from individuals over 60 years of age).

It might then be argued that the 4.1 g acceleration presents a risk of injury to 10% of the population with a body mass similar to the IP. If their body mass were greater, then the compression forces would be greater, and the risk of injury would be greater for a similar UCS.

6.1.6 Ultimate compressive strength (UCS) of vertebrae

Reported compressive strengths of isolated vertebrae show high variability, between 3 to 12 kN (Brinkmann et al. (32), cited in Boocock (2)). Milnes (7) reports a wider data set for compression forces measured to produce a variety of fractures, including that presented by Hansson et al. (33), cited in Milnes (7)) whose sample included subjects aged over 60 years.

Taking data across all studies, (n=90) the minimum, mean and maximum reported L1 UCS were 1520 N, 5299 N and 12535 N respectively.

6.1.7 Compression forces generated by acceleration exposure

Studies of instrumented cadavers subjected to seat to head accelerations (while seated) with varying forward trunk flexion have reported compression forces within the lower end of the range stated above (Hodgson et al (34), cited in Milnes (7)). For example, King and Vulcan (35), cited in Milnes (7)) report an acceleration of 9 g at an onset rate of 1500 g/s as producing a vertebral compression force of 3.6 kN. Boocock (2) suggests this as a possible upper protective limit. This may be because the compression force value corresponds to an established biomechanical risk criterion for compression force within the spine during manual lifting.

6.1.8 Compressive strength of vertebrae and body weight

Milnes (7) reports that UCS is associated with body weight, and greater body weight will result in larger compressive forces within the spine when subjected to axial (seat to head) acceleration. Body weight is also reported to be a factor for spinal injury in NATO Publication TR-HFM-090-03 (33).

The strength and nature of the interaction is not reported. The connection is likely to be strongest where individuals have developed their bone structure with a high body weight, and remained physically active, whereas an individual who is sedentary, and or gained weight quickly is less likely to have developed a high bone strength. Weight/Body Mass Index (BMI) will be an influencing factor in the probability of vertebral fractures, but other (interacting) factors such as bone mineral density, age, and gender are likely to be of significant importance.

6.1.9 The effect of load cycles on compressive strength of vertebrae

The Safeco Crazy Frogs ride motion is repetitive, and will impose repetitive compressive loading on the spine of the rider. Brinkmann ((32), cited in Milnes (7)) found that following 20 load cycles, some vertebrae were found to fail at between 43% and 72% of their UCS. It was calculated that repetitive loading at approximately 60 to 70% of the UCS for 10 cycles presented a 9% probability of fracture.

6.1.10 Reaction time and muscle tone

It may be unlikely that reaction time will be sufficiently fast to enable an individual to respond to a single or initial acceleration event. However, it will be possible for riders to respond to successive events. The effect is not certain, but muscle contractions around the spine will generally have the effect of increasing the compressive forces acting within it. However, abdominal muscle contractions may also tend to increase intra-abdominal pressure (IAP), which can have a mitigating effect on spinal loading. Muscle activity is something that is not accounted for in the studies performed on cadaver specimens.

6.2 SITE VISIT – WILKINSON DJ JUMP AMUSEMENT DEVICE (20TH – 22ND NOVEMBER 2012): MEASUREMENT TEST RUN LIST

Run	Description
1	All arms operating. Pressure adjusted when cars lifted to compensate for no load. There is some video of a running check following Run1, because cars 2 and 4 appeared to be running much higher than car 12.
2	All arms operating. During the final free fall pedal operating section for Prog 2, Jonathan operates the pedal after the operator has done it for a short while. The difference in timing of the bounce results in cars becoming out of synchronisation. This is followed by some further attempts by the operator to allow the arms to drop low to the bottom of the travel.
3	Arms 2 and 12 operating. Car 2 GP1 fitted. During the final free fall pedal operation phase the operator attempted to achieve a harder drop to the bottom of the travel.
4	All arms operating. Car 12 only with GP1 fitted. The operator adjusted the pressure to a "lowered setting" based on how he felt the arms were running after lift, 3.5 – 4.5 bar on the setting dial. This was lower than normal operation.
5	All cars running. 6 bar displayed on the pressure dial
6	Repeat of Run 5. All cars running, 6 bar displayed on the pressure dial.
7	Only cars 12 and 6 running, both loaded with 160 kg of pea gravel. 7 bar displayed on the pressure dial.
8	Repeat of Run 7. Recorded consecutive to Run 7.
9	Only cars 12 and 6 running, both loaded with 160 kg of pea gravel. "Low pressure" setting, 6.5 bar was displayed on the pressure dial.
10	Repeat of Run 9. Cars 12 and 6 loaded with 160 kg of pea gravel. Operator attempted more 'aggressive' use of the foot pedal during program 2, by allowing the arms to drop further before the pedal is released.
11	Only cars 12 and 6 running, both loaded with 160 kg of pea gravel. "Low pressure" setting, 6 bar was displayed on the pressure dial.
12	Only cars 12 and 6 running, both loaded with 160 kg of pea gravel. "High pressure" setting, 7.5 bar was displayed on the pressure dial. Recorded consecutive to Run 11.
13	Only Car 12 running, unloaded, with central hub stationary. This run was an attempt to investigate the effects of the pneumatic cushion at the bottom of the ram. This was to be done by achieving an arm drop from the lowest possible height with the hub stationary. The starting position was programme 1, in the default "floating" position between programme inputs, i.e. in a low position. The drop was triggered by use of the foot pedal. The arm height was controlled by altering the pressure. The adjustment of the exhaust valve at the base of the ram was investigated. The screw head slot was horizontal at start, and was screwed in through 2.5 turns to reach a hard stop position. This resulted in the air cushion being apparent, but the arm would not lower to its stop position. The exhaust valve was then backed off ¼ turn. This appeared to achieve a cushion at the bottom of the ram travel which very slowly lowered the arm when switched to off/end position.
14	Only Car 12 running, unloaded, with central hub stationary. 5 bar was displayed on the pressure dial. Some programmes plus the foot pedal were used to try to bounce the

	arms to bottom of ram travel. Exhaust valve ¼ turn open from fully closed.
15	Repeat of Run 14. Only Car 12 running, unloaded, with central hub stationary. 4 bar was displayed on the pressure dial. Cushion exhaust valve ¼ turn out from fully in.
16	Repeat of Run 14, using a few programmes plus foot pedal use. The pressure was down to around 4 bar on the dial at the end of Run 15. Only cars 12 and 6 running, both loaded with 160 kg of pea gravel. “High pressure” setting, 7 bar was displayed on the pressure dial. Recorded consecutive to Run 15.
17	6 bar was displayed on the pressure dial. Void data on GP1
18	7.5 bar was displayed on the pressure dial. Recorded consecutive to Run 17. Void data on GP1
19	Arms 6 and 12 operating. 6 bar was displayed on the pressure dial. Cushion exhaust valve ¼ turn out from fully in.
20	Arms 6 and 12 operating. 7.5 bar on dial. Cushion exhaust valve ¼ turn out from fully in. Recorded consecutive to Run 19.
21	A succession of free-fall pedal actions to investigate changes in exhaust valve adjustment: Part 1. ½ turn out from fully in; Part 2. ¾ turn out from fully in; Part 3. 1 turn out from fully in; Part 4. 1 ¼ turns out from fully in; Part 5. Fully in.
22	A ‘typical routine’ run through. Initially, all arms were lifted to the ‘float’ position and then only arms 6 and 12 operated. The operator reported that this it was typical practise to raise the unloaded arms, usually to the top position, for situations where the ride was operated partially loaded, as lifting the cars afford better visibility of the ride surrounds for safety reasons. Subsequently, all arms were activated (at around 6 minutes). At around 8:45 minutes the unloaded arms are deactivated once more, and held at the ‘float’ position while arms 6 and 12 operate. This was done largely as a work around for the different loading conditions. There was some adjustment of pressure during the ride session.

6.3 ACCELERATION MEASUREMENT DATA SET

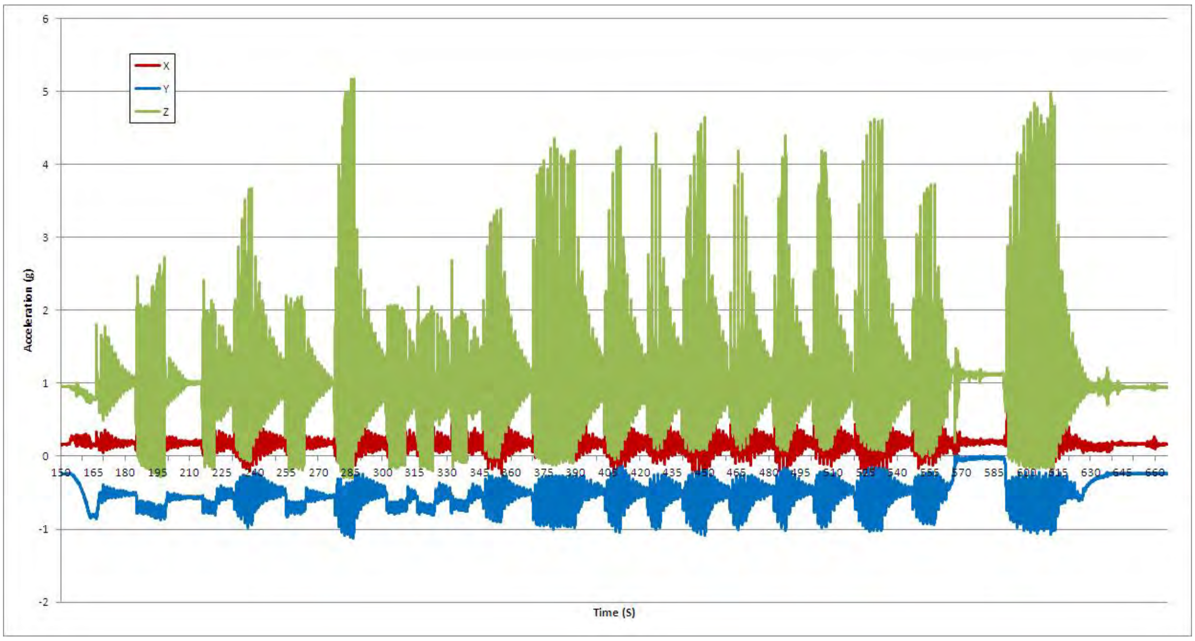

Figure 37 Test run 1 full

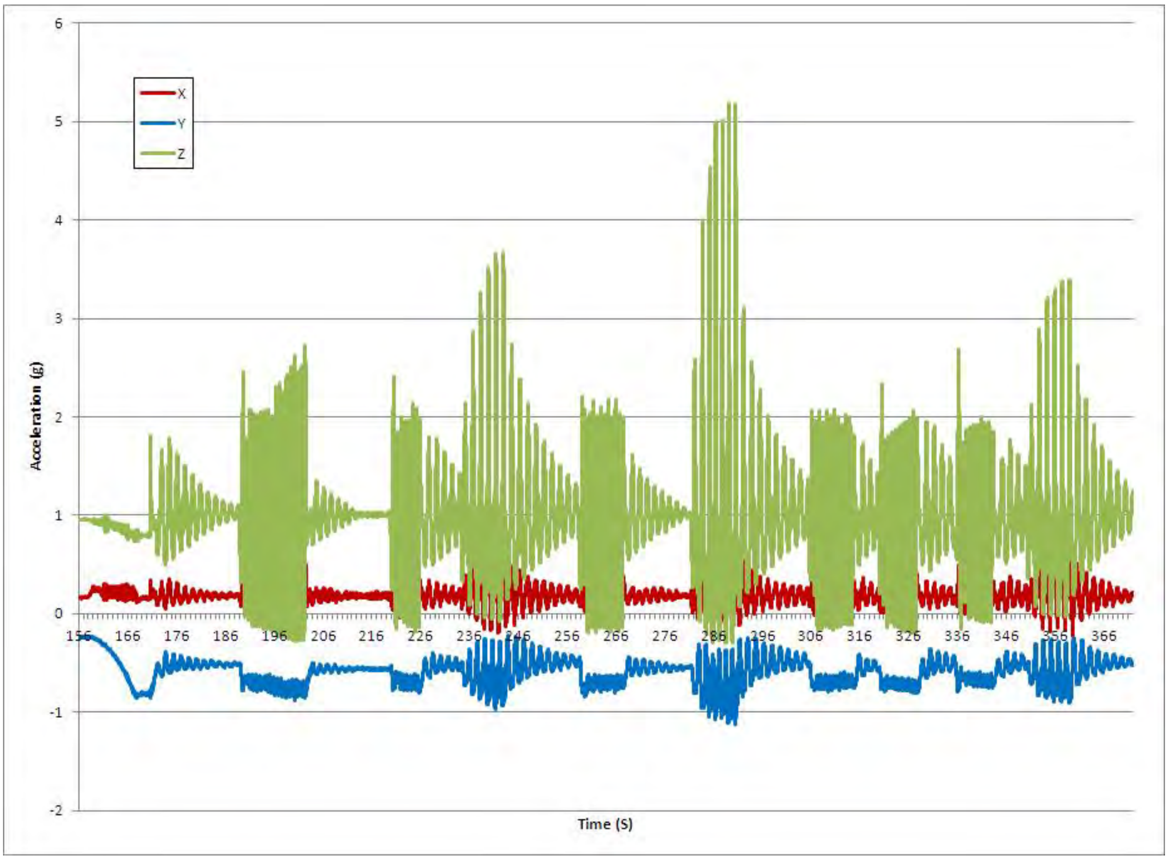

Figure 38 Test run 1, Program 1

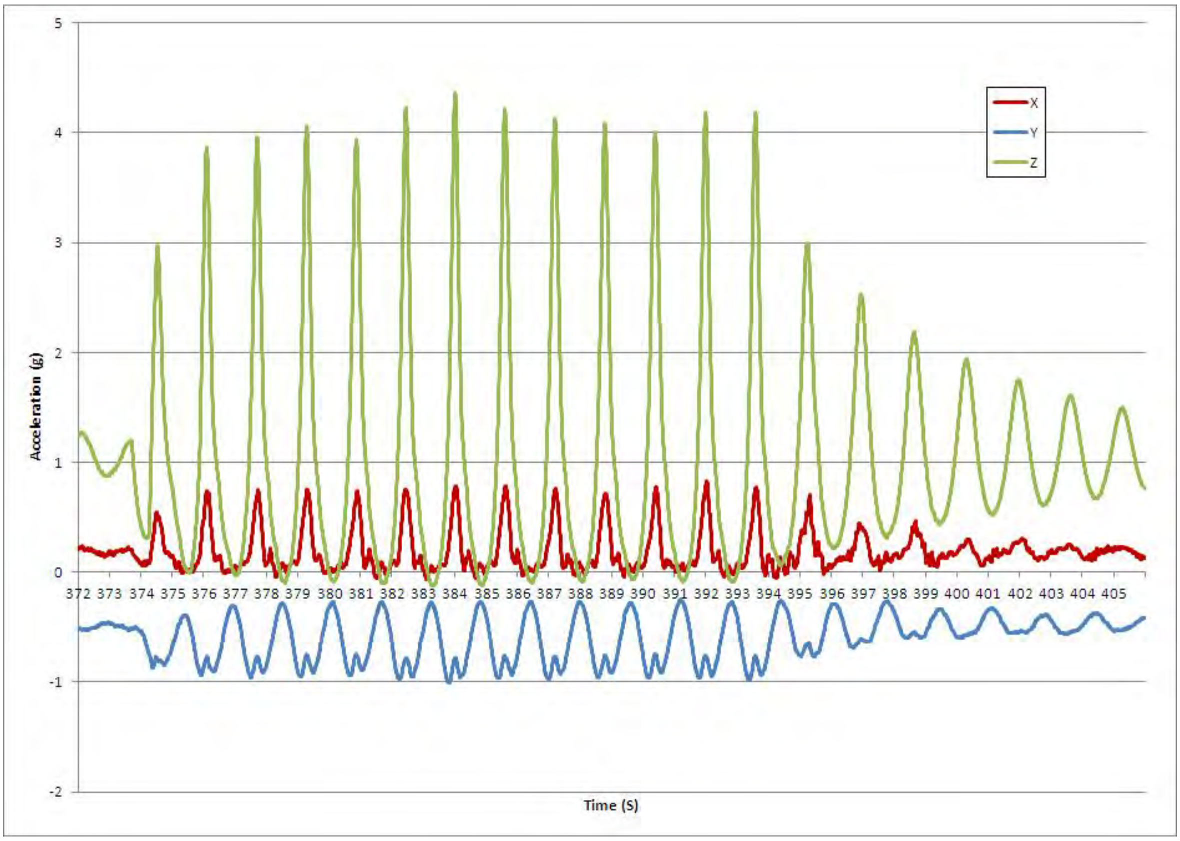

Figure 39 Test run 1, Program 1, Foot Pedal

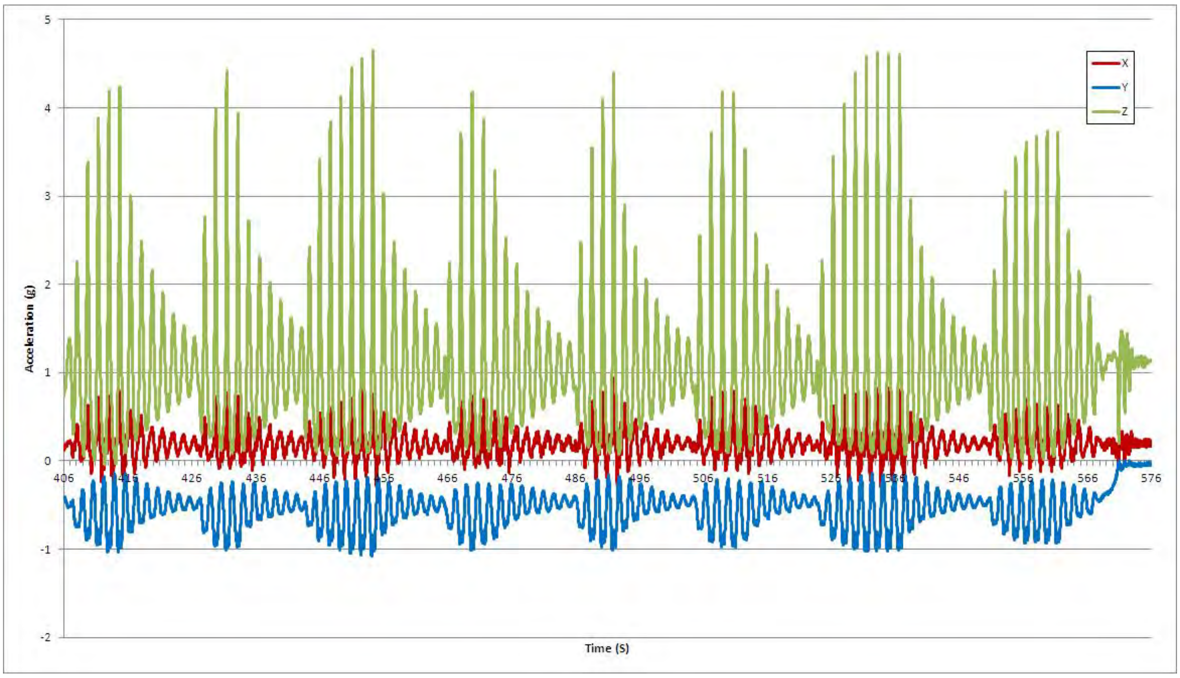

Figure 40 Test run 1, Program 2

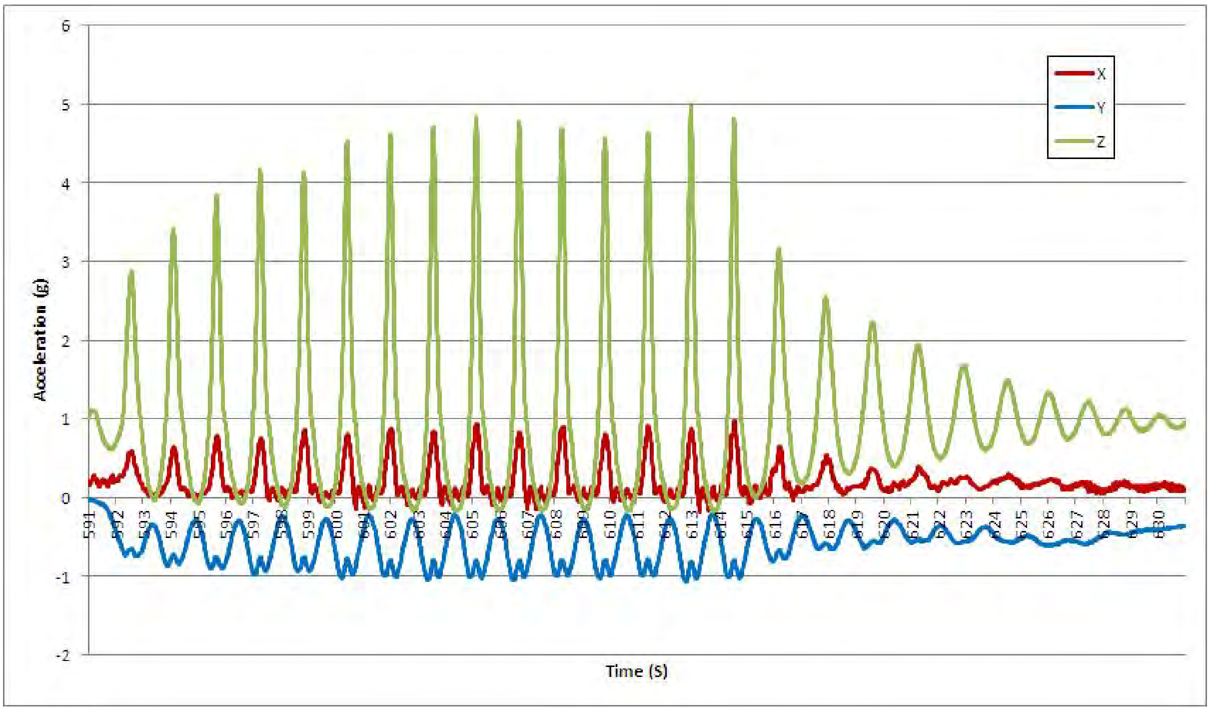

Figure 41 Test run 1, Program 2, Foot pedal

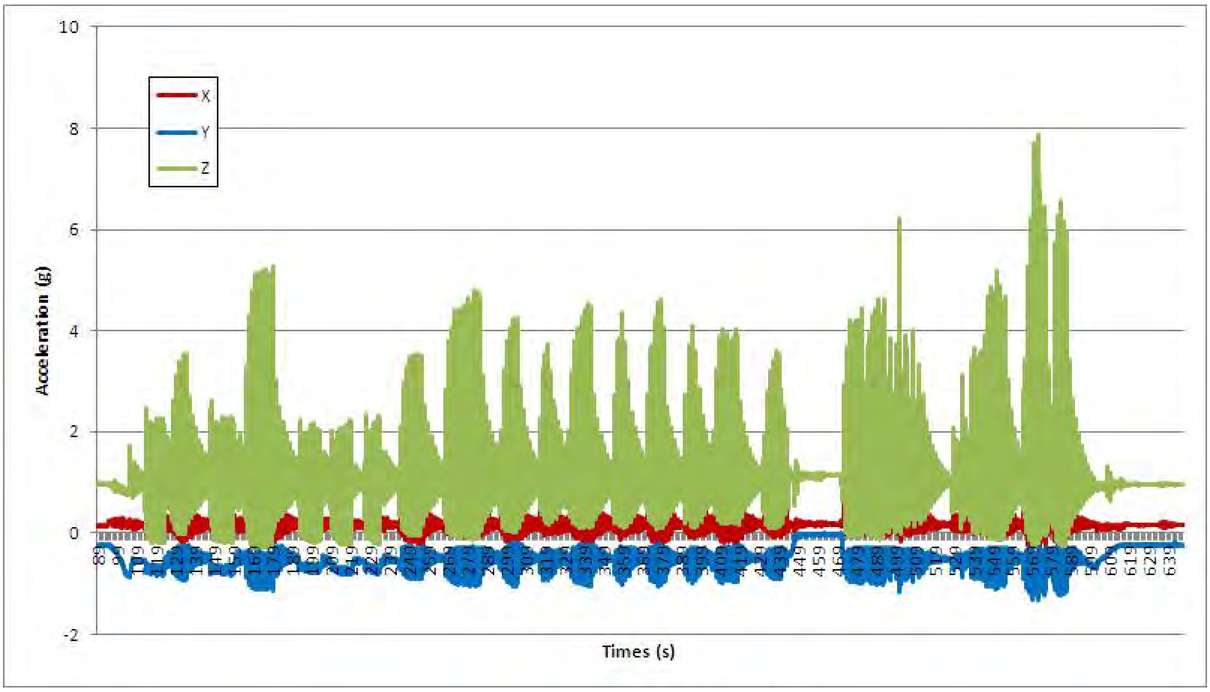

Figure 42 Test run 2 Full

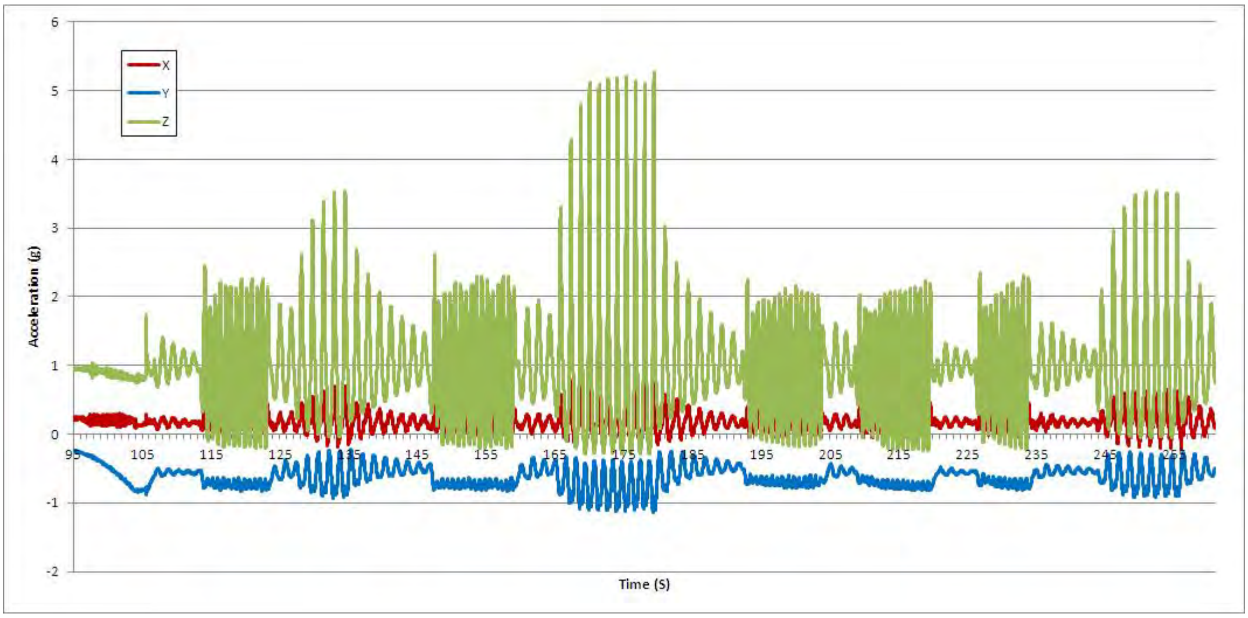

Figure 43 Test run 2, Program 1

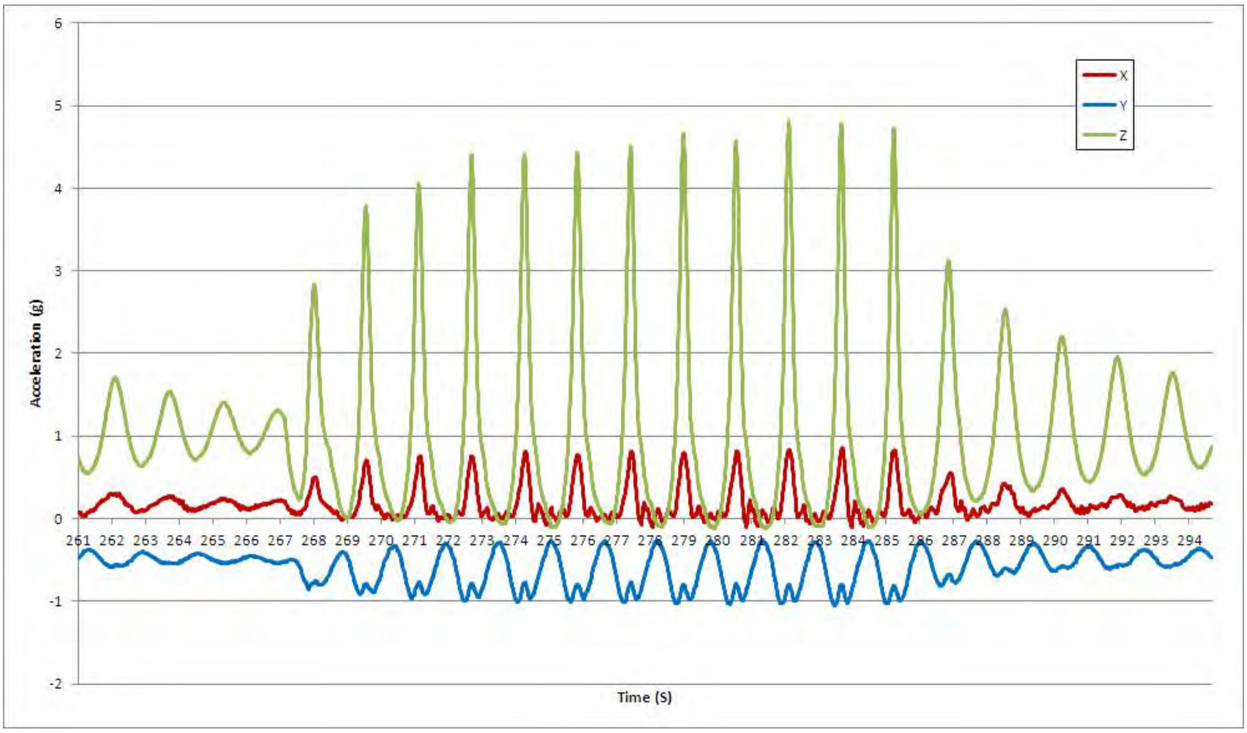

Figure 44 Test run 2, Program 1, Foot pedal

Figure 45 Test run 2, Program 2

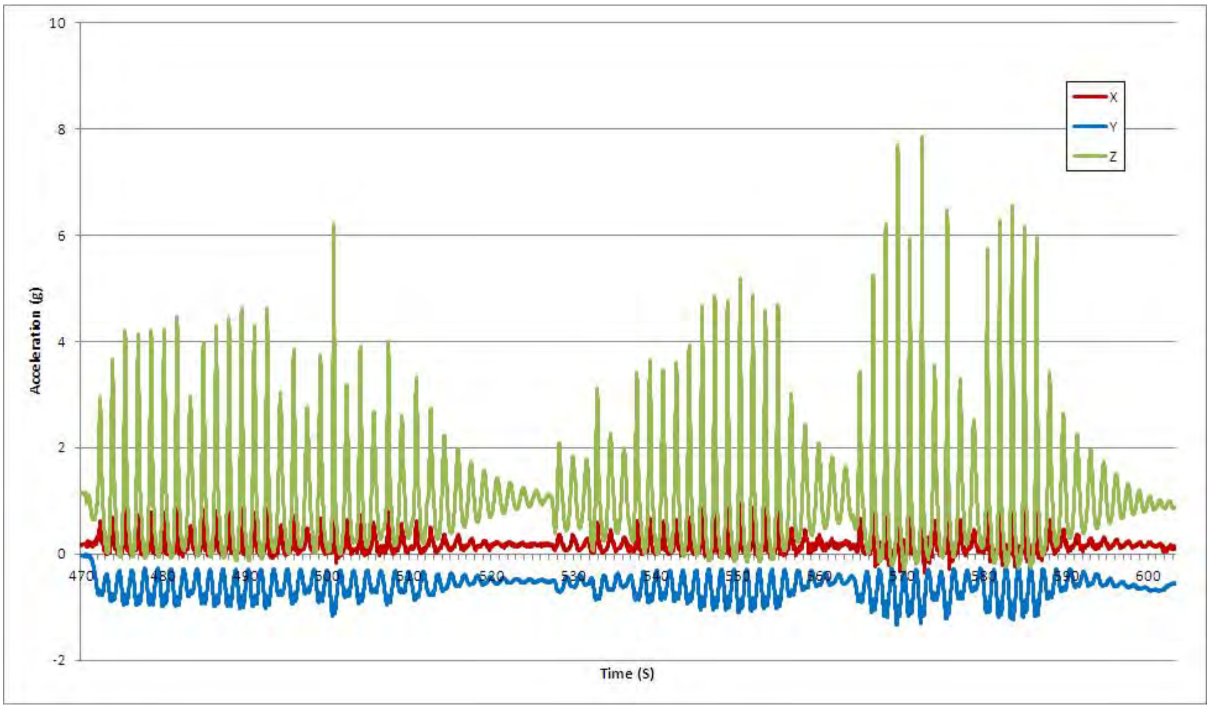

Figure 46 Test run 2, Program 2, Foot pedal

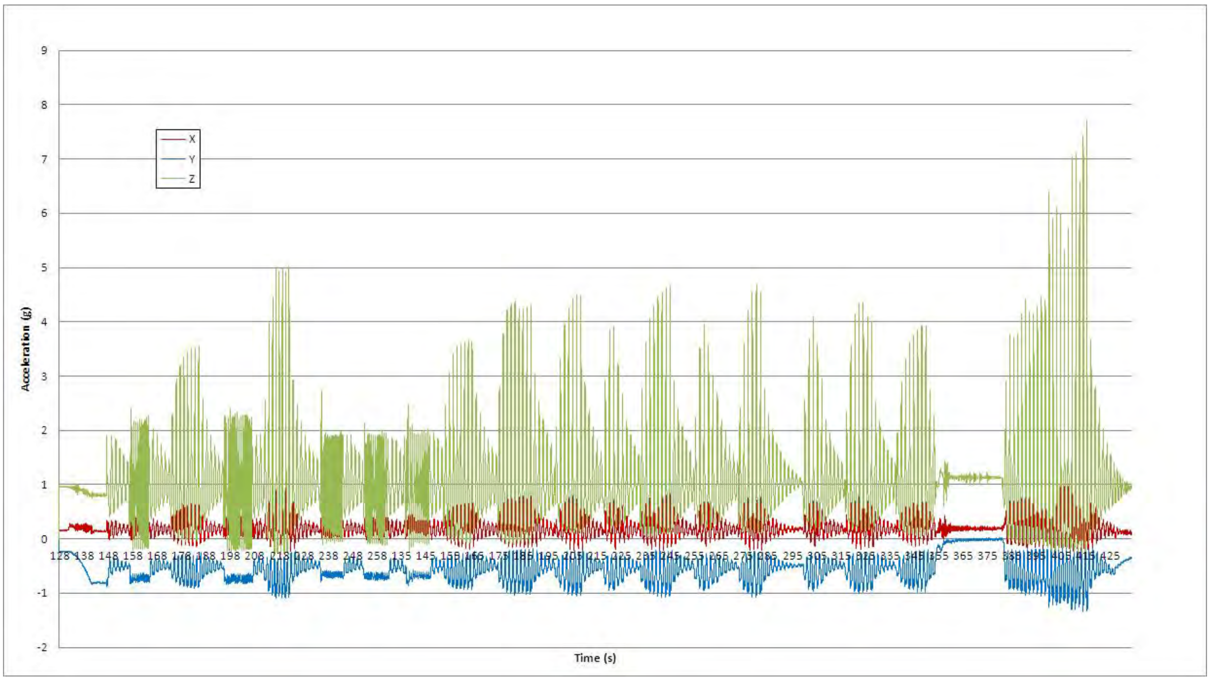

Figure 47 Test run 3 Full

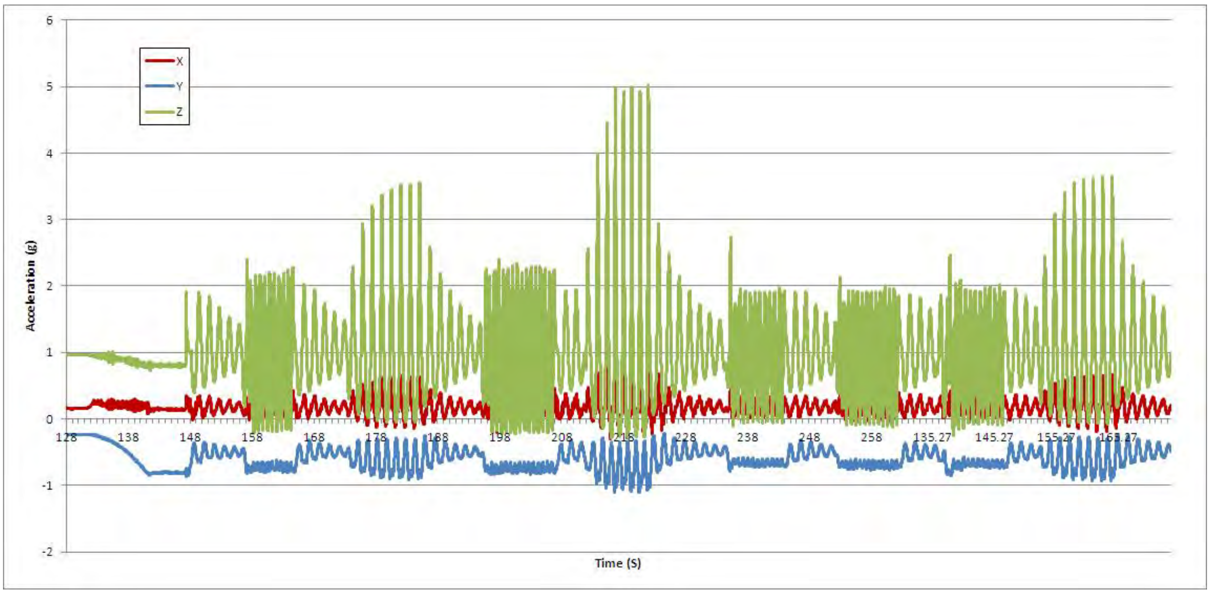

Figure 48 Test run3, Program 1

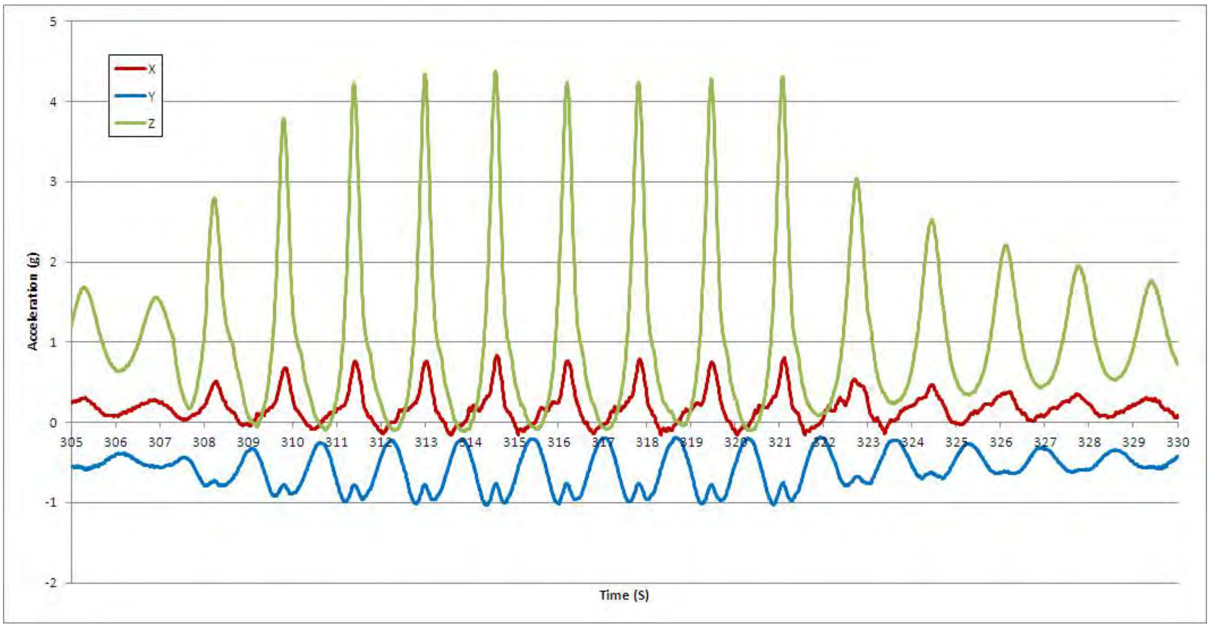

Figure 49 Test run 3, Program 1, Foot pedal

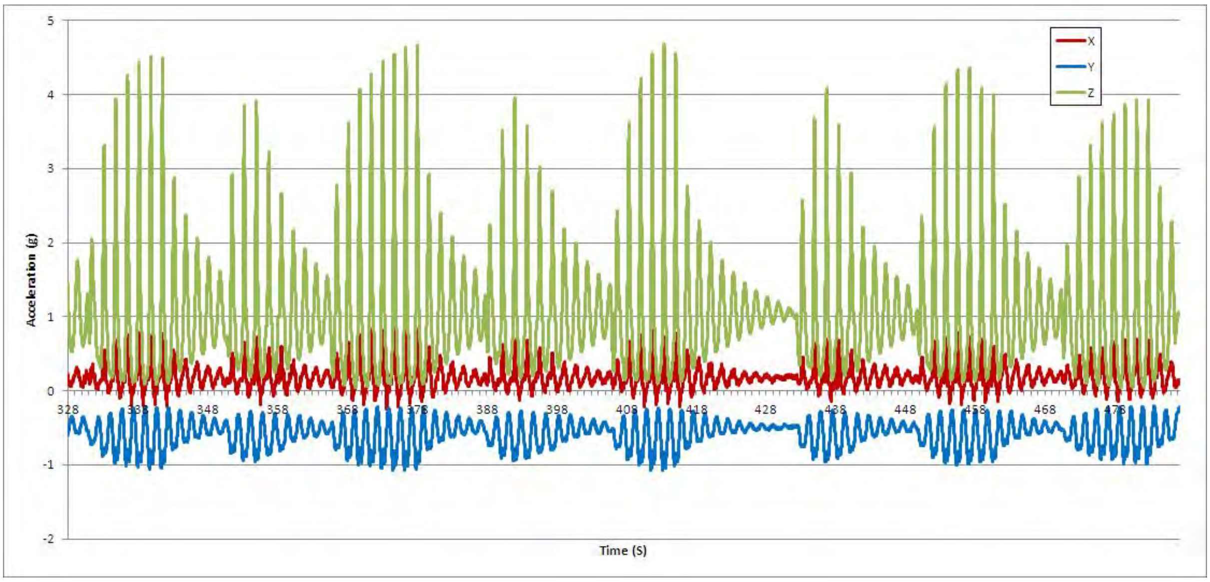

Figure 50 Test run 3, Program 2

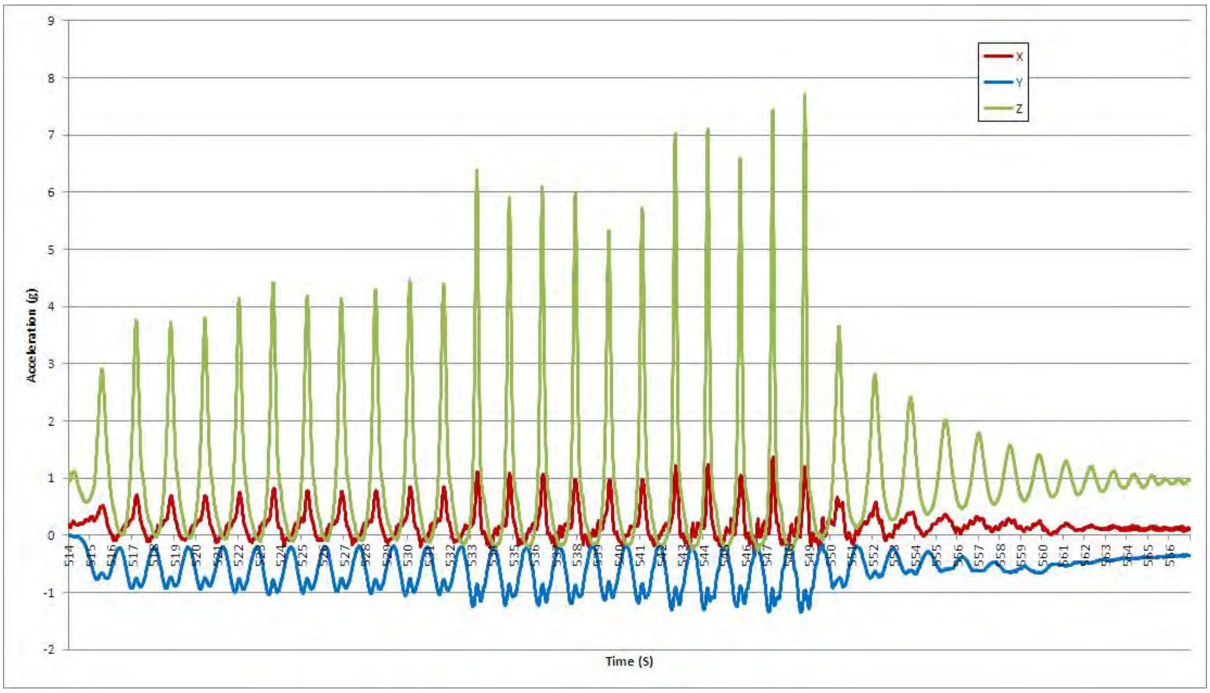

Figure 51 Test run 3, Program 2, Foot pedal

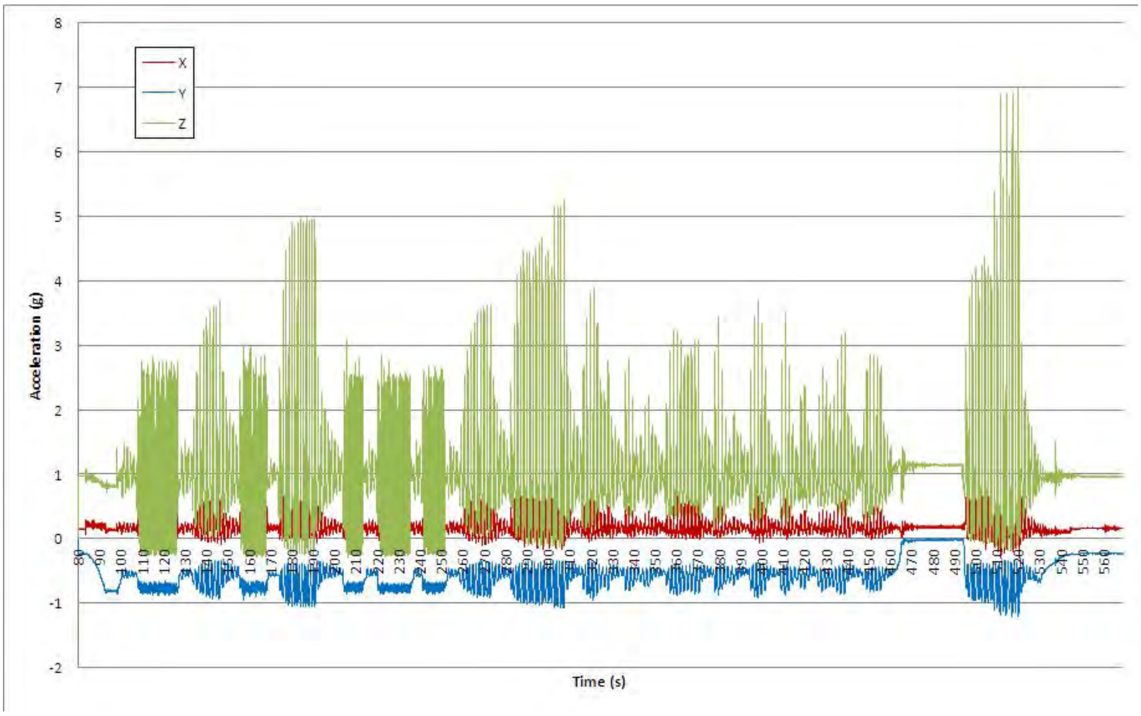

Figure 52 Test run 4 Full

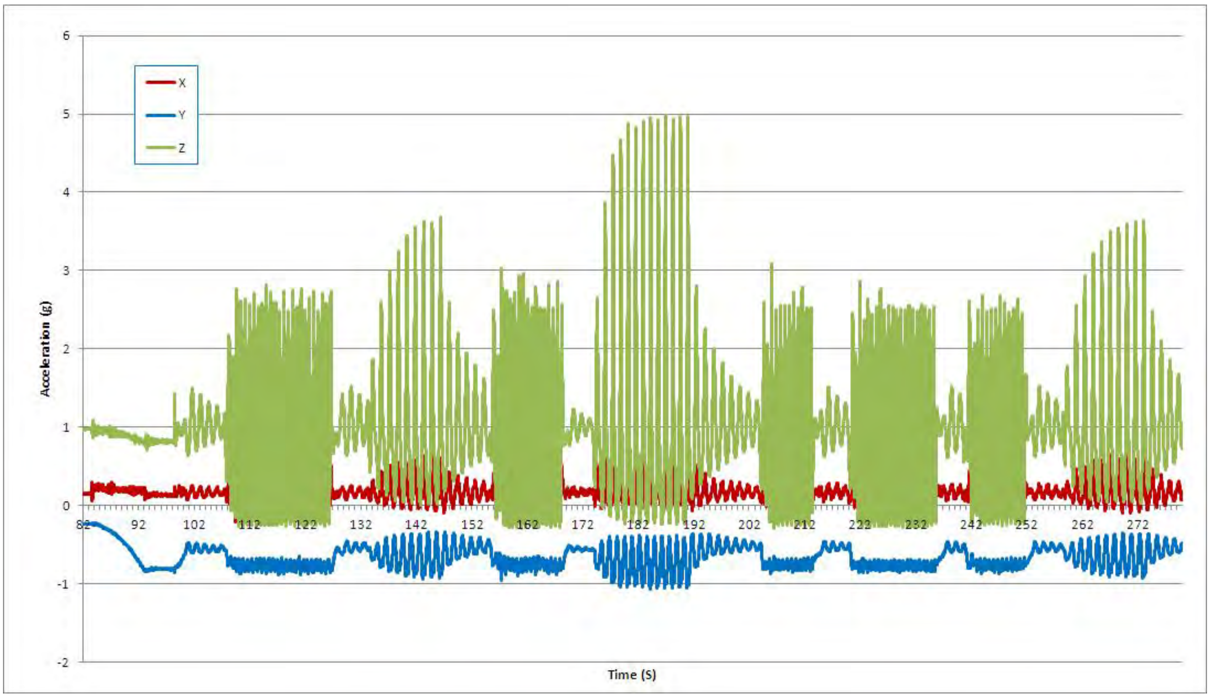

Figure 53 Test run 4 Program 1

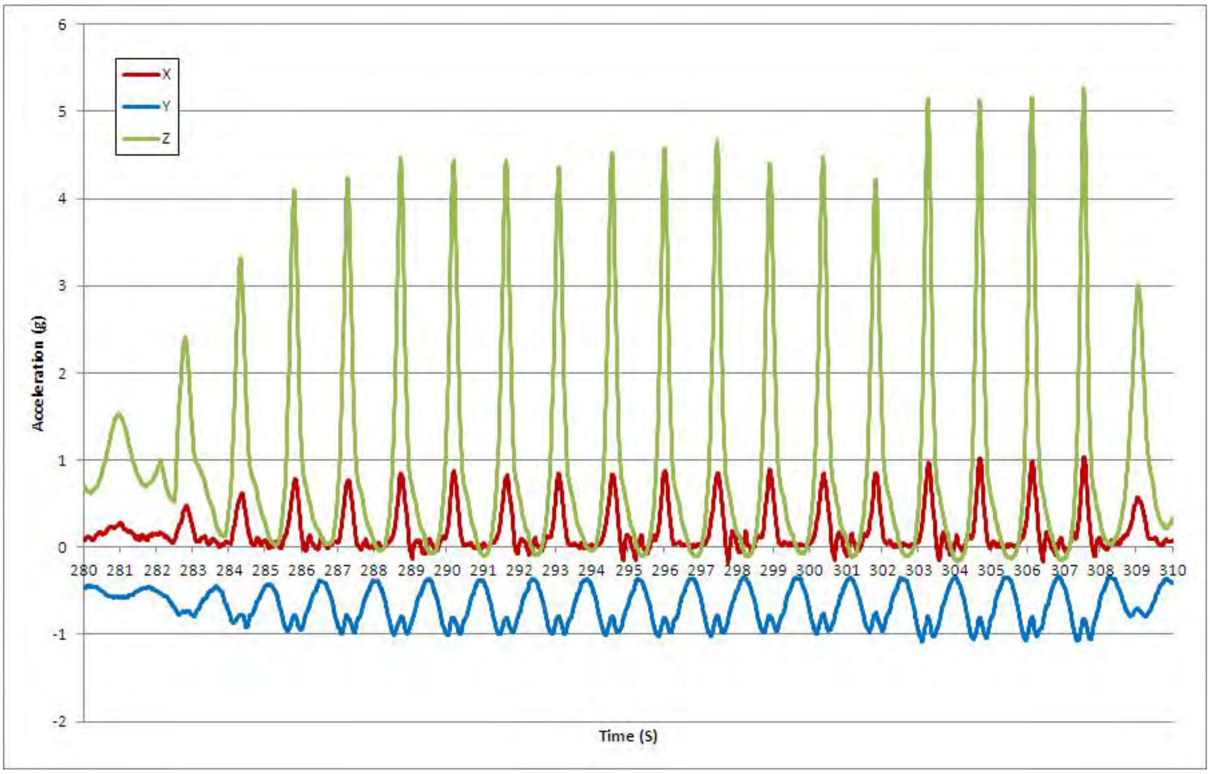

Figure 54 Test run 4, Program 1, Foot pedal

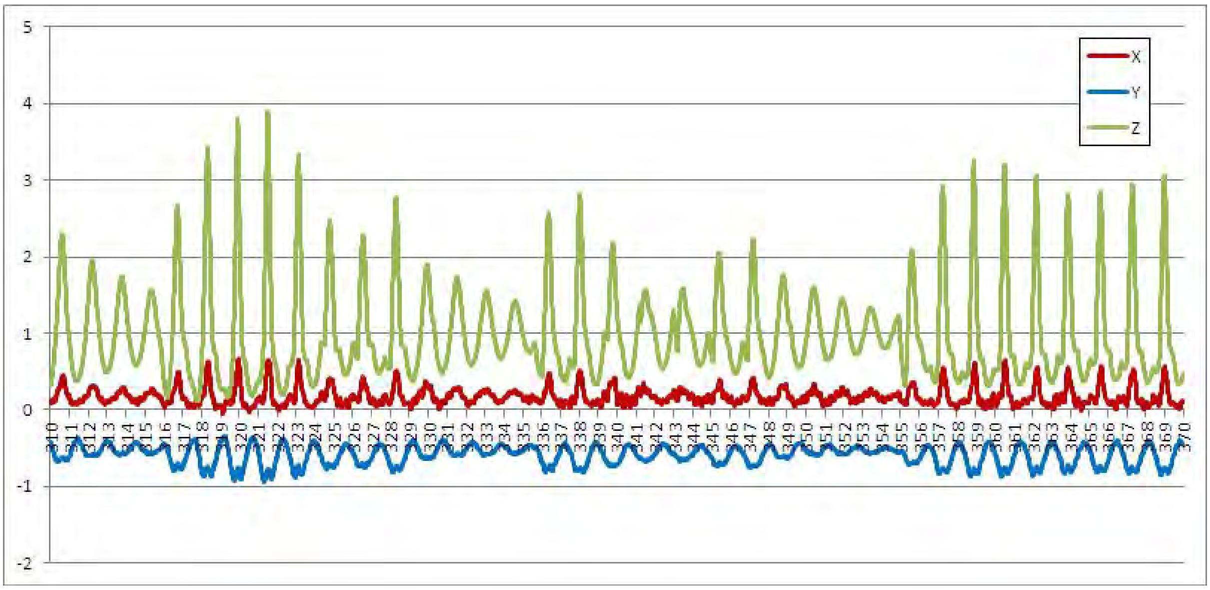

Figure 55 Test run 4, Program 2

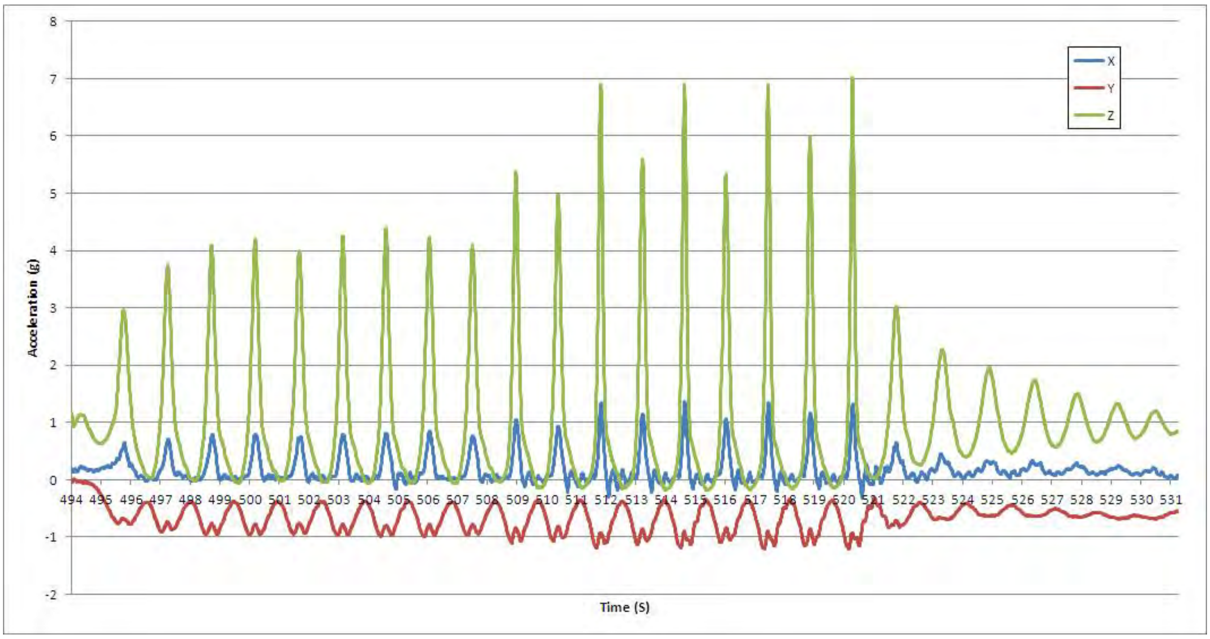

Figure 56 Test run 4, Program 2, Foot pedal

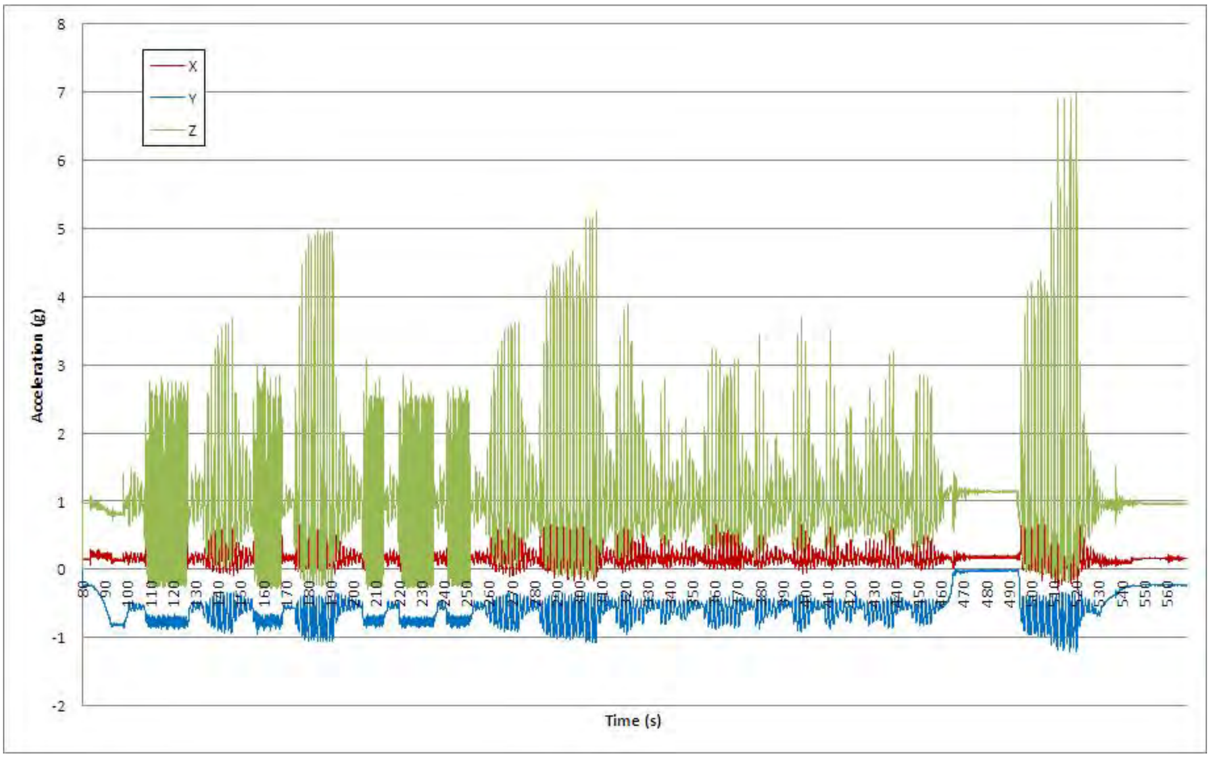

Figure 57 Test run 5 Full

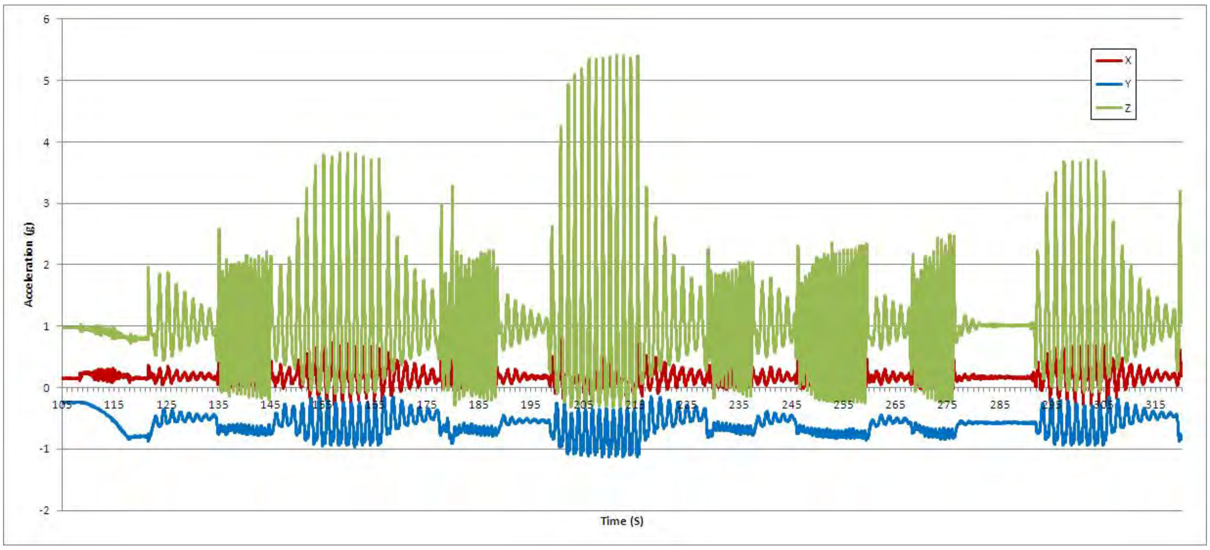

Figure 58 Test run 5, Program 1

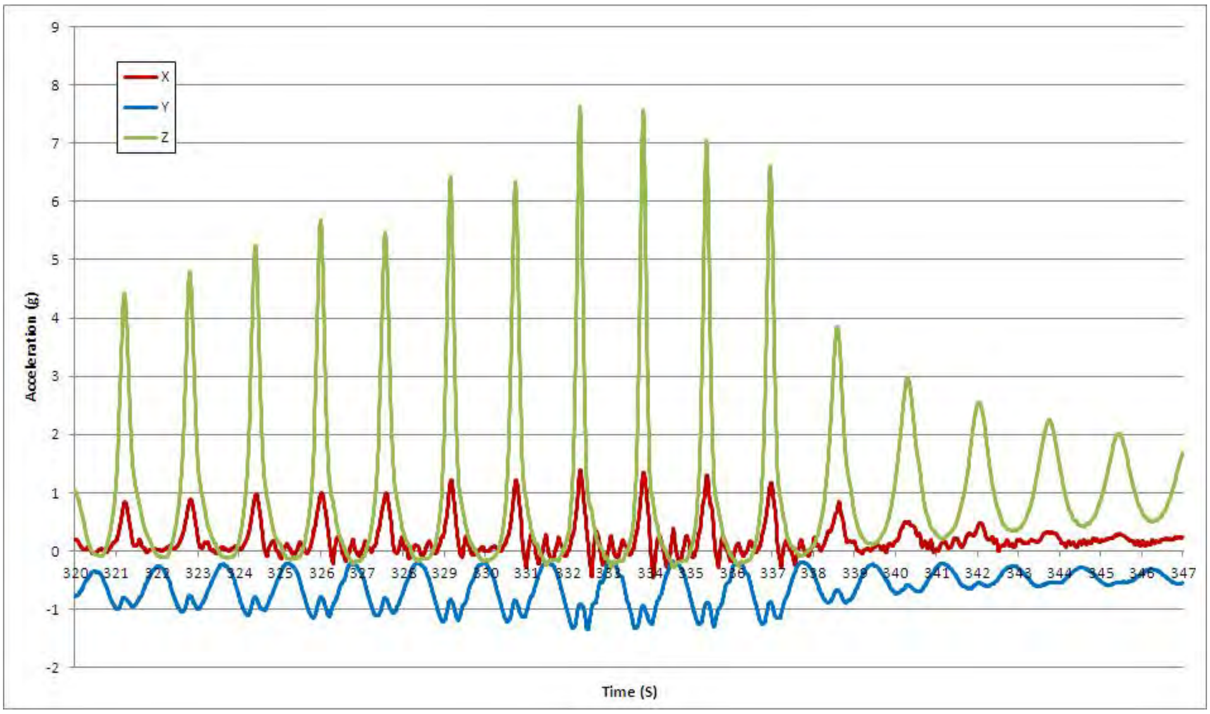

Figure 59 Test run 5, Program 1, Foot pedal

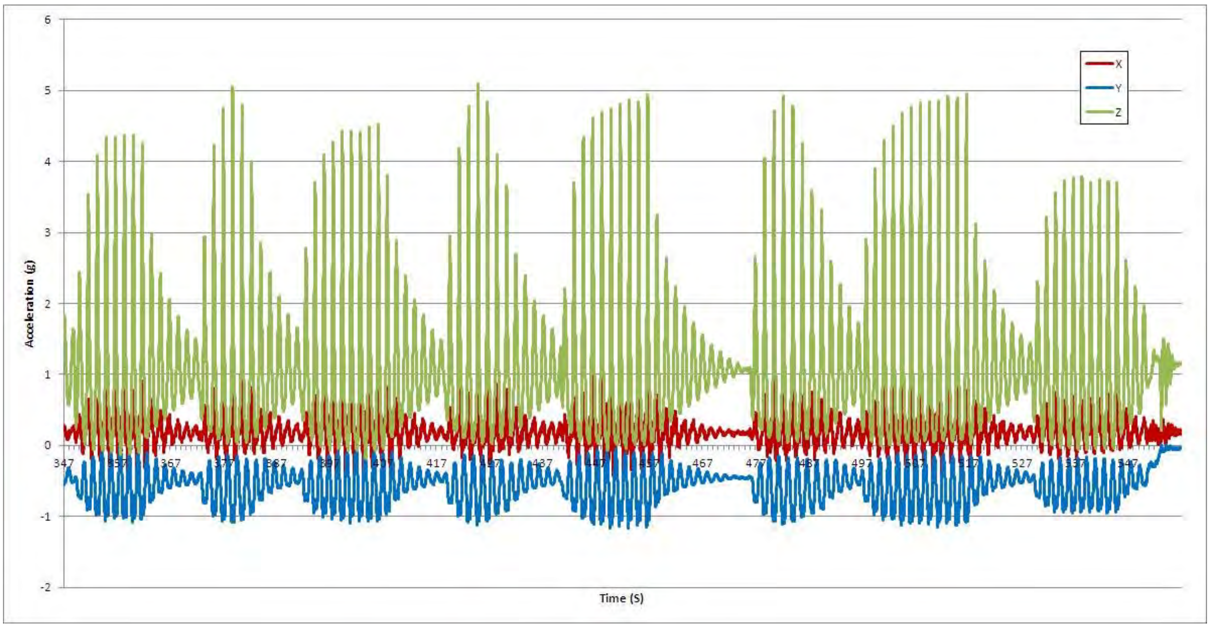

Figure 60 Test run 5, Program 2

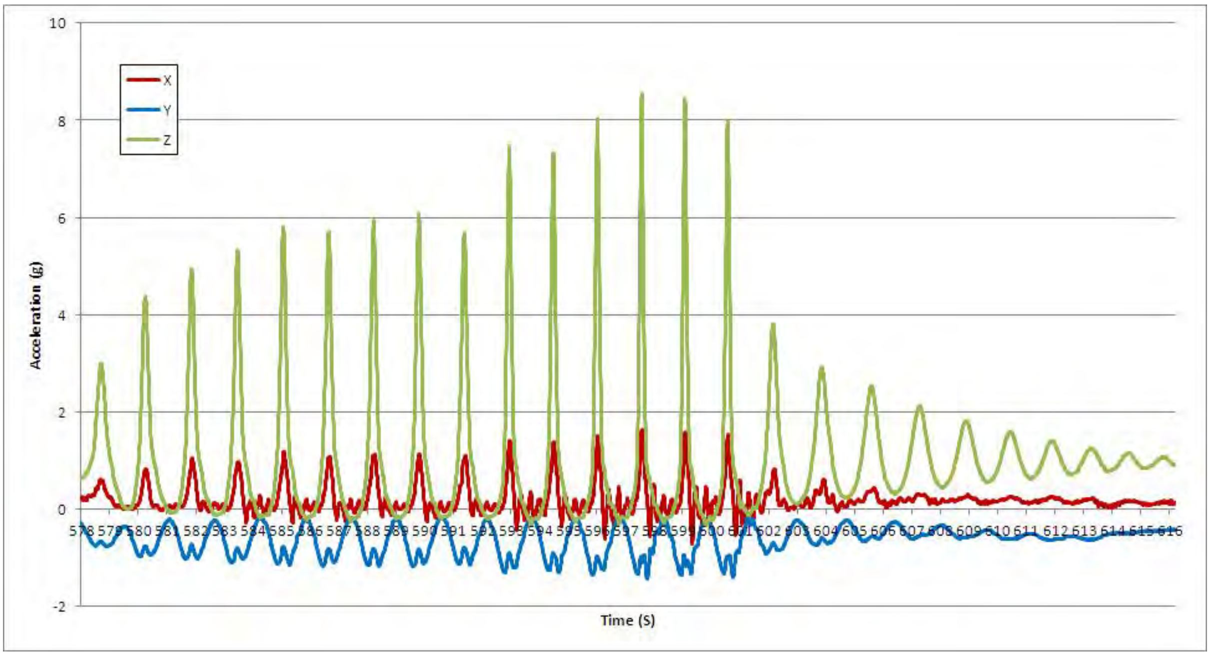

Figure 61 Test run 5, Program 2, Foot pedal

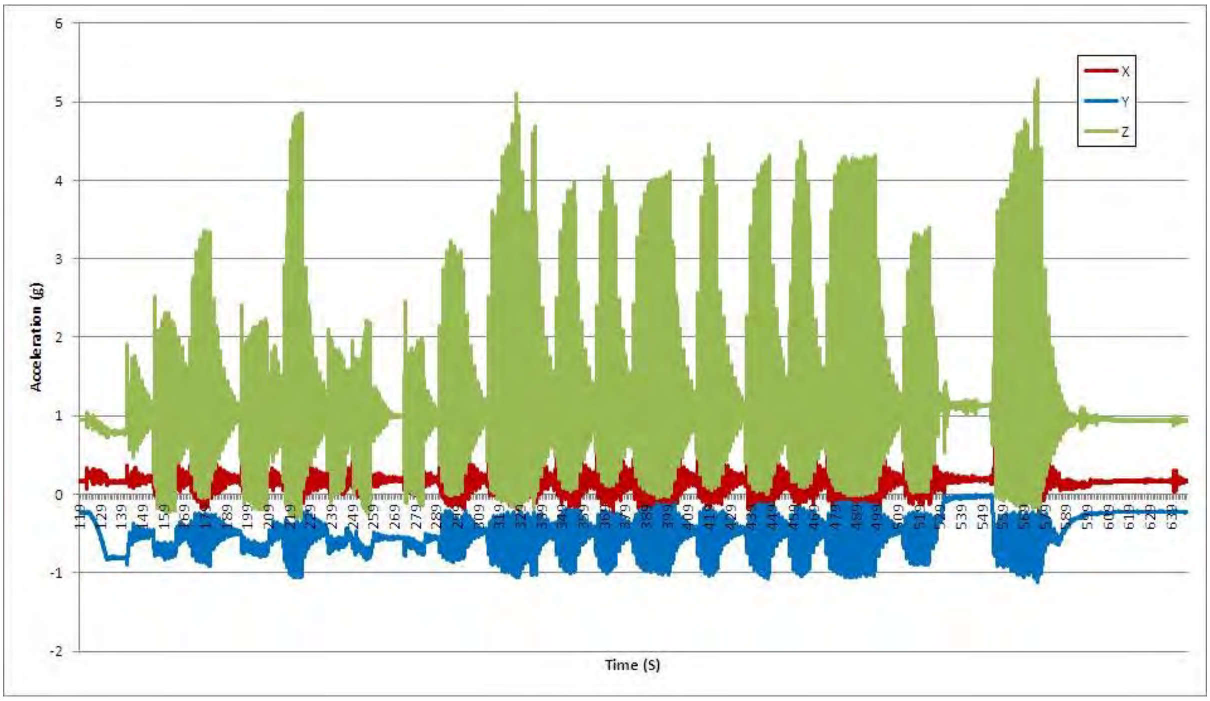

Figure 62 Test run 6 Full

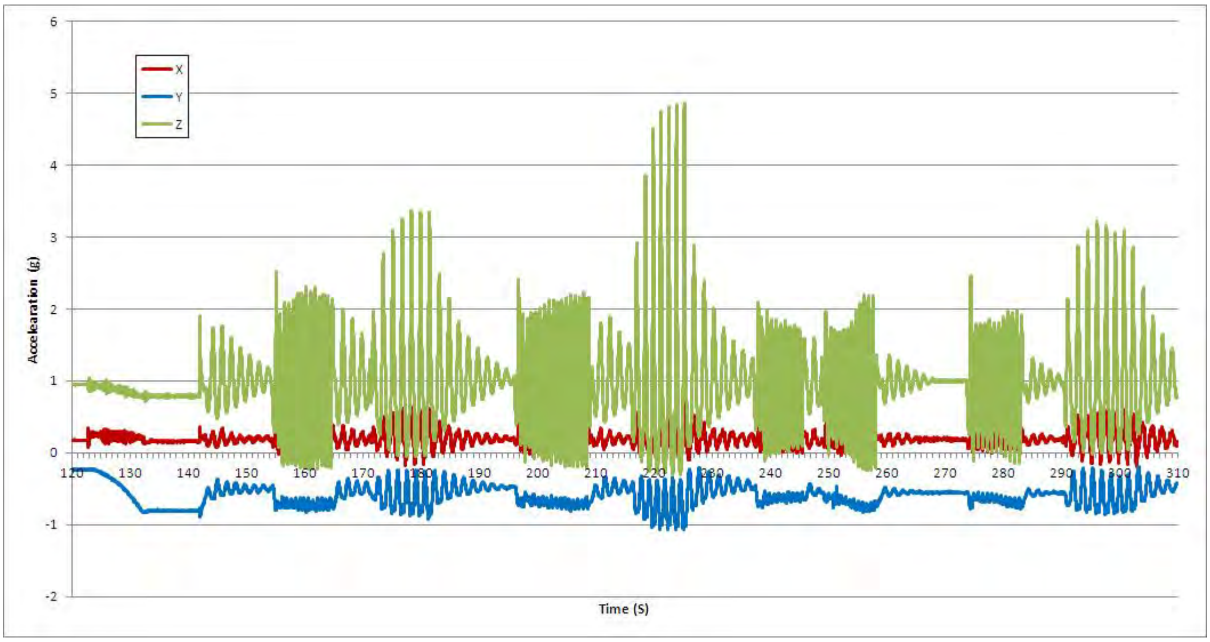

Figure 63 Test run 6, Program 1

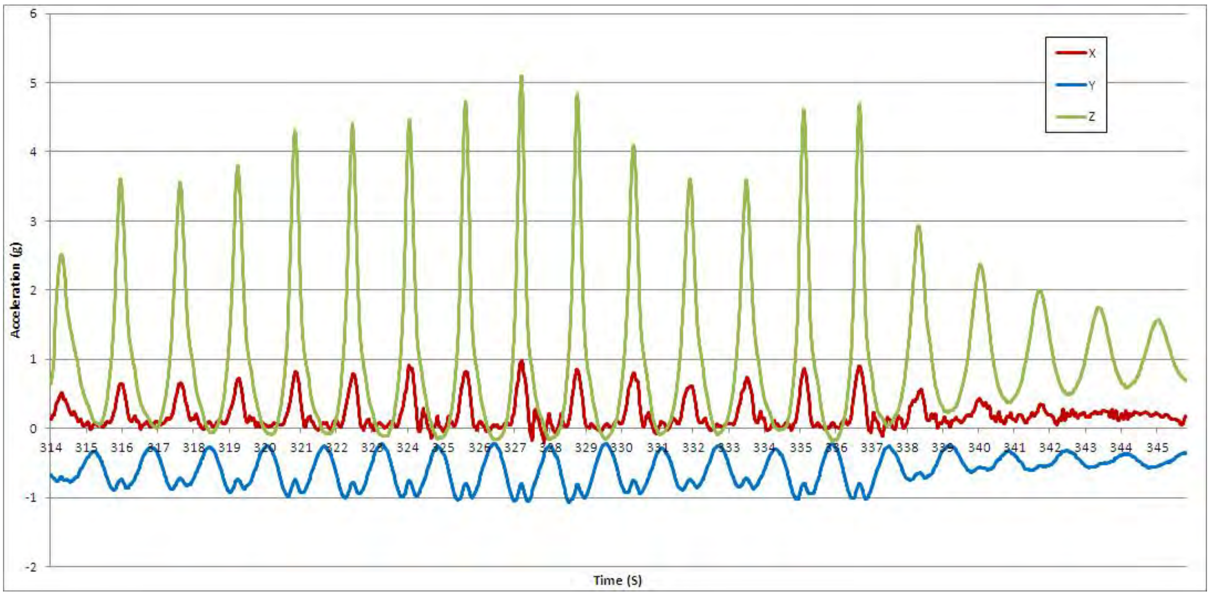

Figure 64 Test run 6, Program 1, Foot pedal

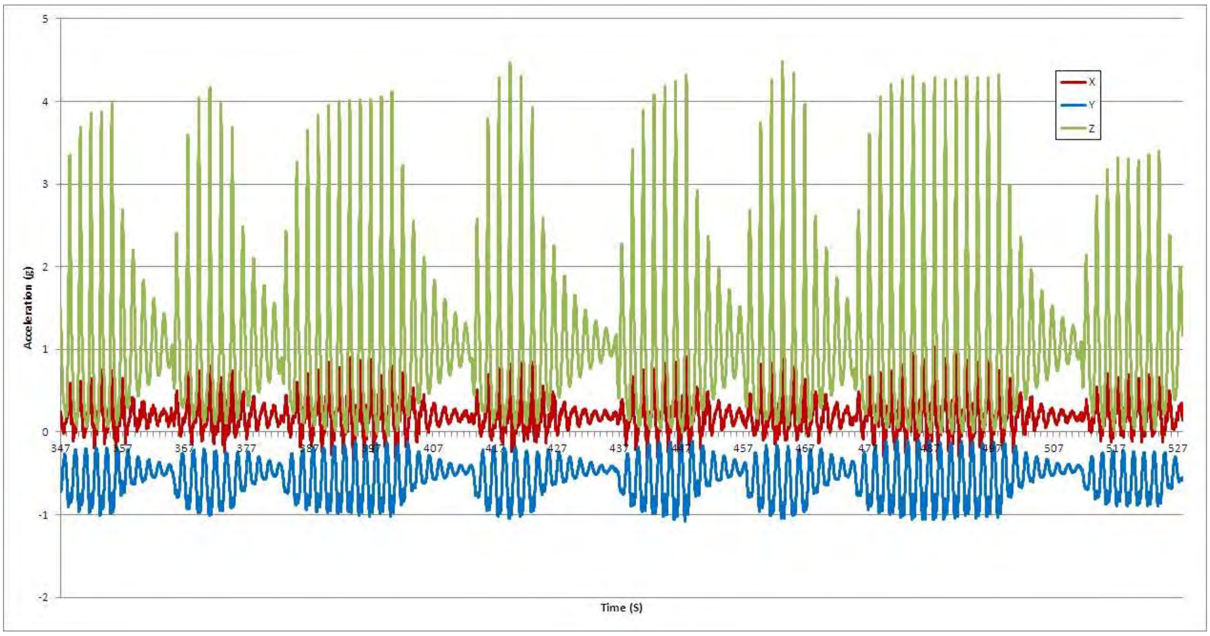

Figure 65 Test run 6, Program 2

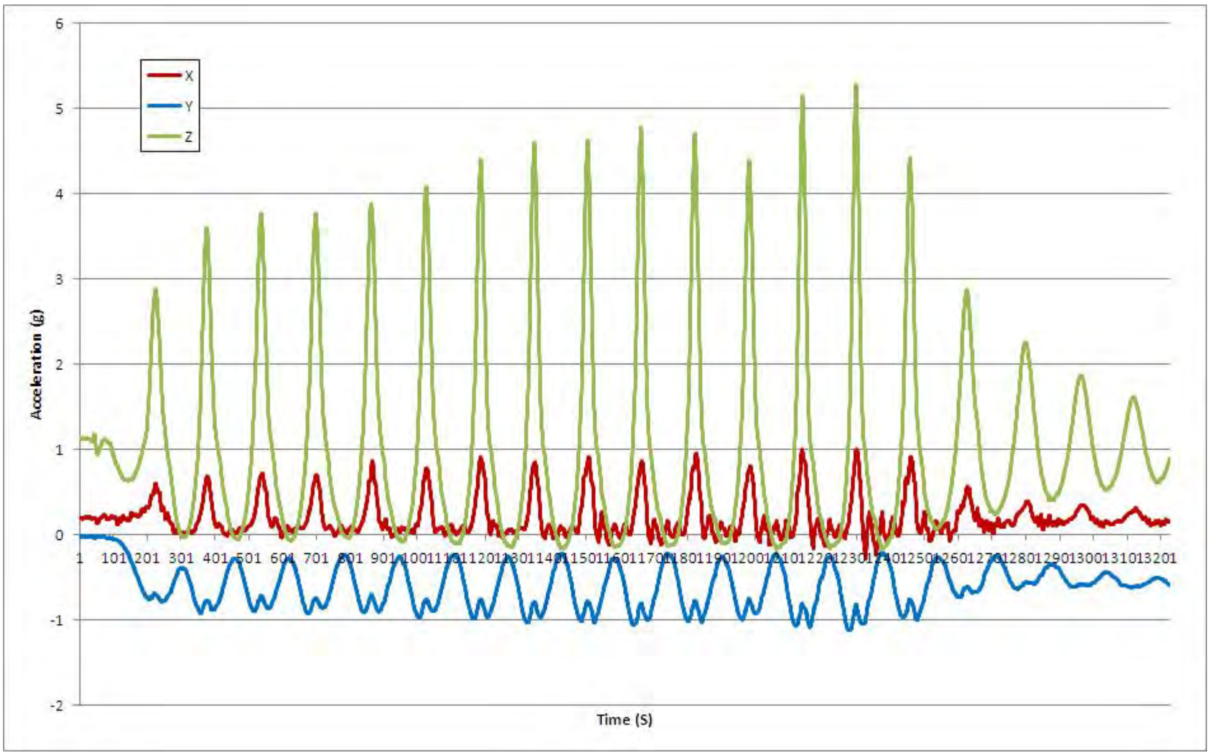

Figure 66 Test run 6, Program 2, Foot pedal

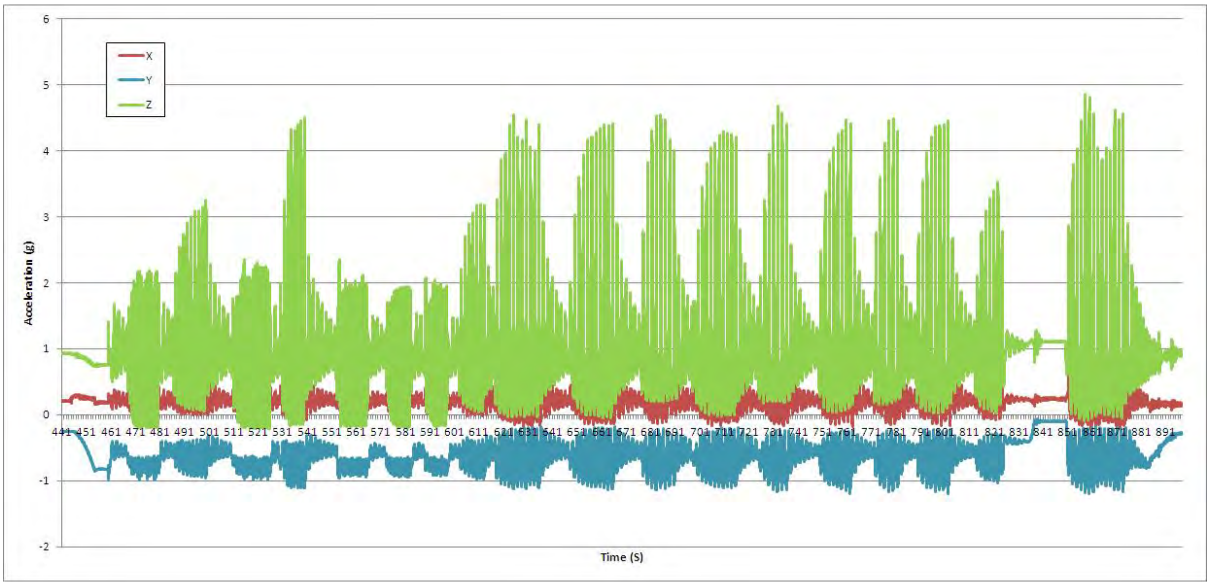

Figure 67 Test run 7 Full

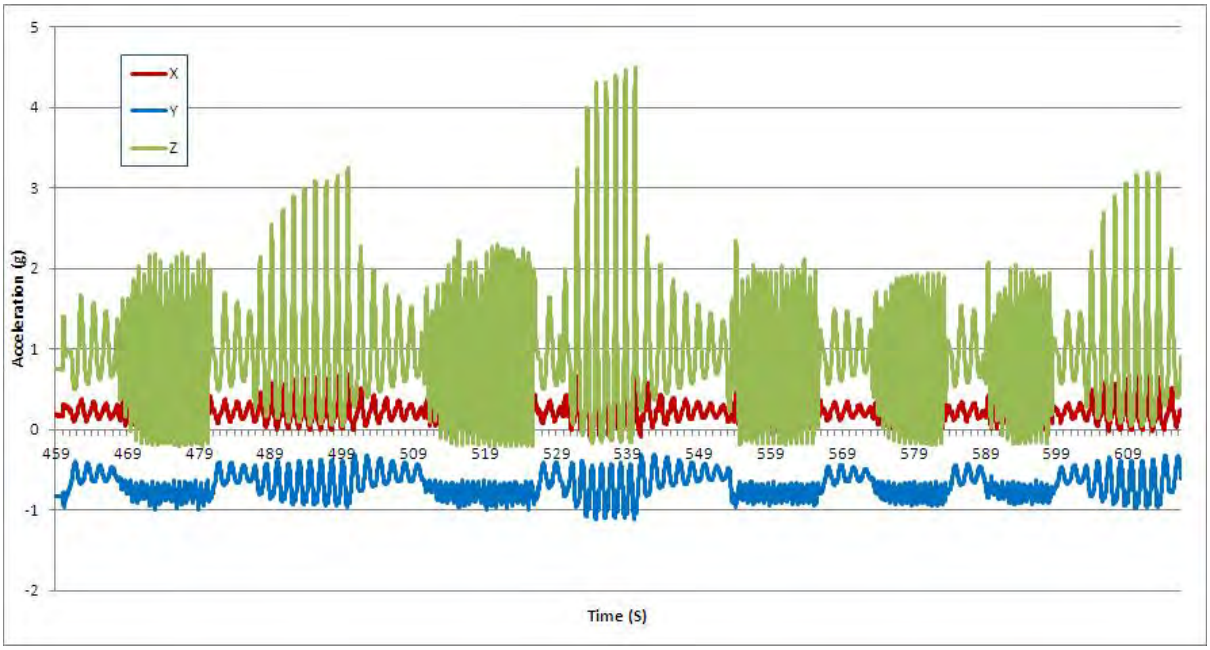

Figure 68 Test run 7, Program 1

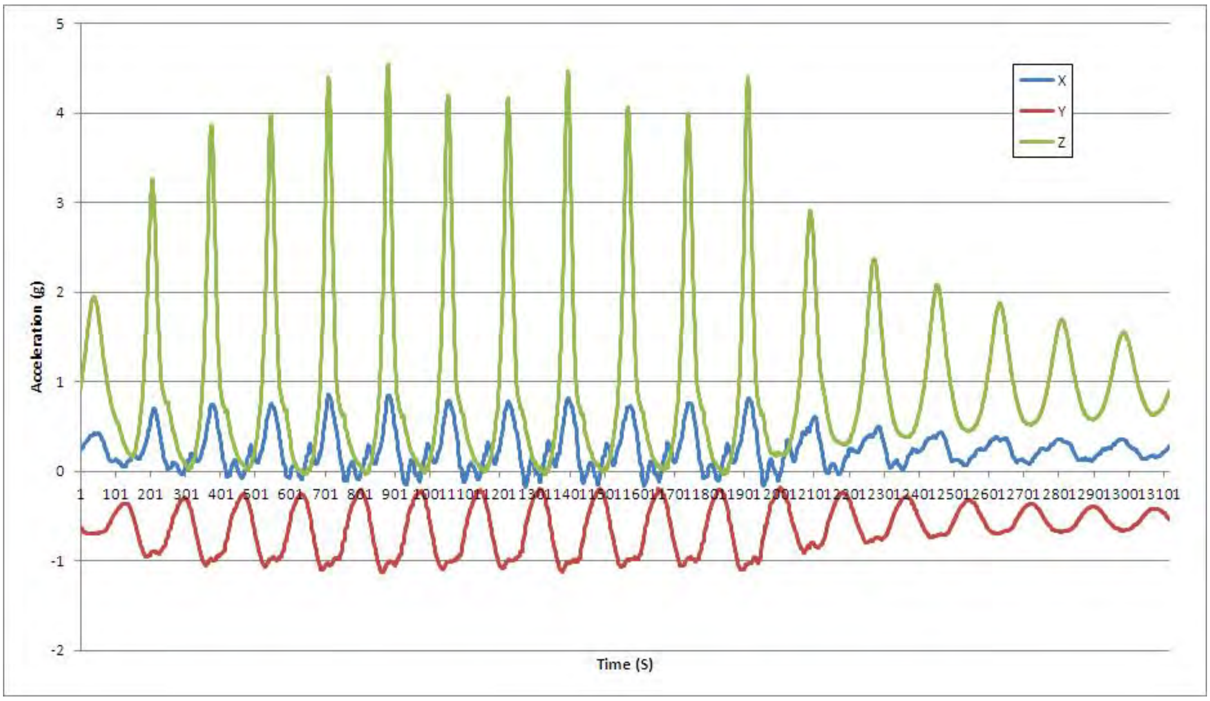

Figure 69 Test run 7, Program 1, Foot pedal

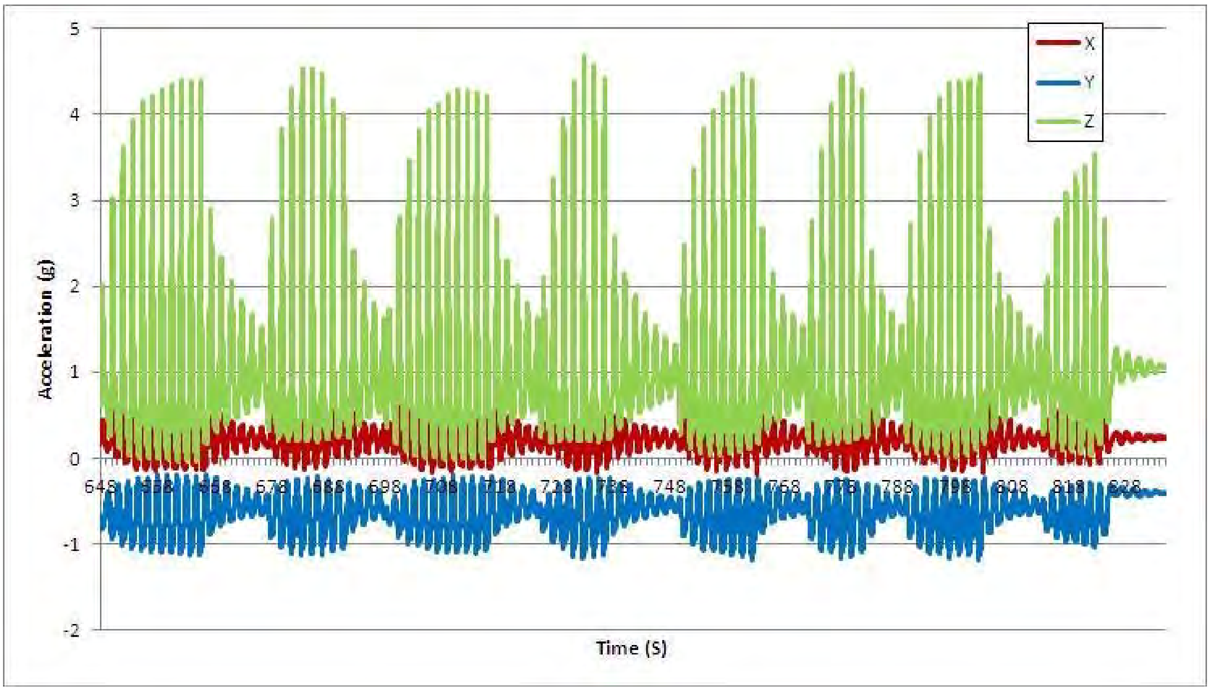

Figure 70 Test run 7, Program 2

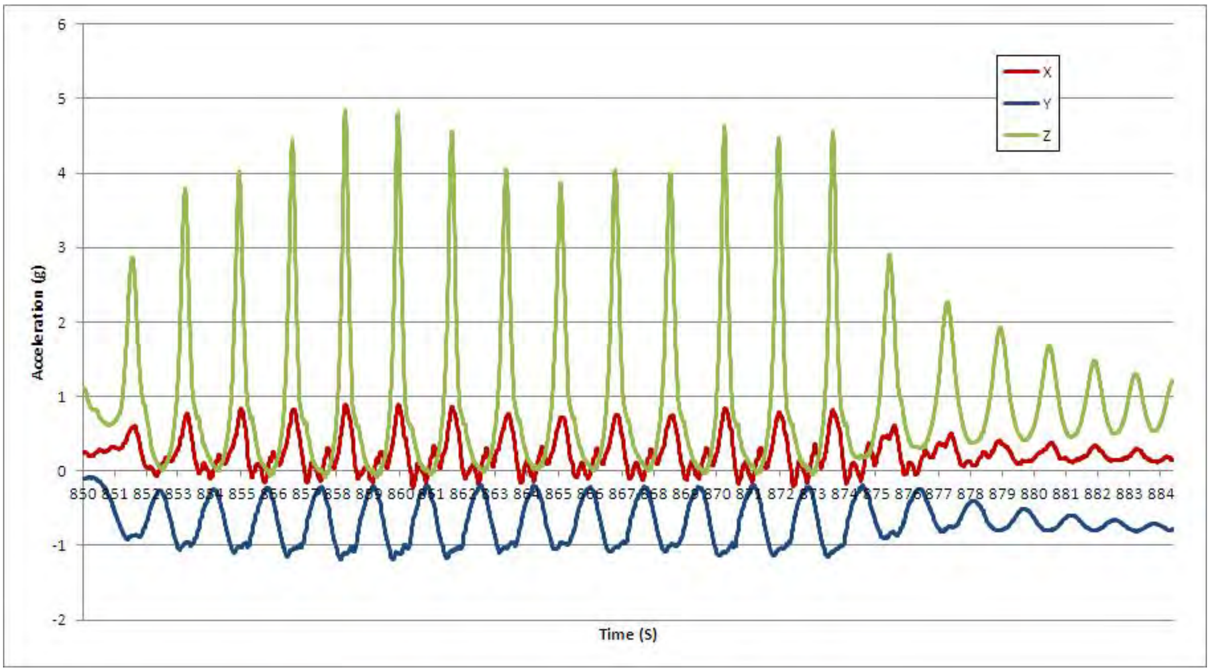

Figure 71 Test run 7, Program 2, Foot pedal

Figure 72 Test run 8 Full

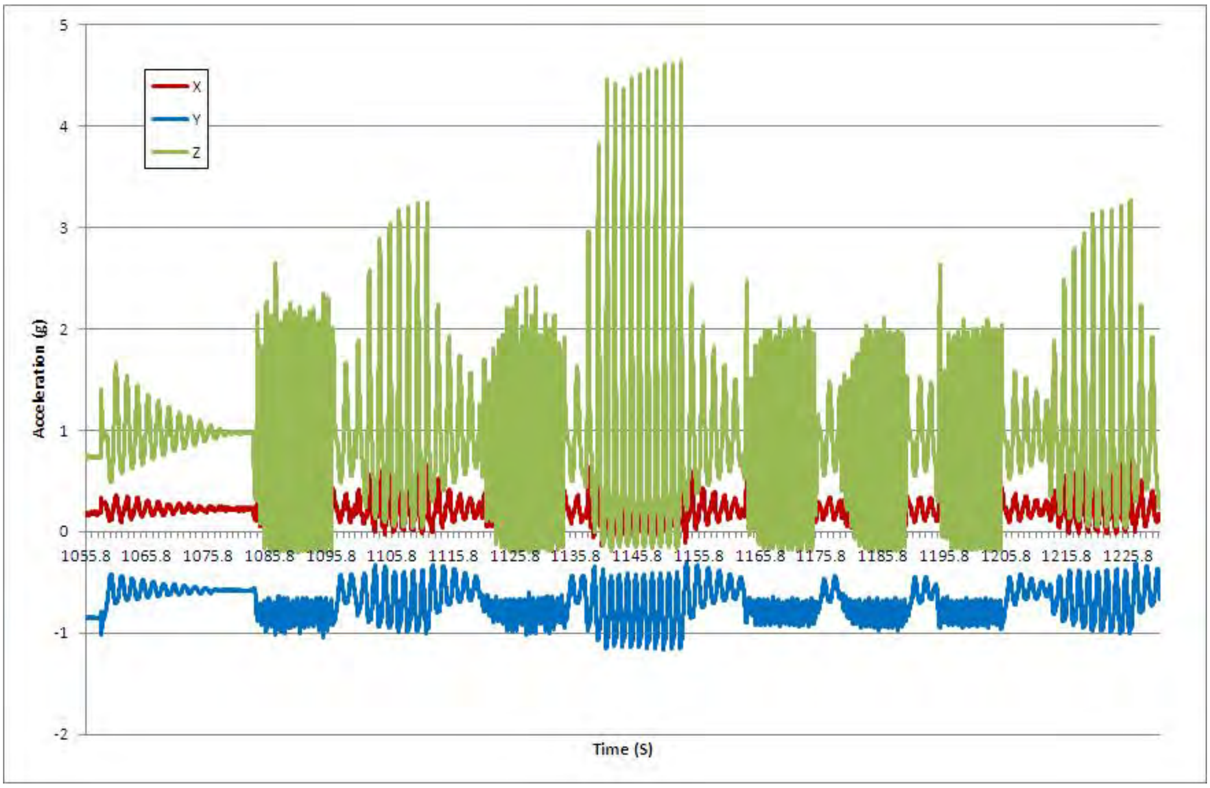

Figure 73 Test run 8, Program 1

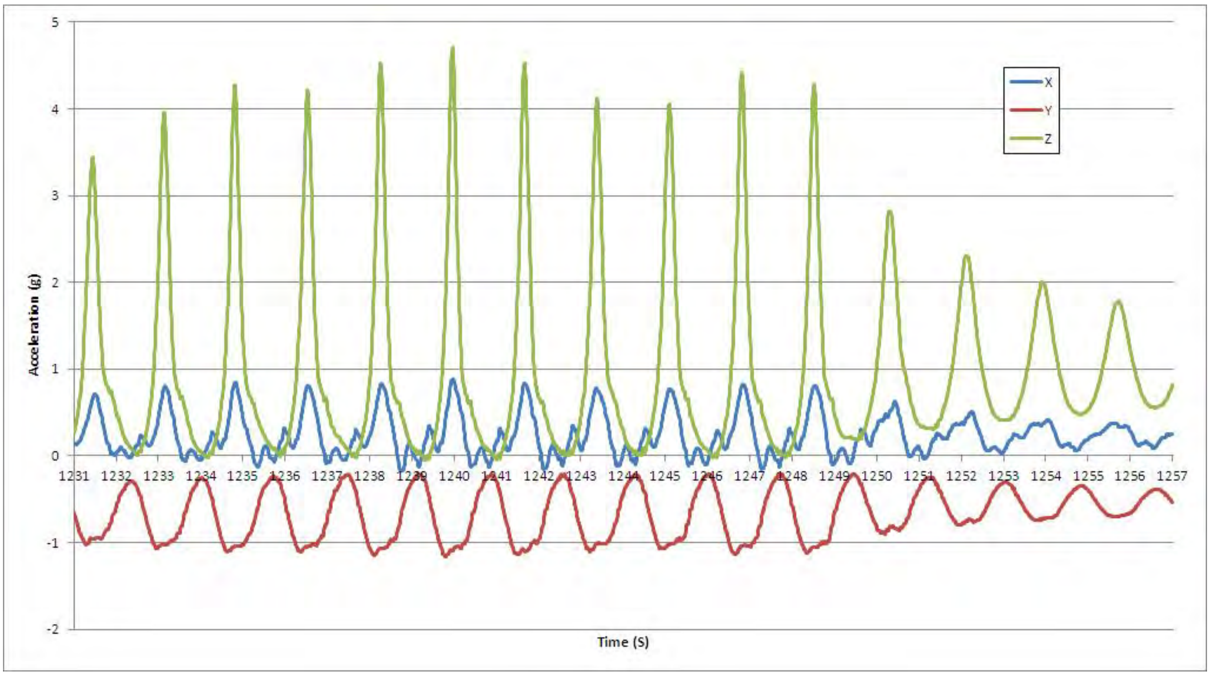

Figure 74 Test run 8, Program 1, Foot pedal

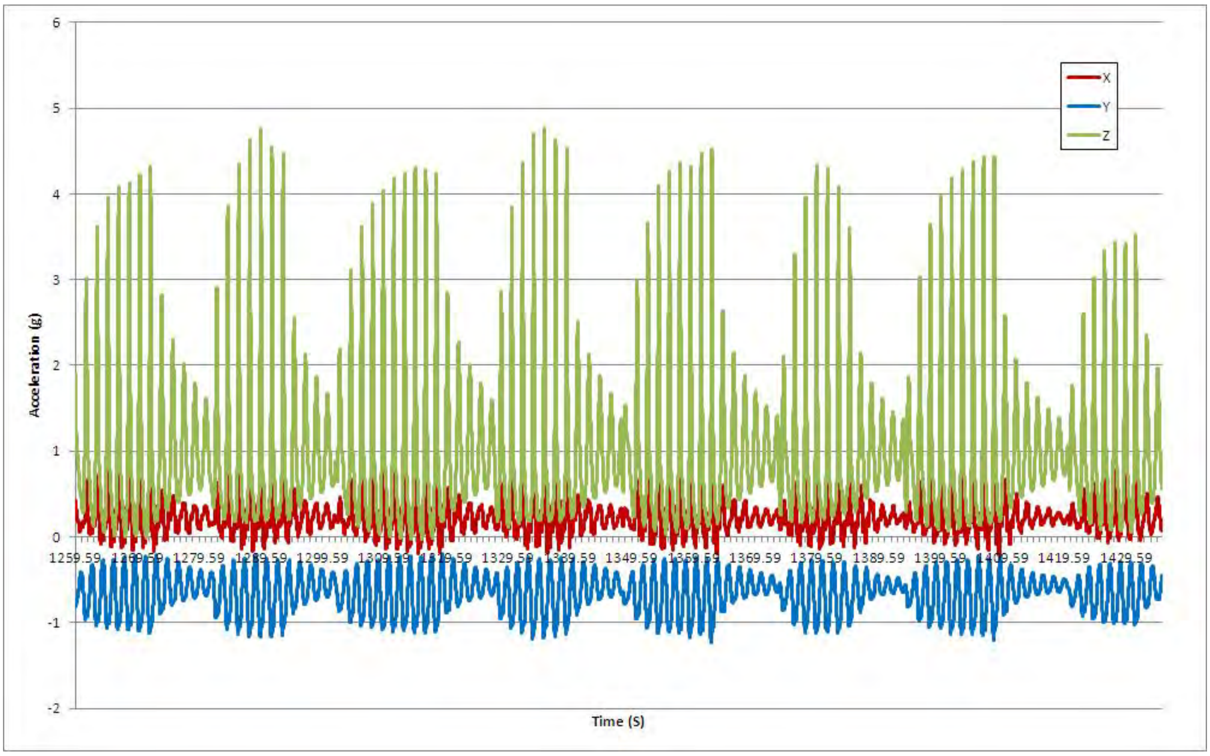

Figure 75 Test run 8, Program 2

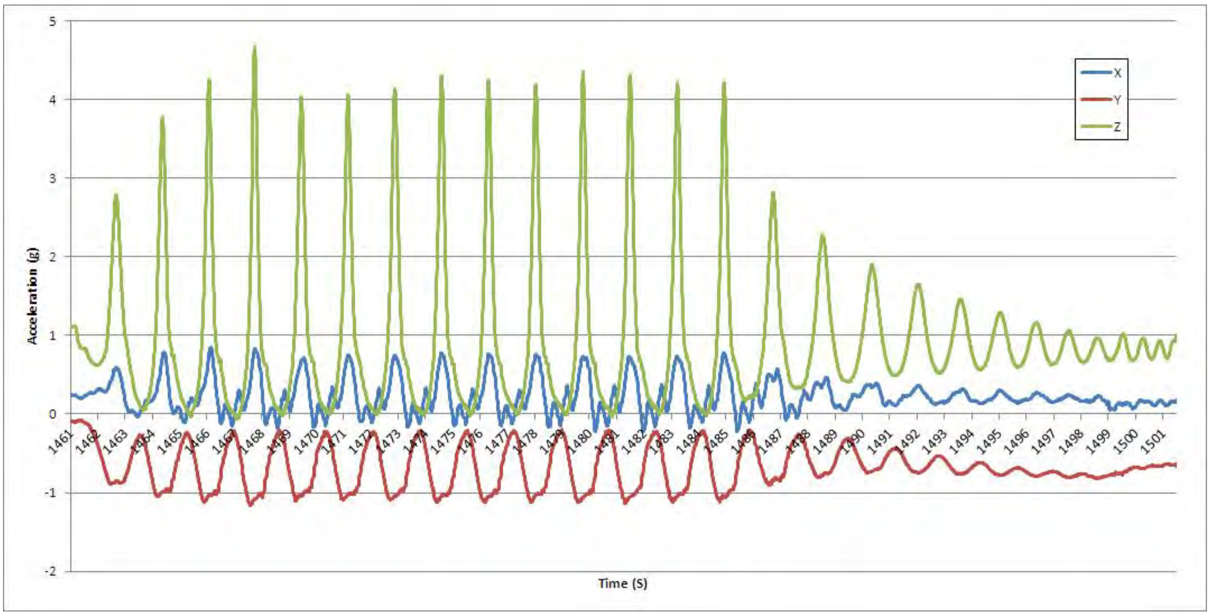

Figure 76 Test run 8, Program 2, Foot pedal

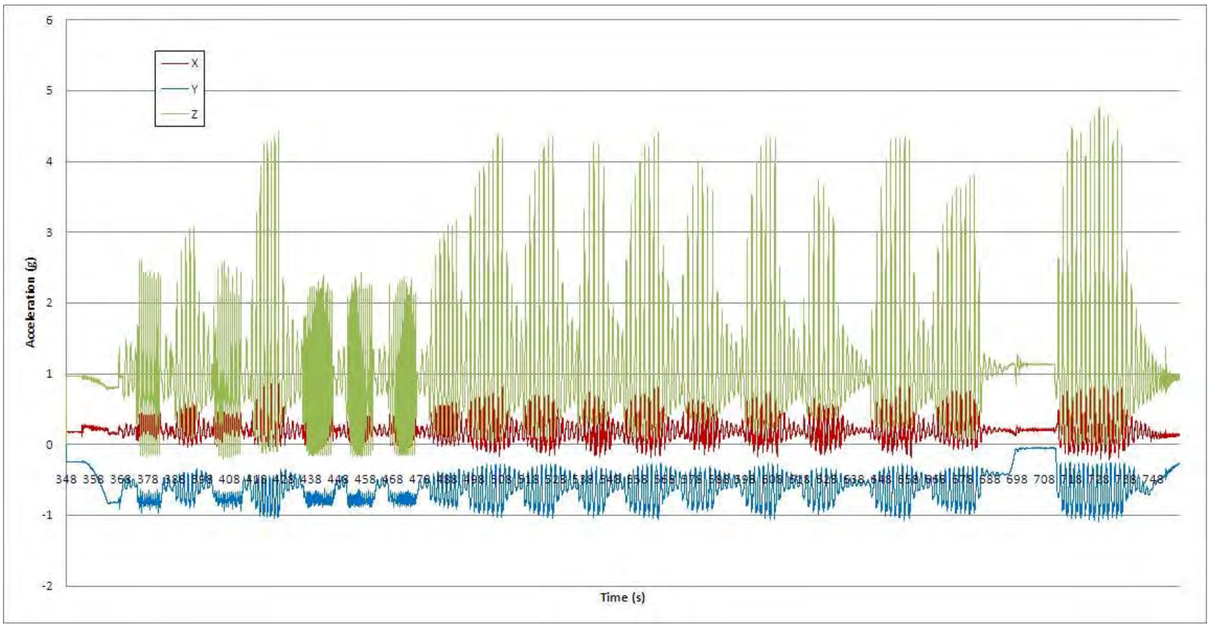

Figure 77 Test run 9 Full

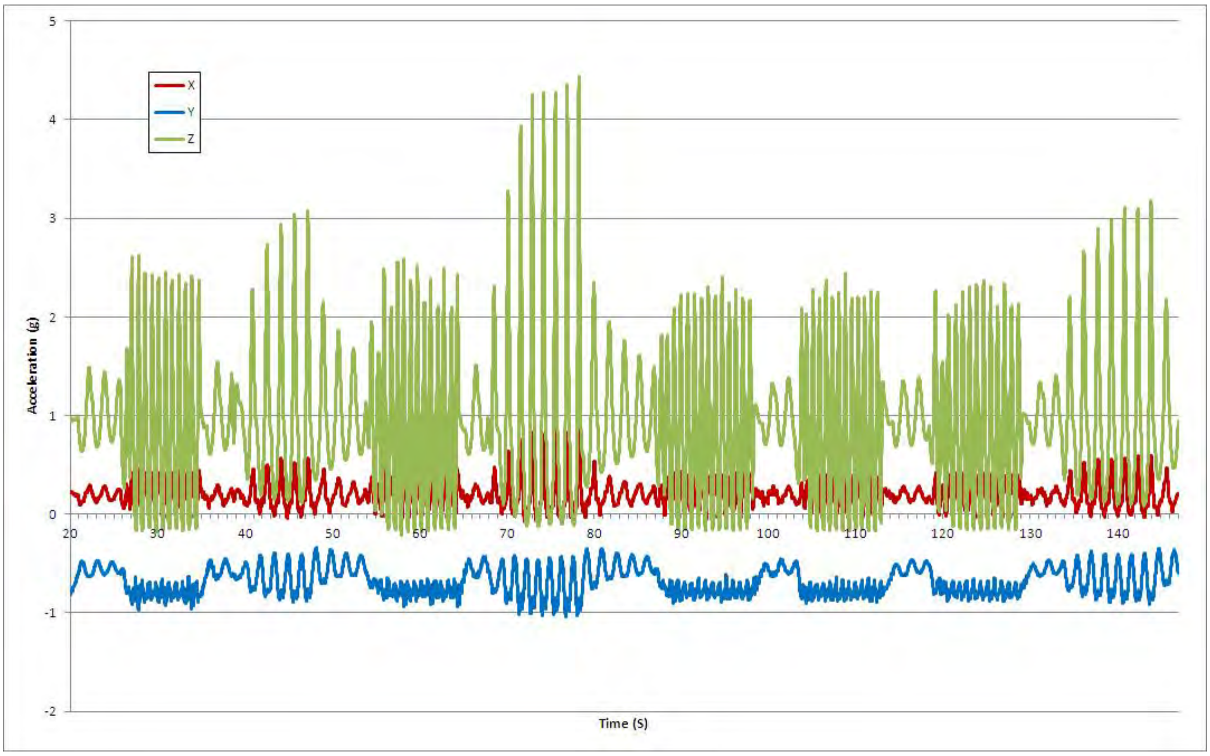

Figure 78 Test run 9, Program 1

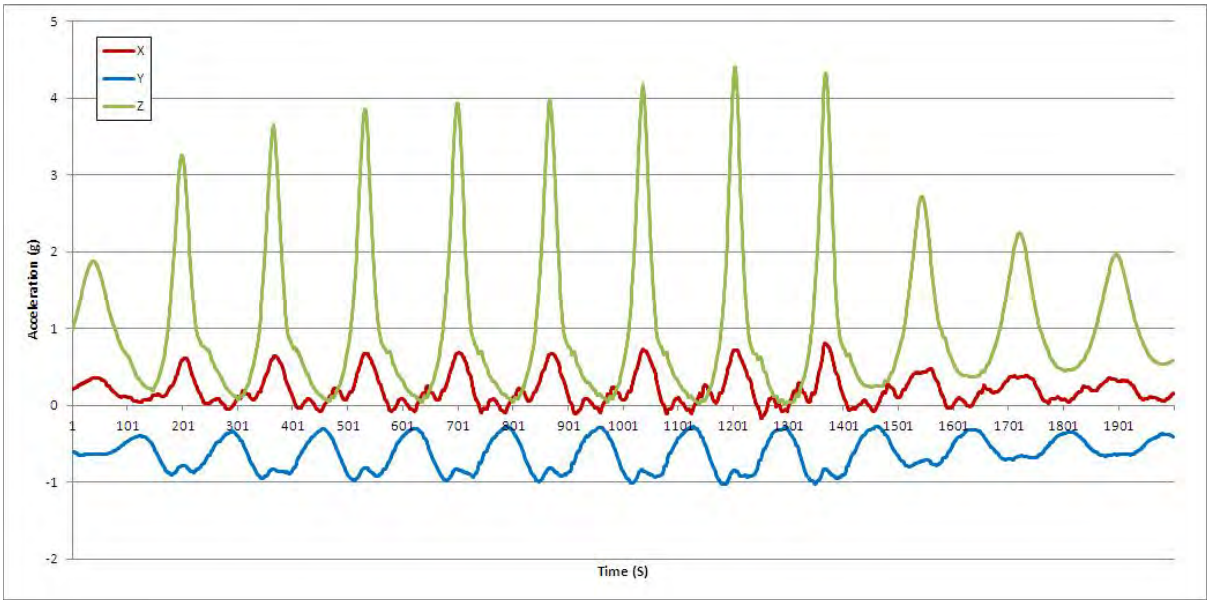

Figure 79 Test run 9, Program 1, Foot pedal

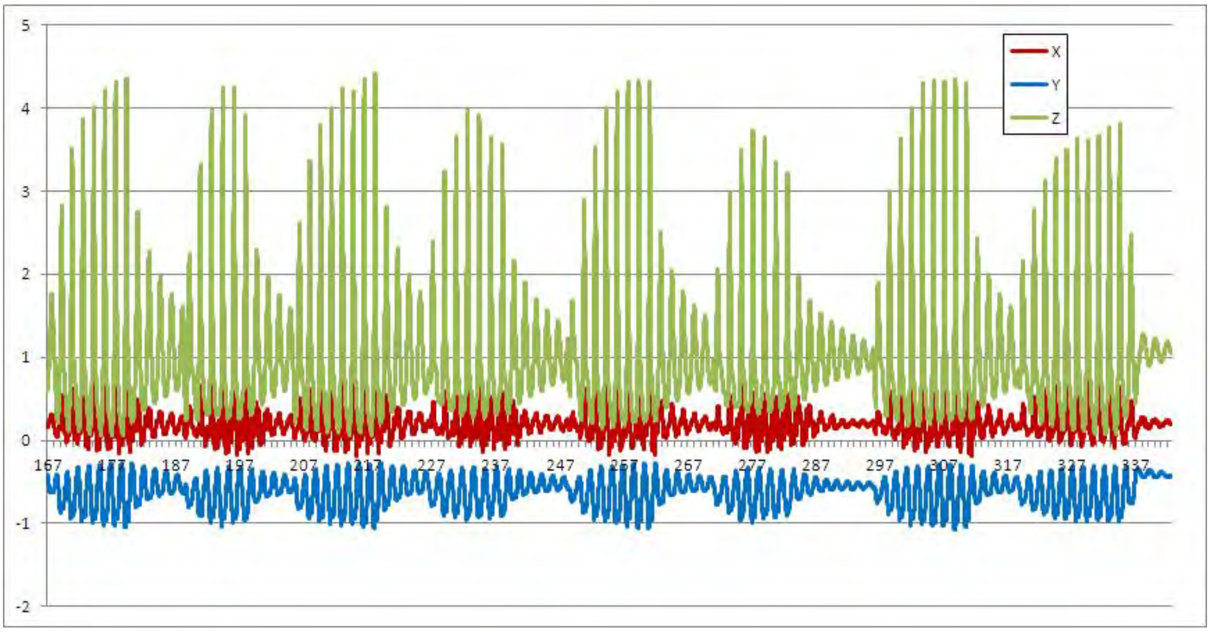

Figure 80 Test run 9, Program 2

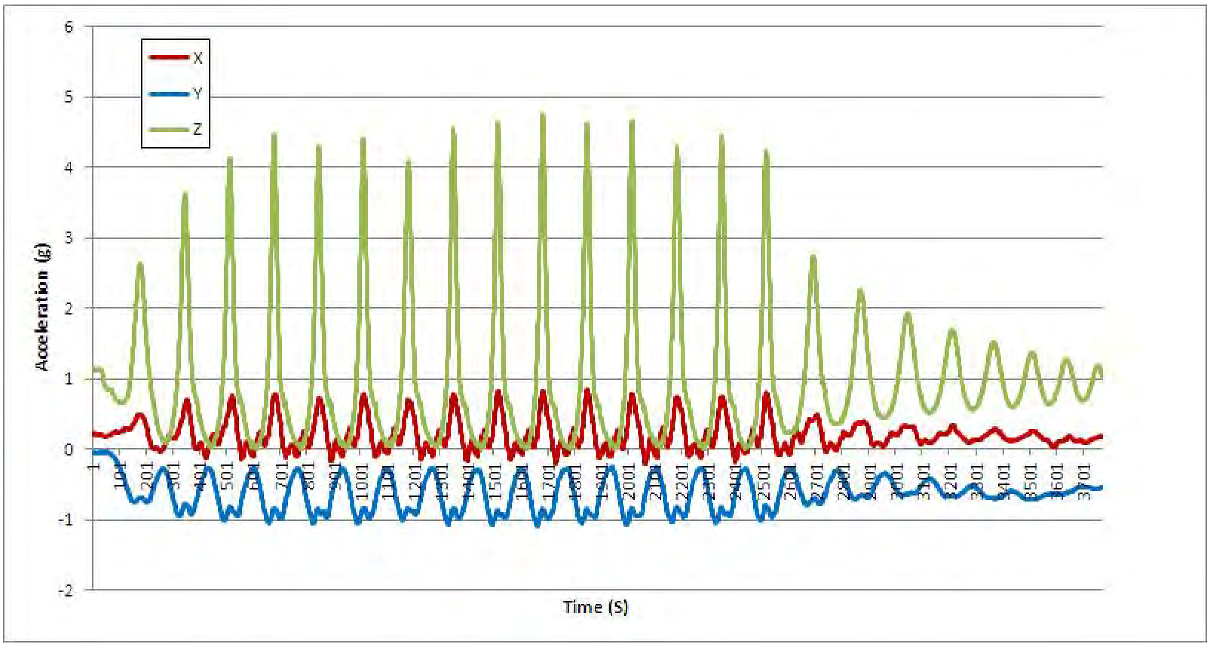

Figure 81 Test run 9, Program 2, Foot pedal

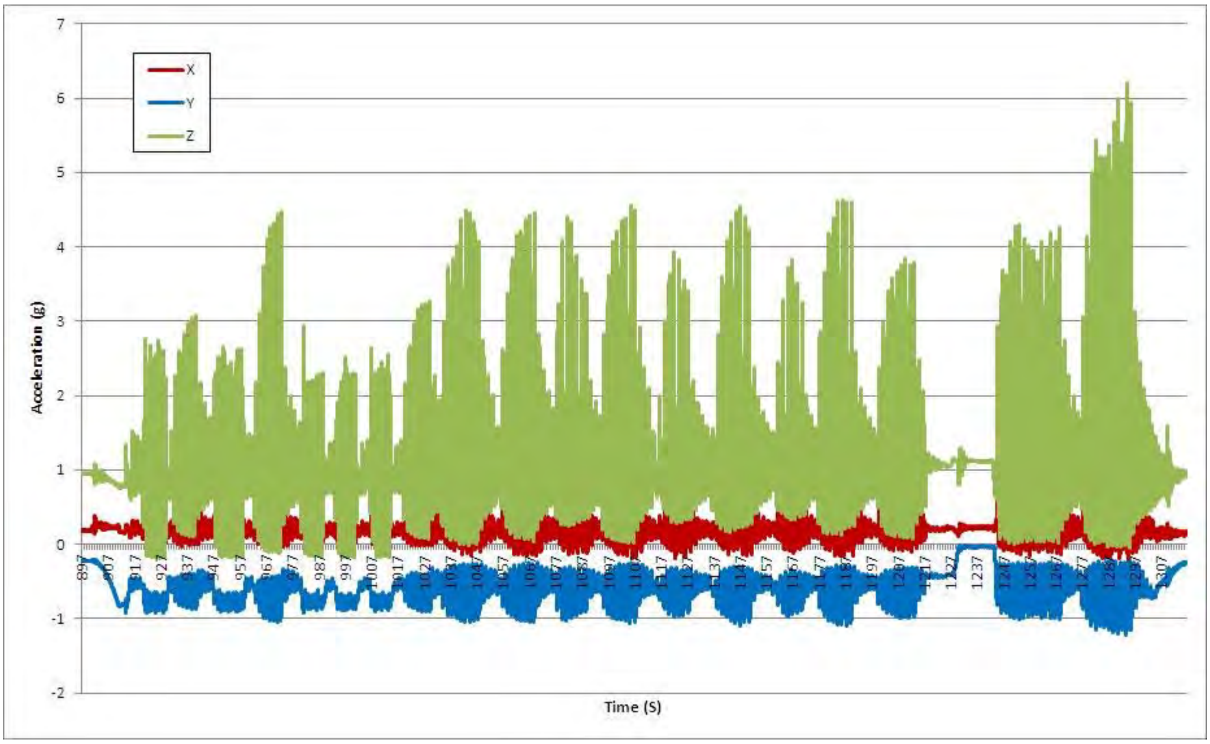

Figure 82 Test run 10 Full

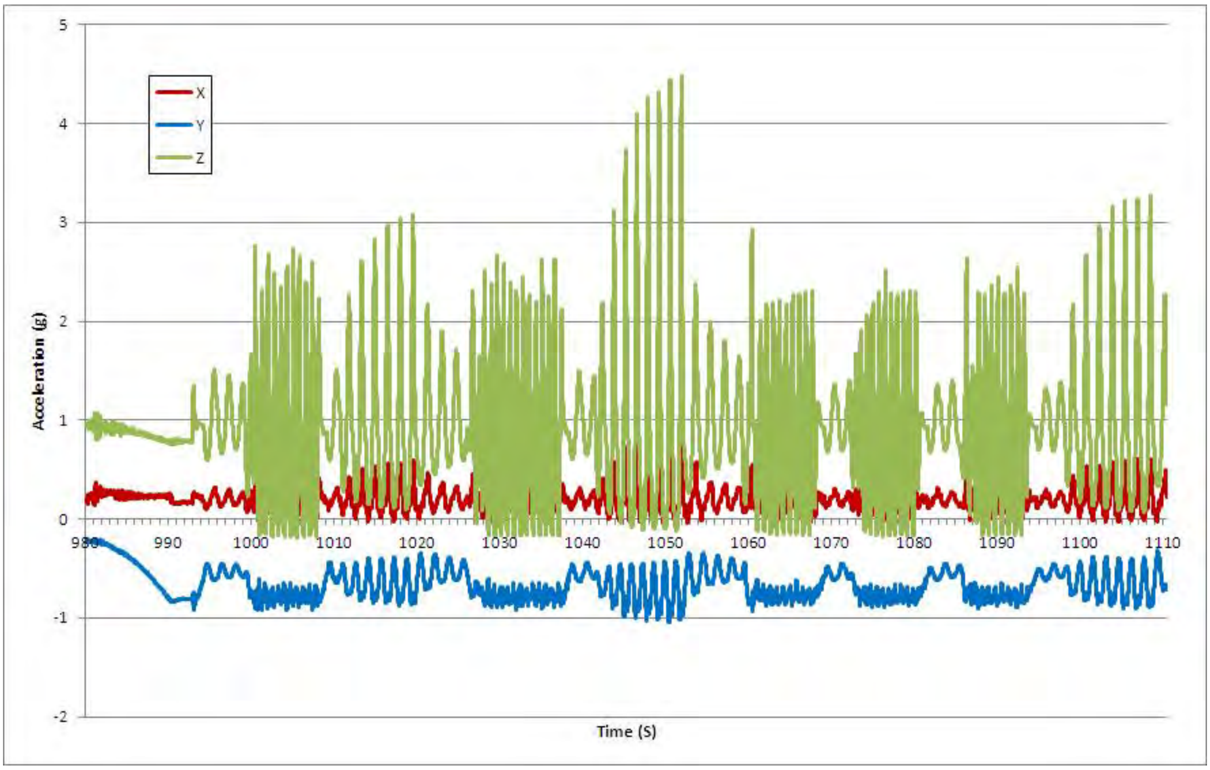

Figure 83 Test run 10, Program 1

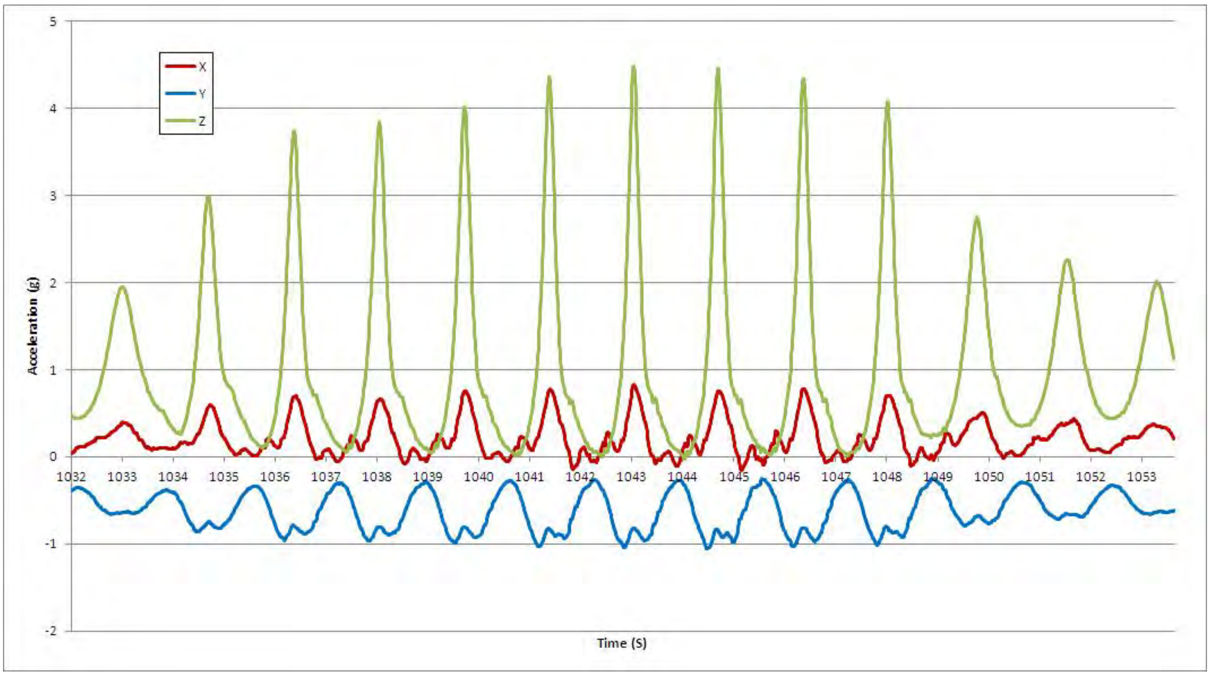

Figure 84 Test run 10, Program 1, Foot pedal

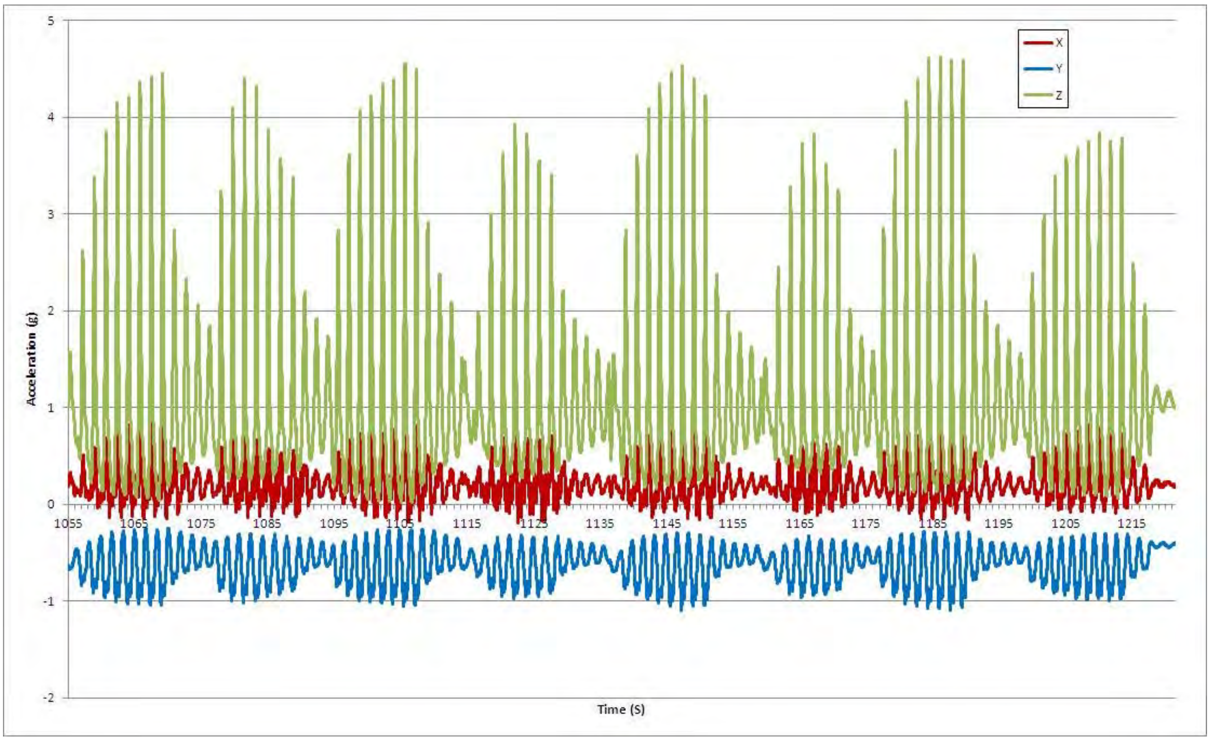

Figure 85 Test run 10, Program 2

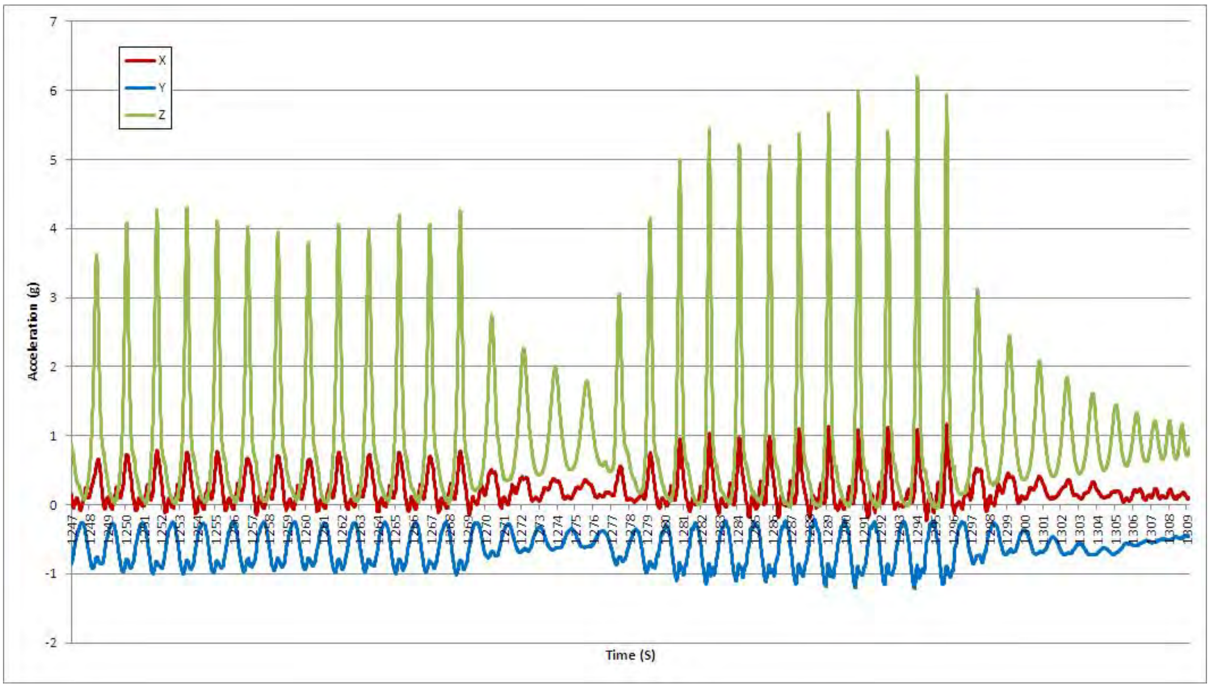

Figure 86 Test run 10, Program 2, Foot pedal

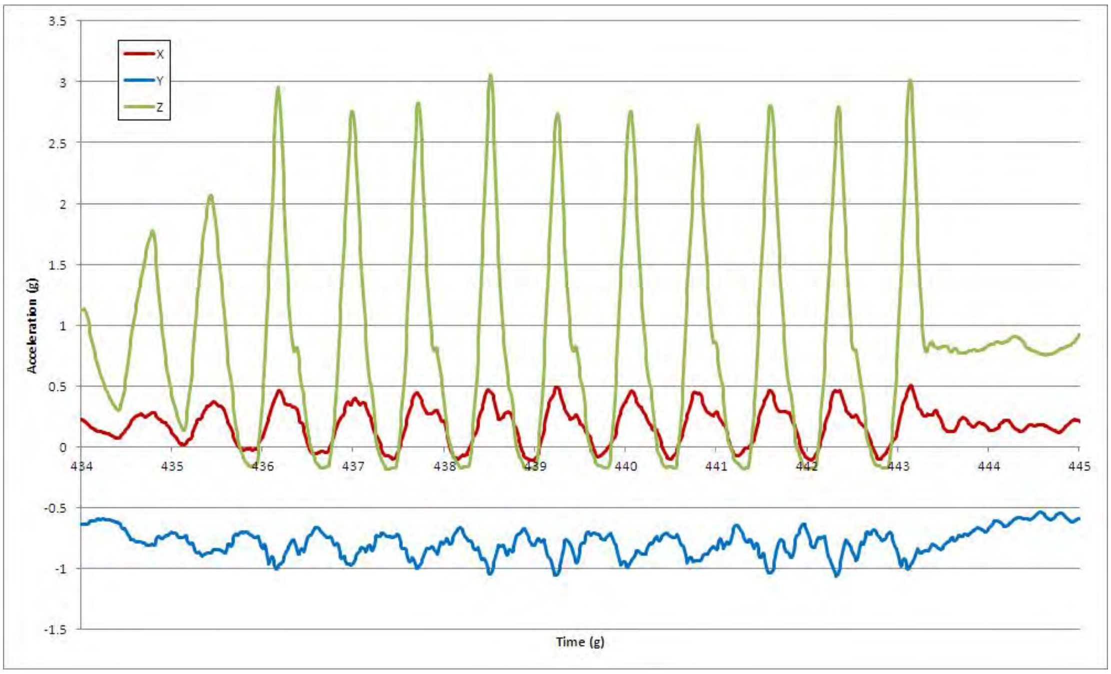

Figure 87 Test run 11, Prog 1, A

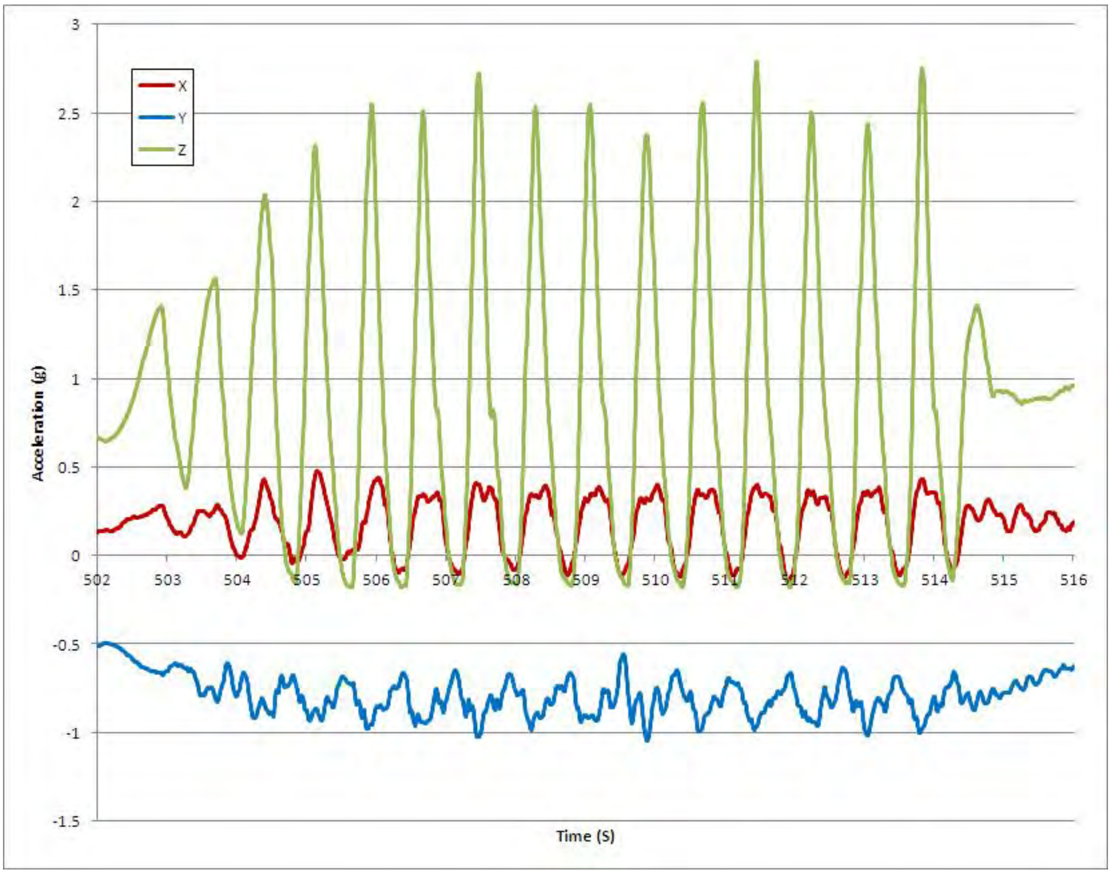

Figure 88 Test run 11, Prog 1, AA

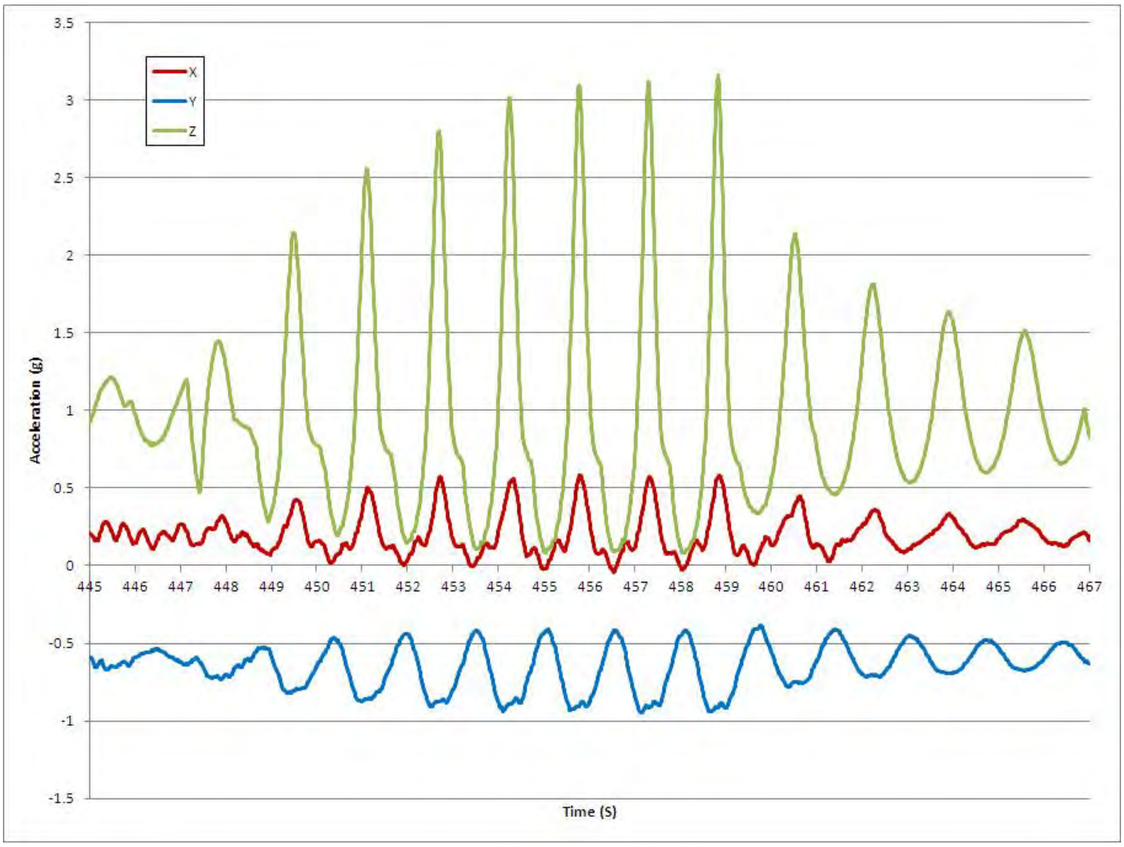

Figure 89 Test run 11, Prog 1, B

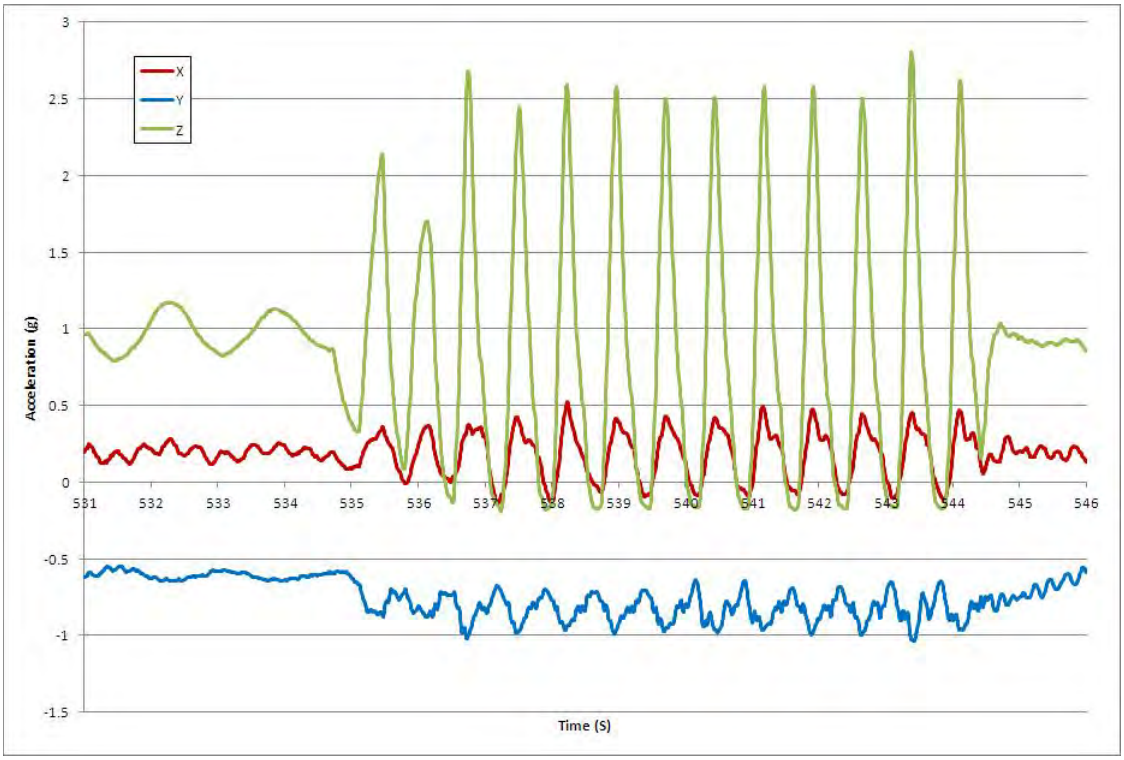

Figure 90 Test run 11, Prog 1, BB

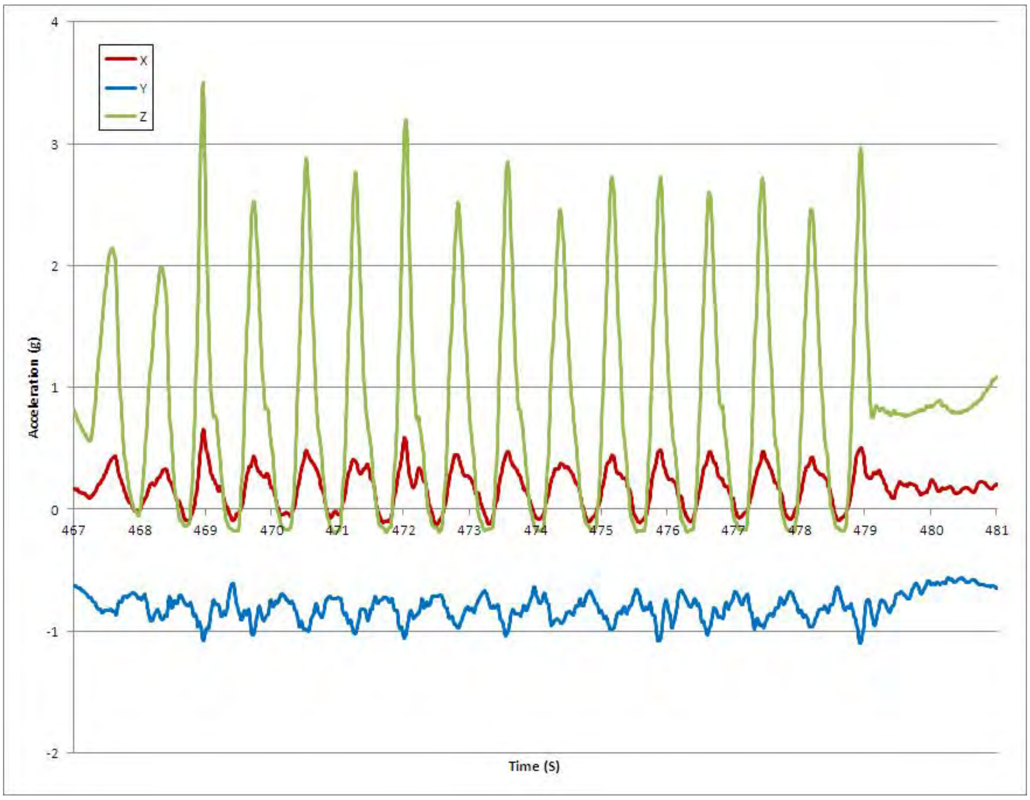

Figure 91 Test run 11, Prog 1, C

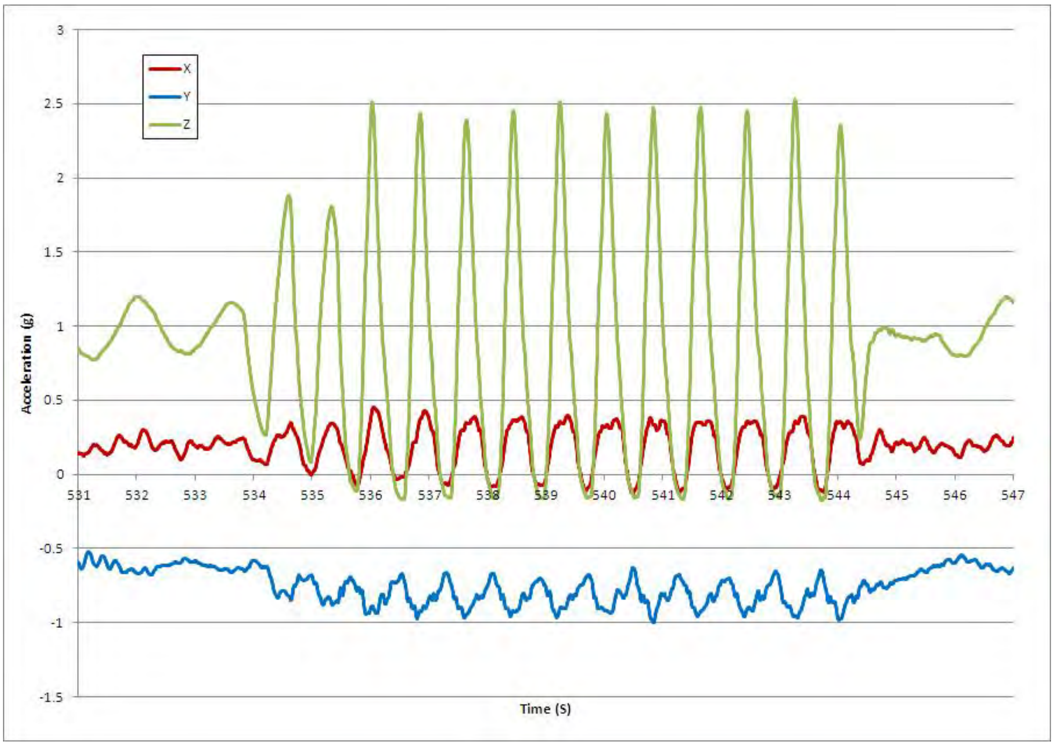

Figure 92 Test run 11, Prog 1, CC

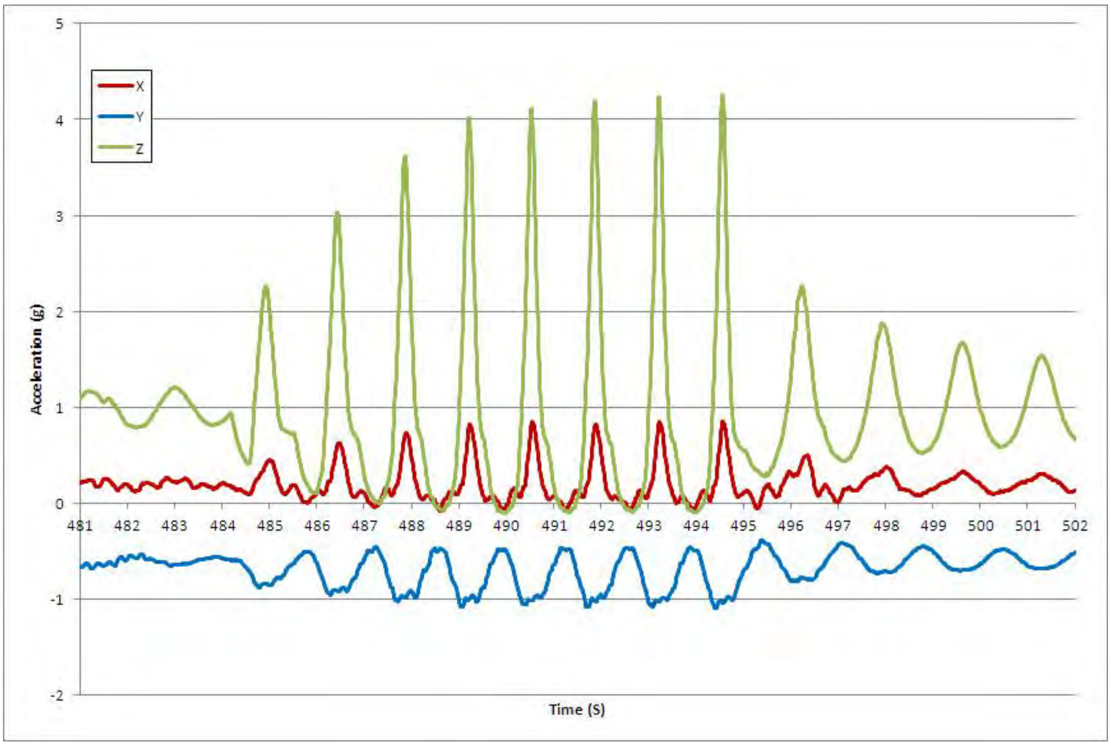

Figure 93 Test run 11, Prog 1, D

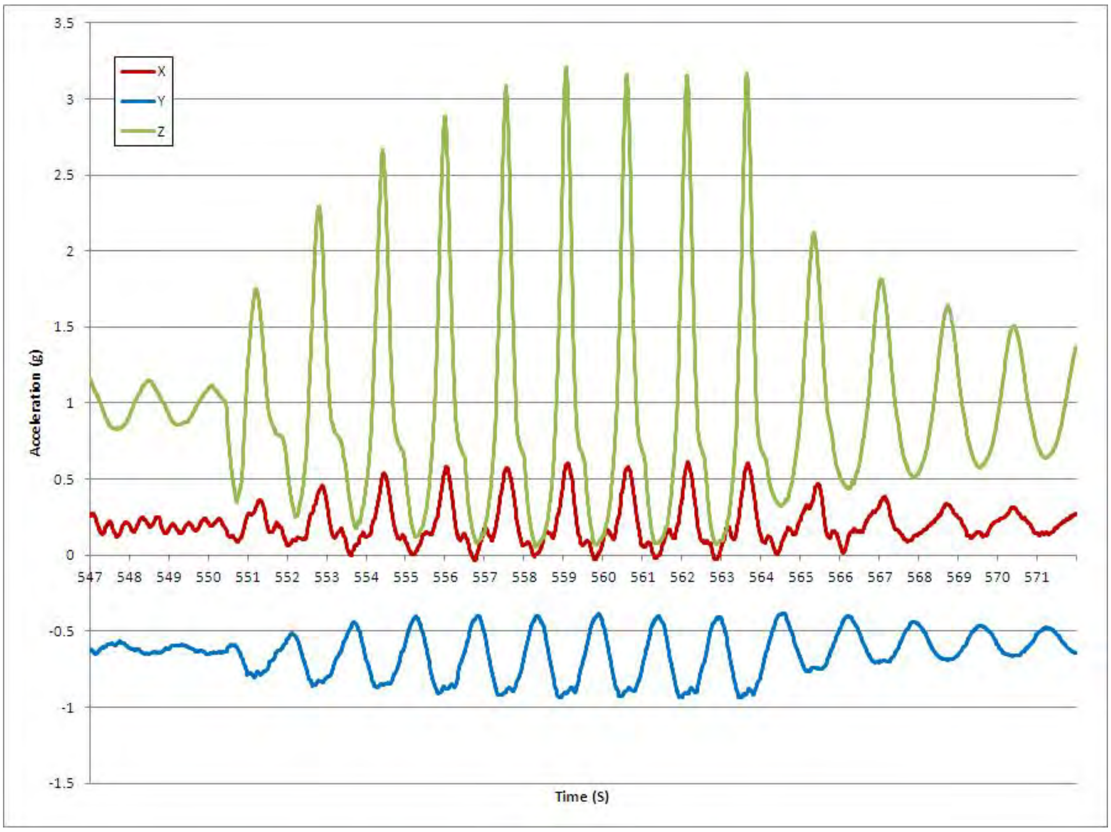

Figure 94 Test run 11, Prog 1, DD

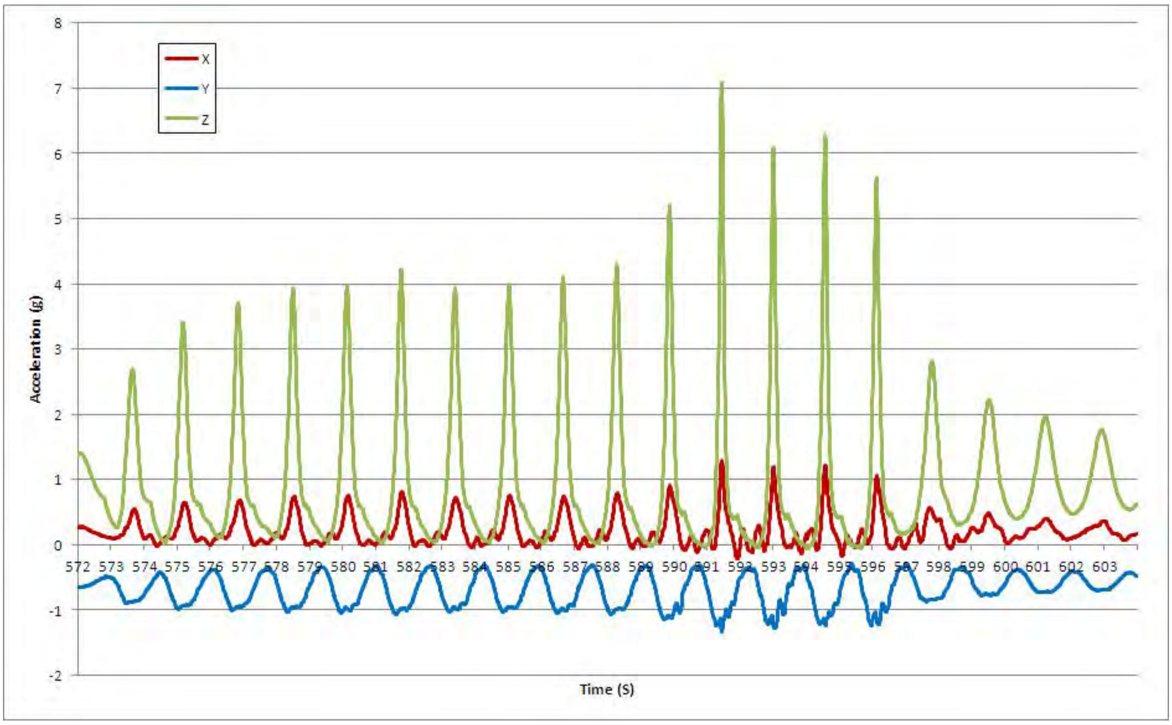

Figure 95 Test run 11, Prog 1, Foot pedal

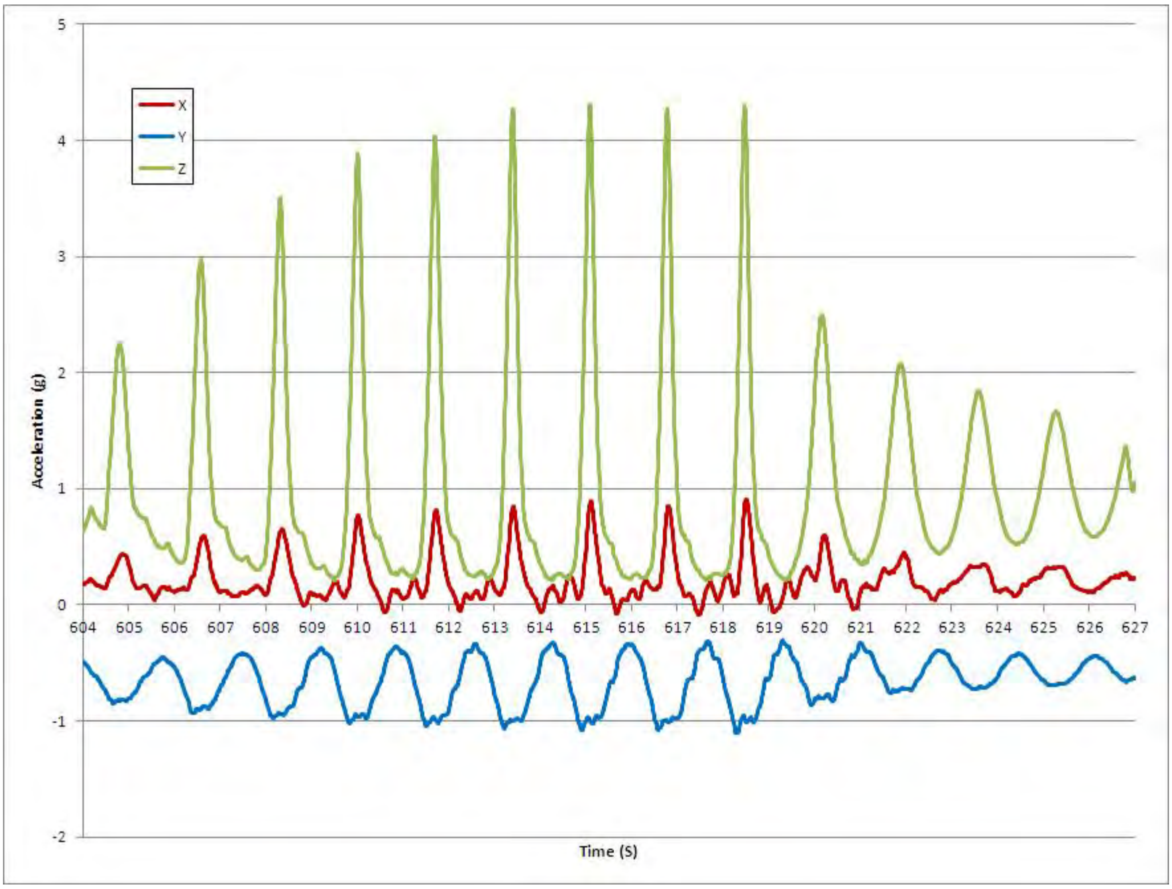

Figure 96 Test run 11, Program 2, A

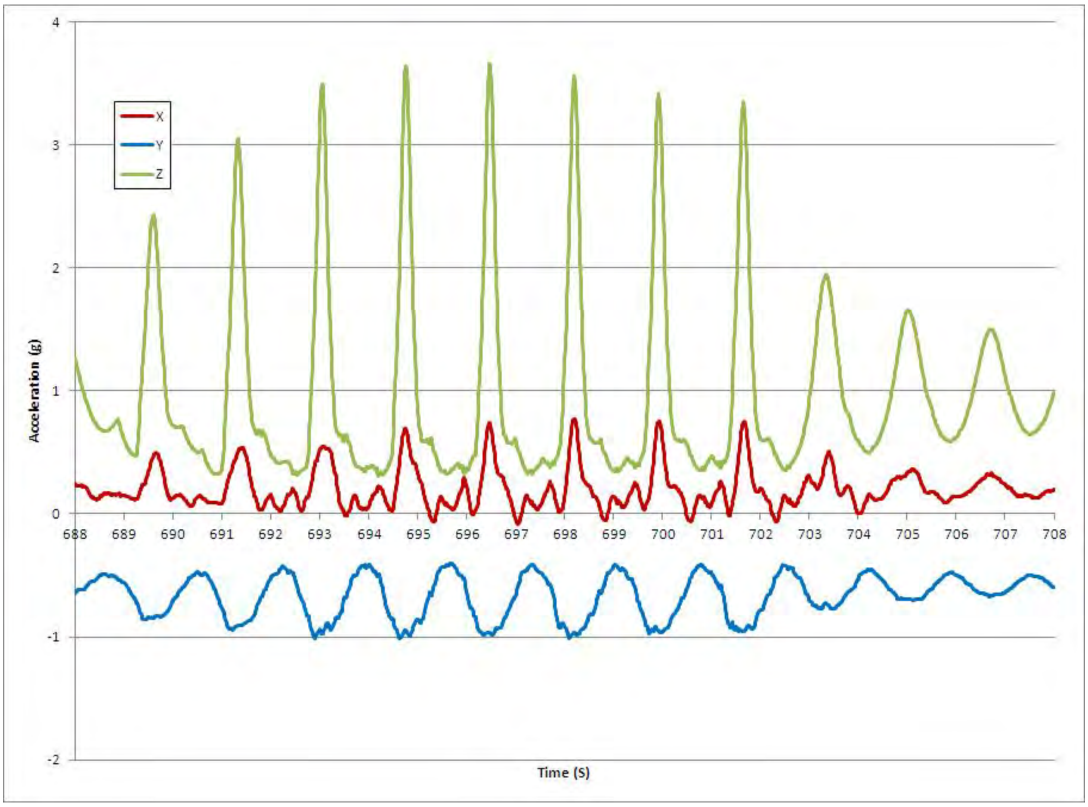

Figure 97 Test run 11, Program 2, AA

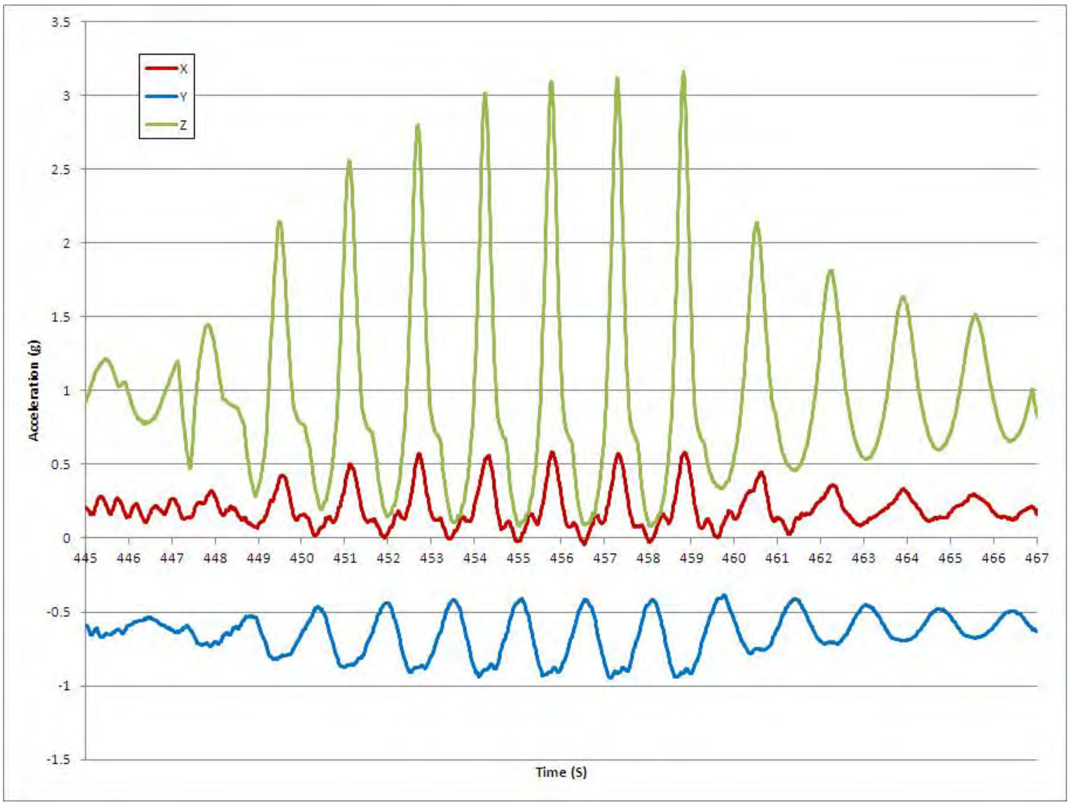

Figure 98 Test run 11, Program 2, B

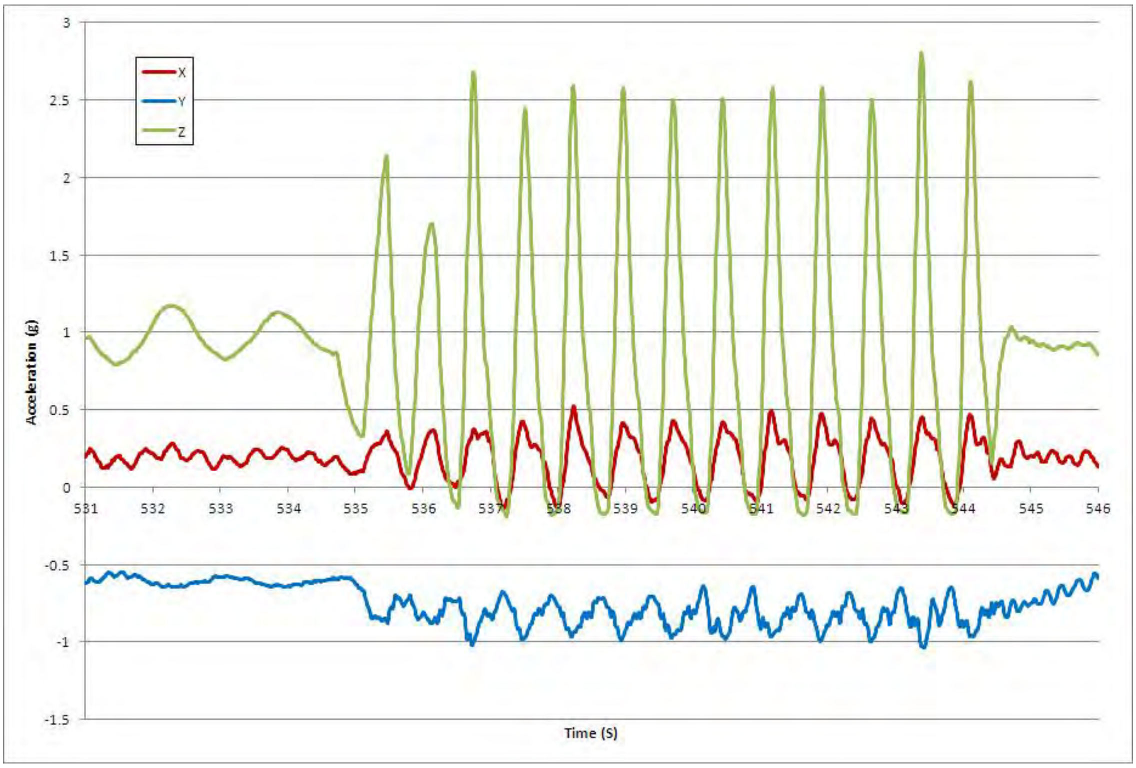

Figure 99 Test run 11, Program 2, BB

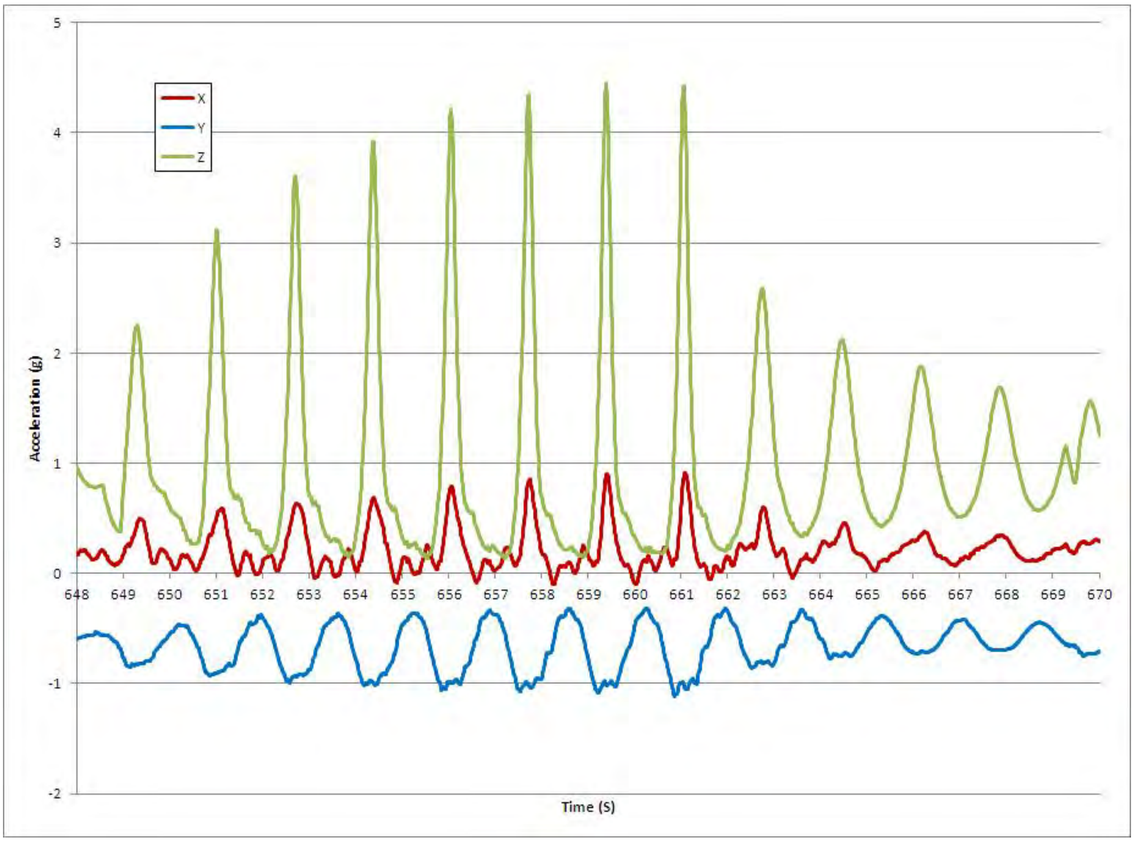

Figure 100 Test run 11, Program 2, C

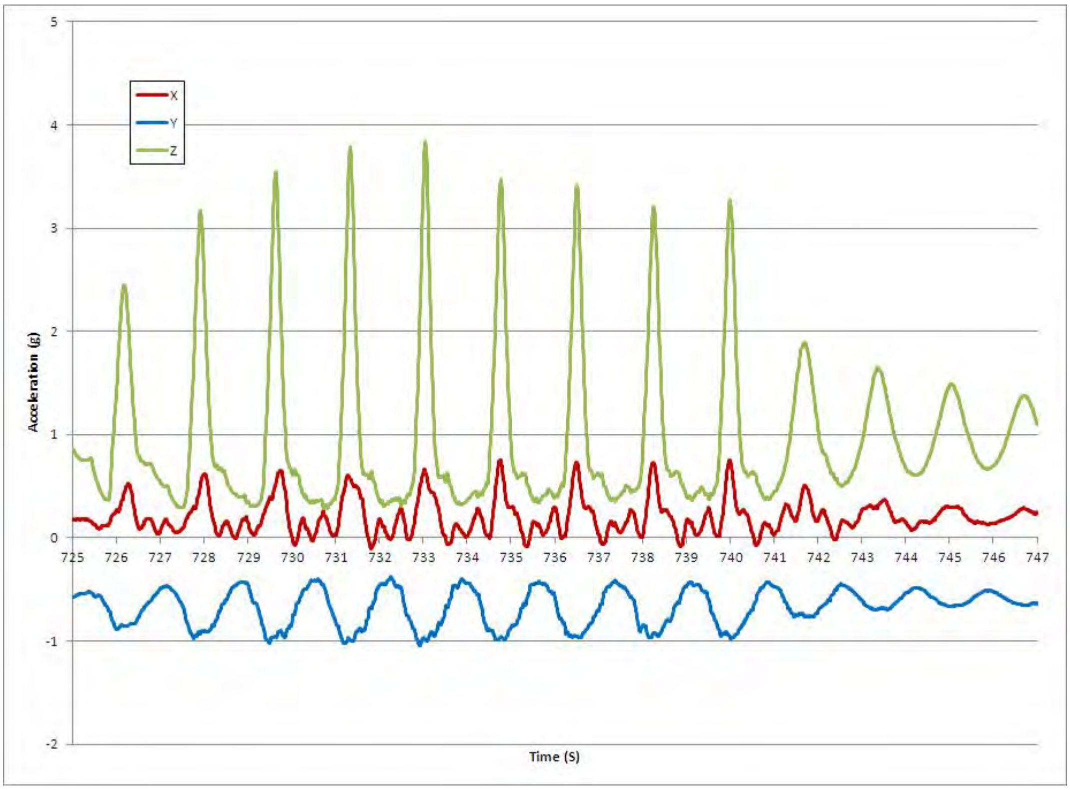

Figure 101 Test run 11, Program 2, CC

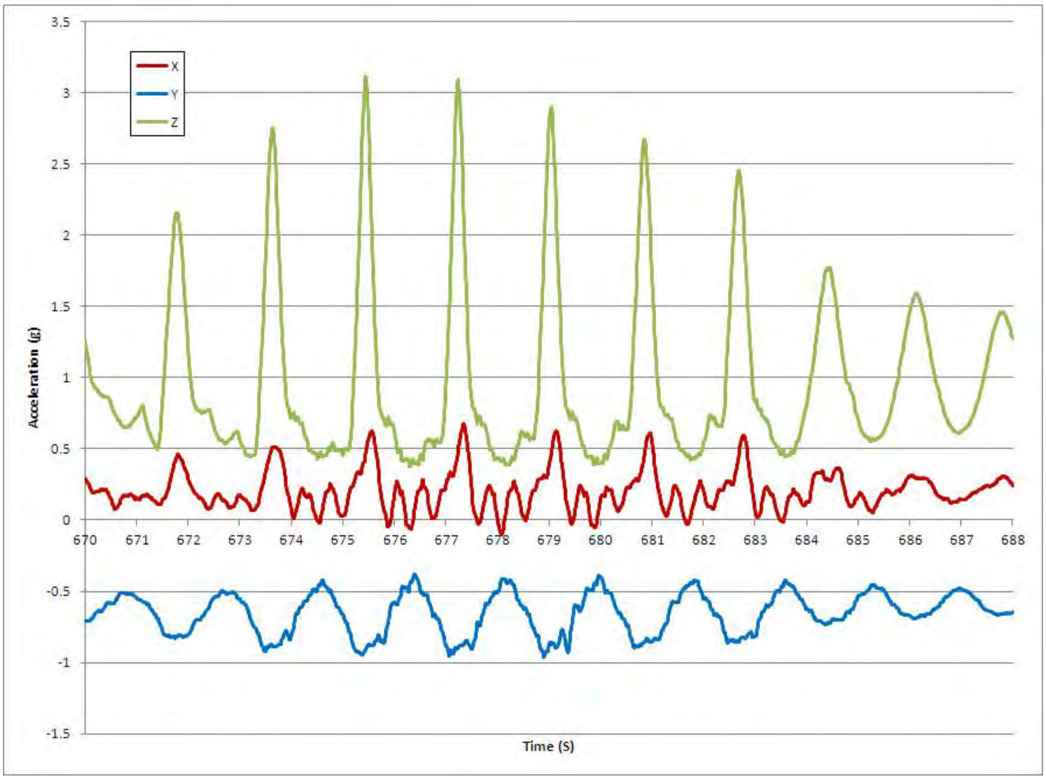

Figure 102 Test run 11, Program 2, D

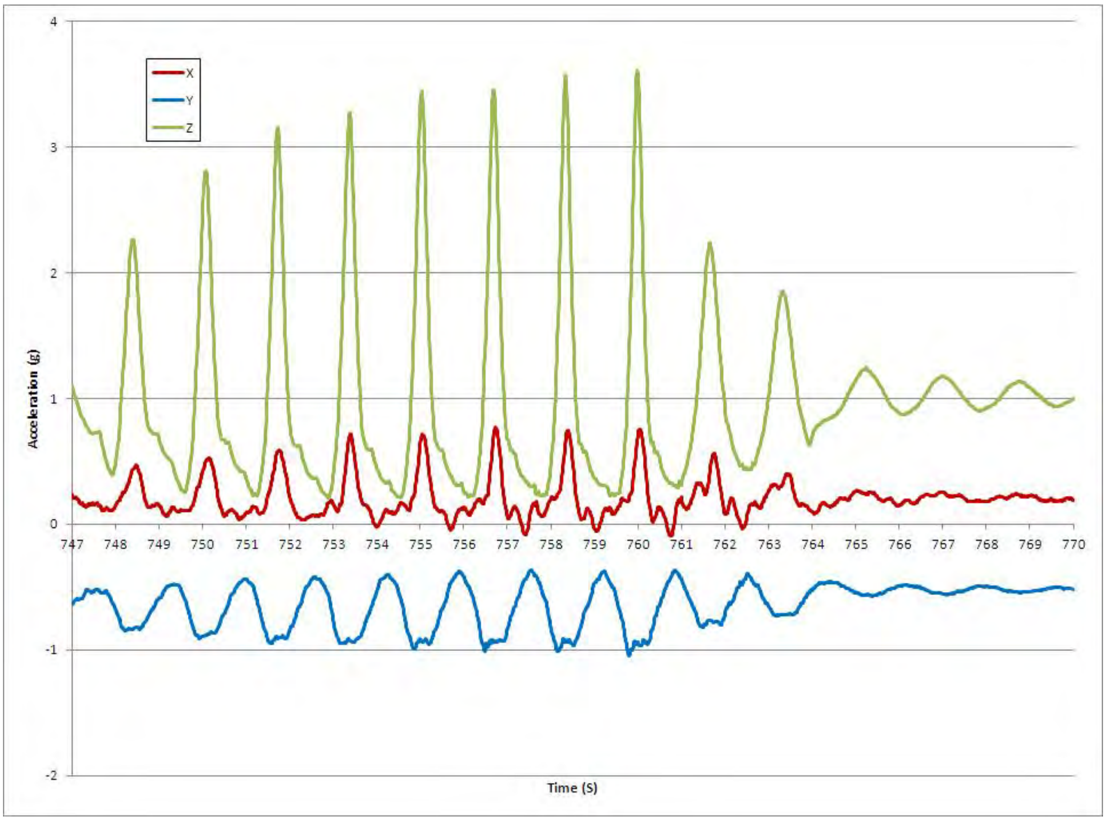

Figure 103 Test run 11, Program 2, DD

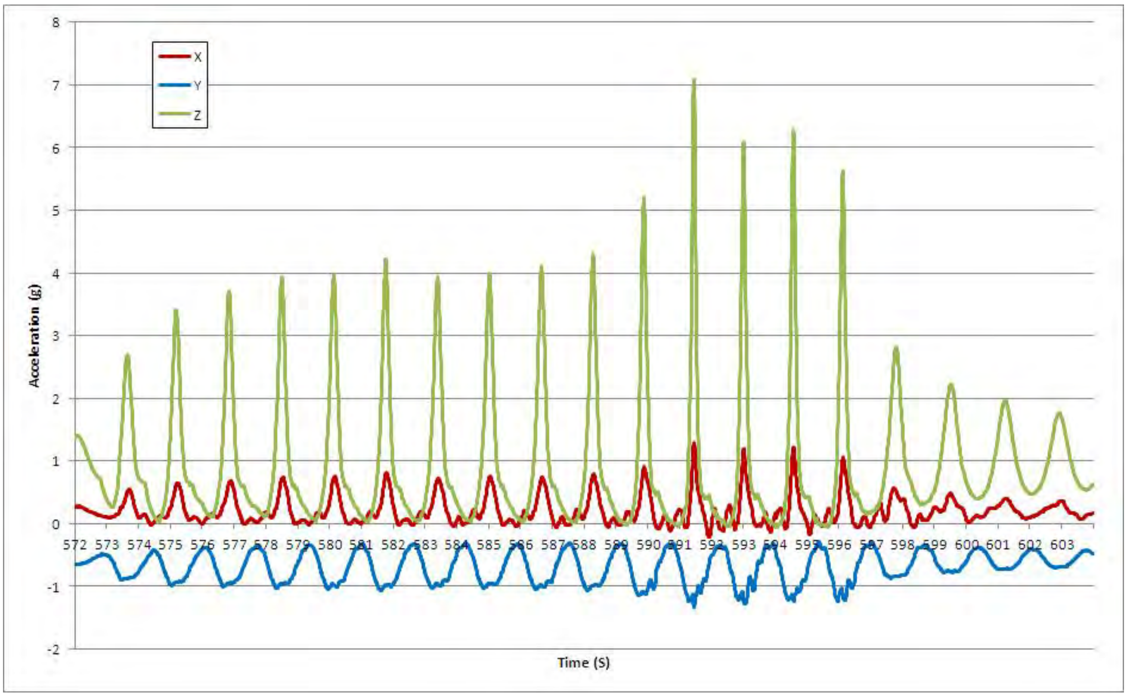

Figure 104 Test run 11, Program 2, Foot pedal

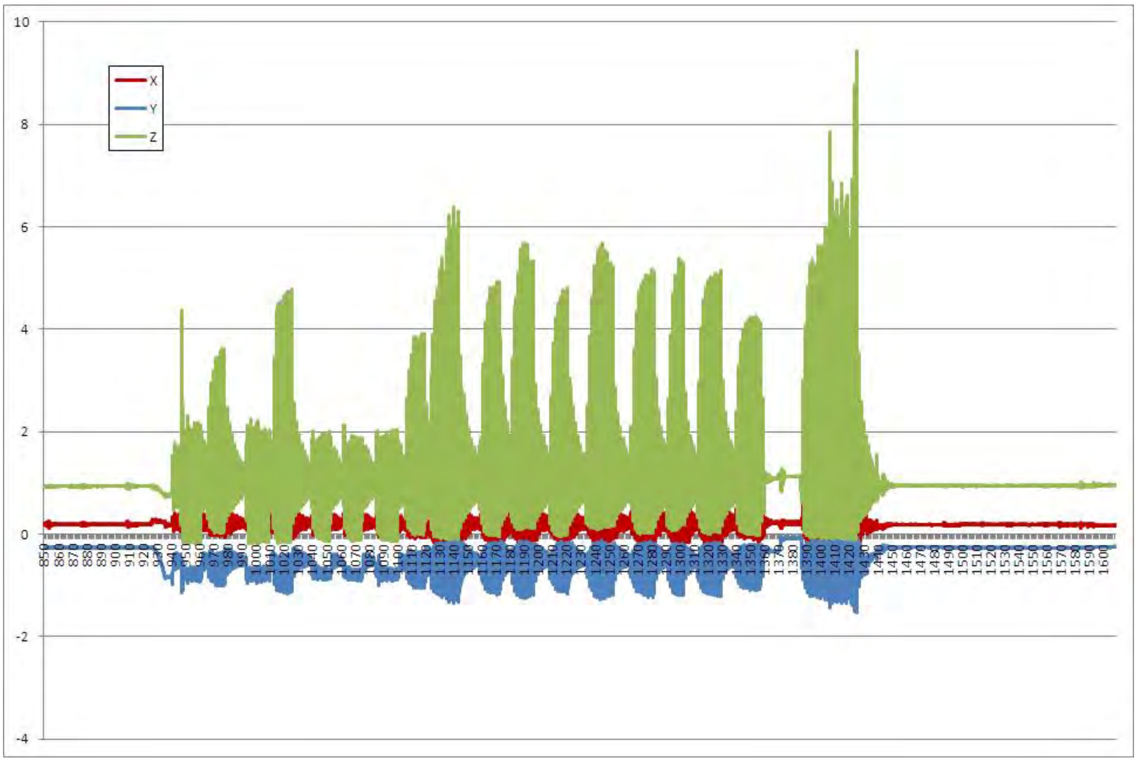

Figure 105 Test run 12 Full

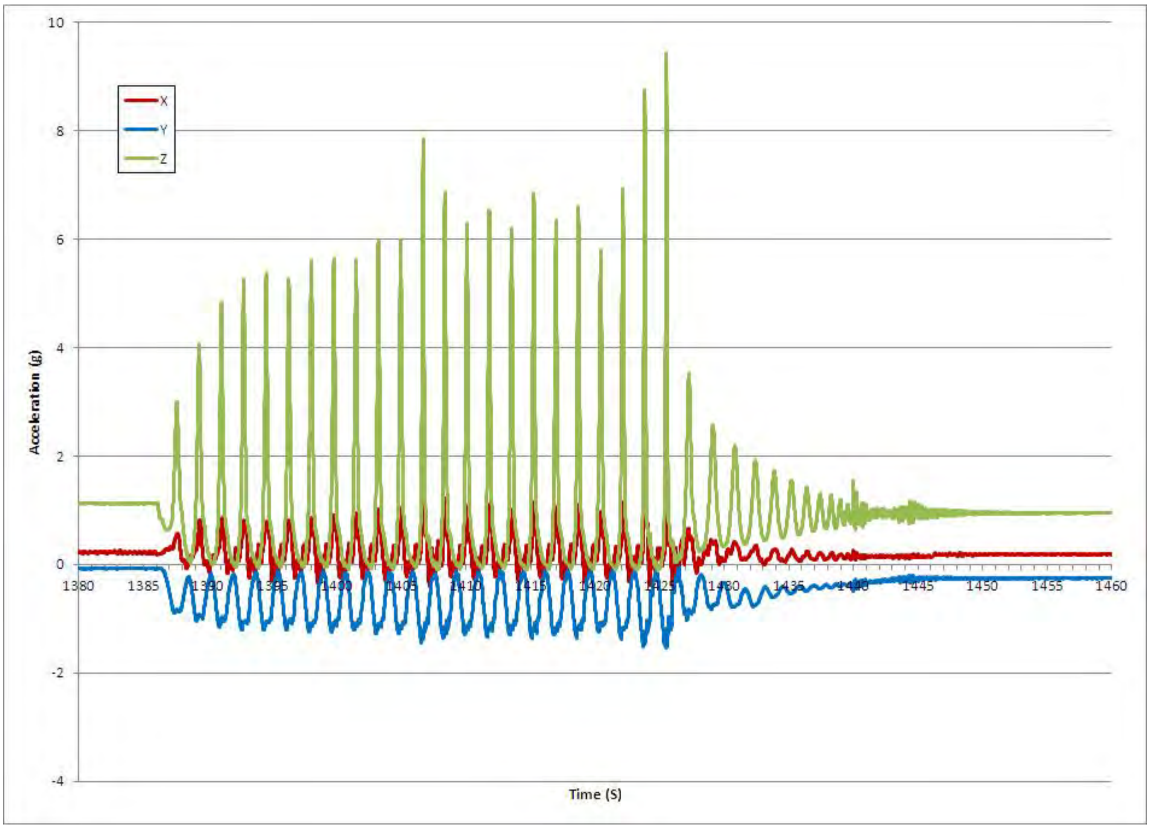

Figure 106 Test run 12, Program 2, Foot pedal

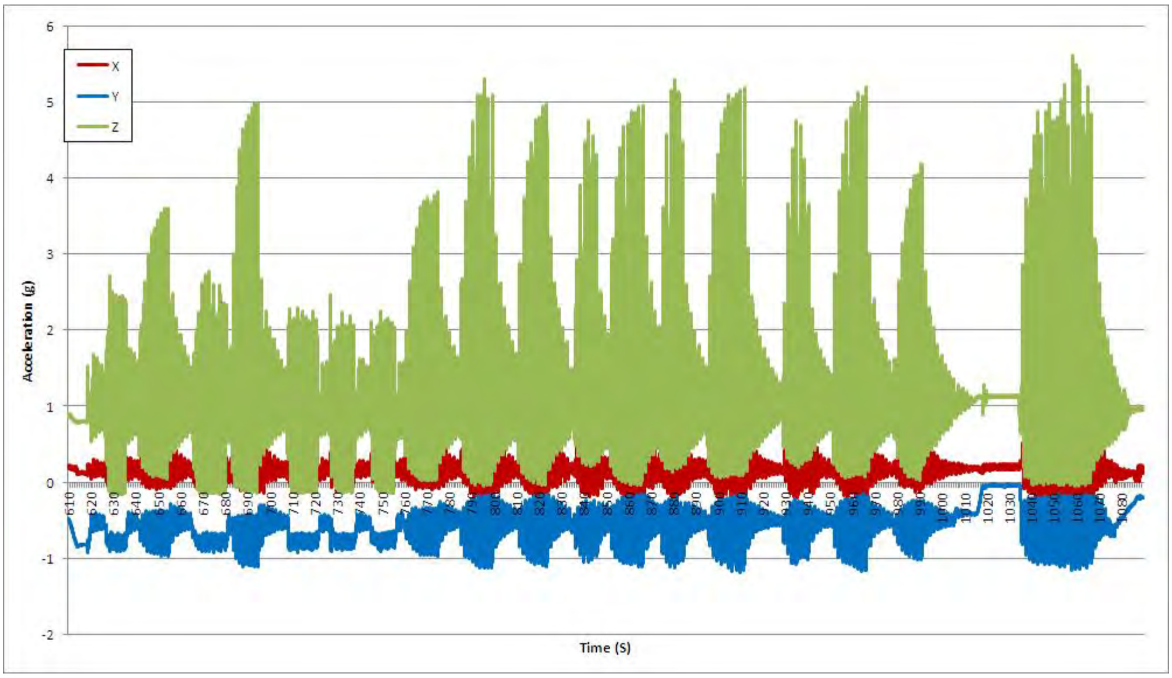

Figure 107 Test run 16 Full

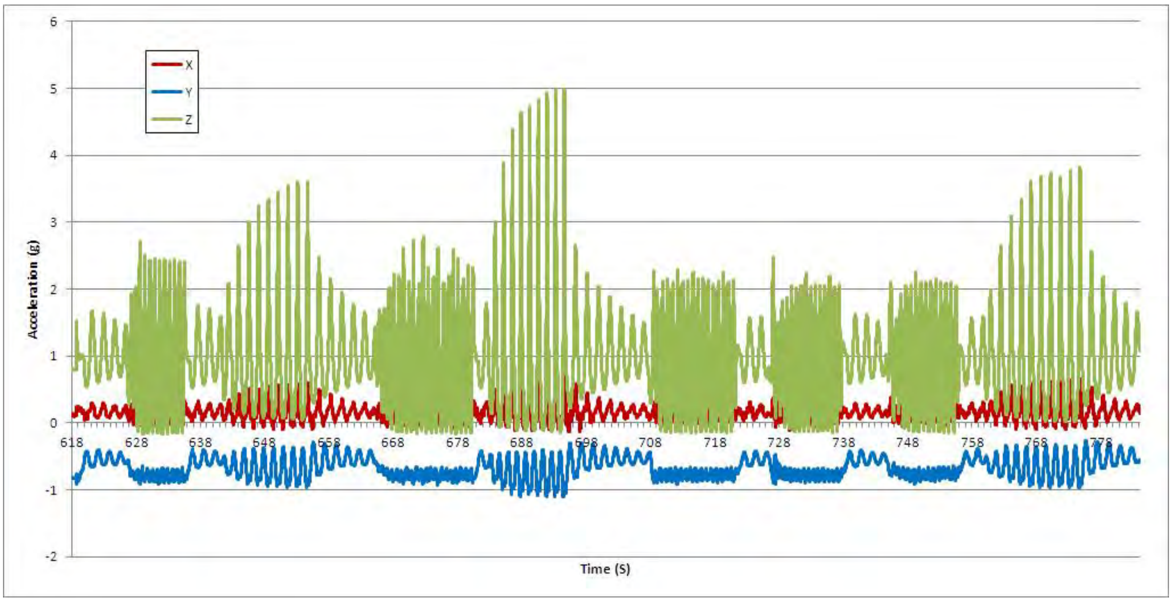

Figure 108 Test run 16, Program 1

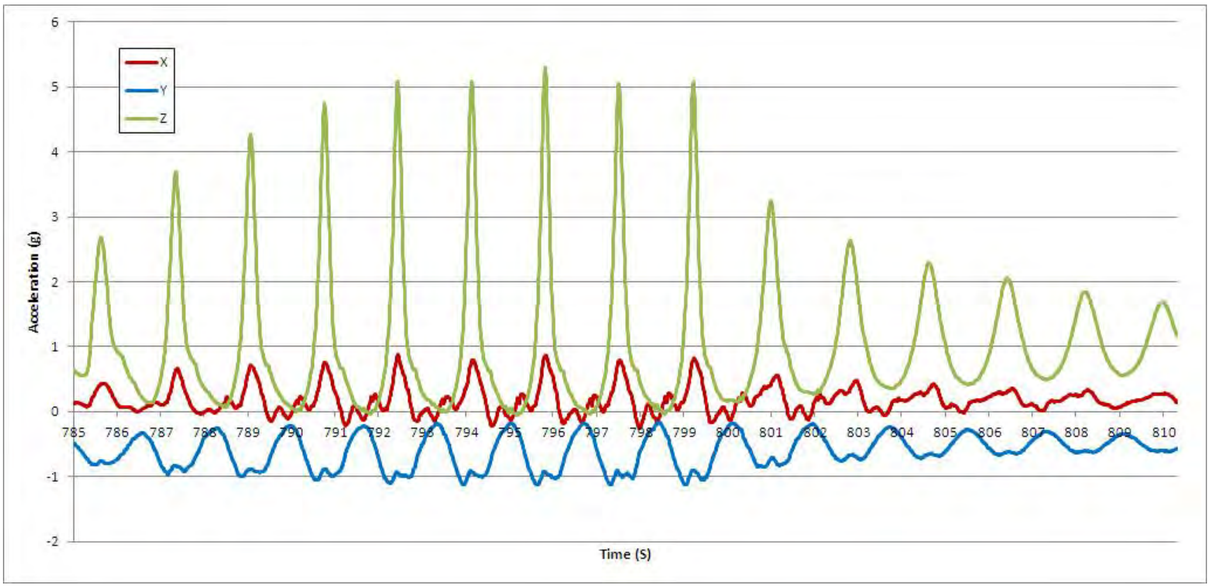

Figure 109 Test run 16, Program 1, Foot pedal

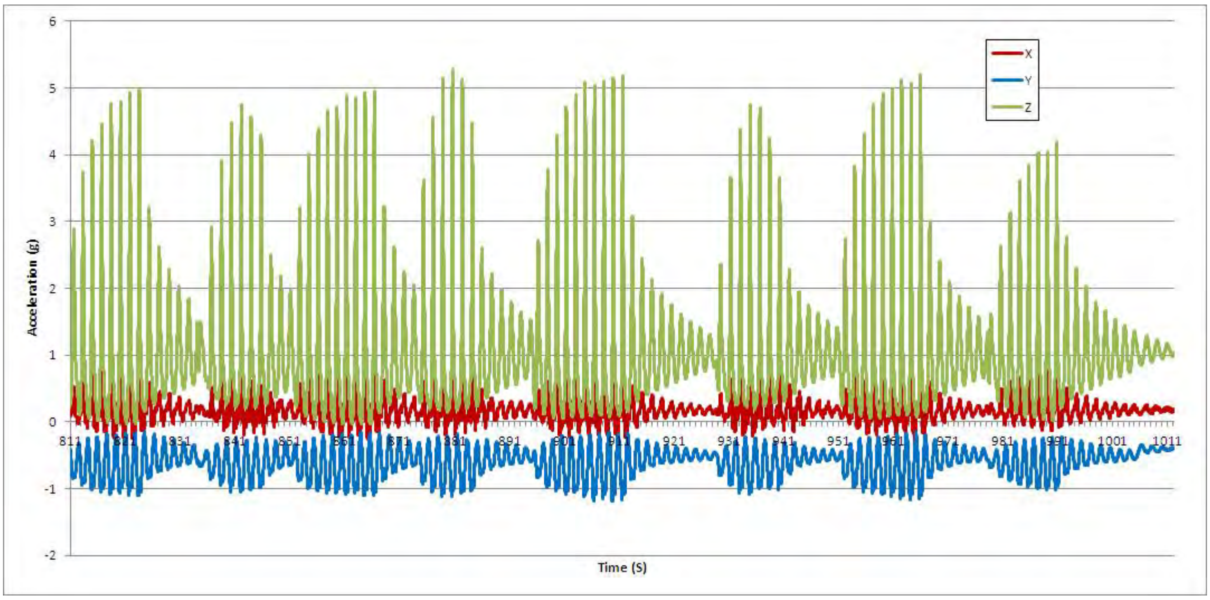

Figure 110 Test run 16, Program 2

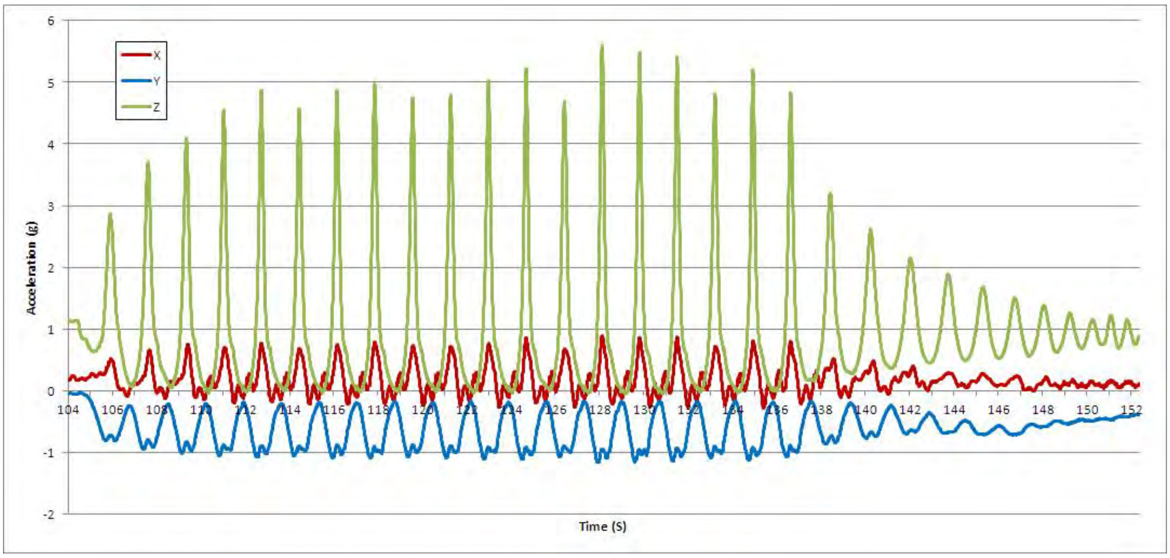

Figure 111 Test run 16, Program 2, Foot pedal

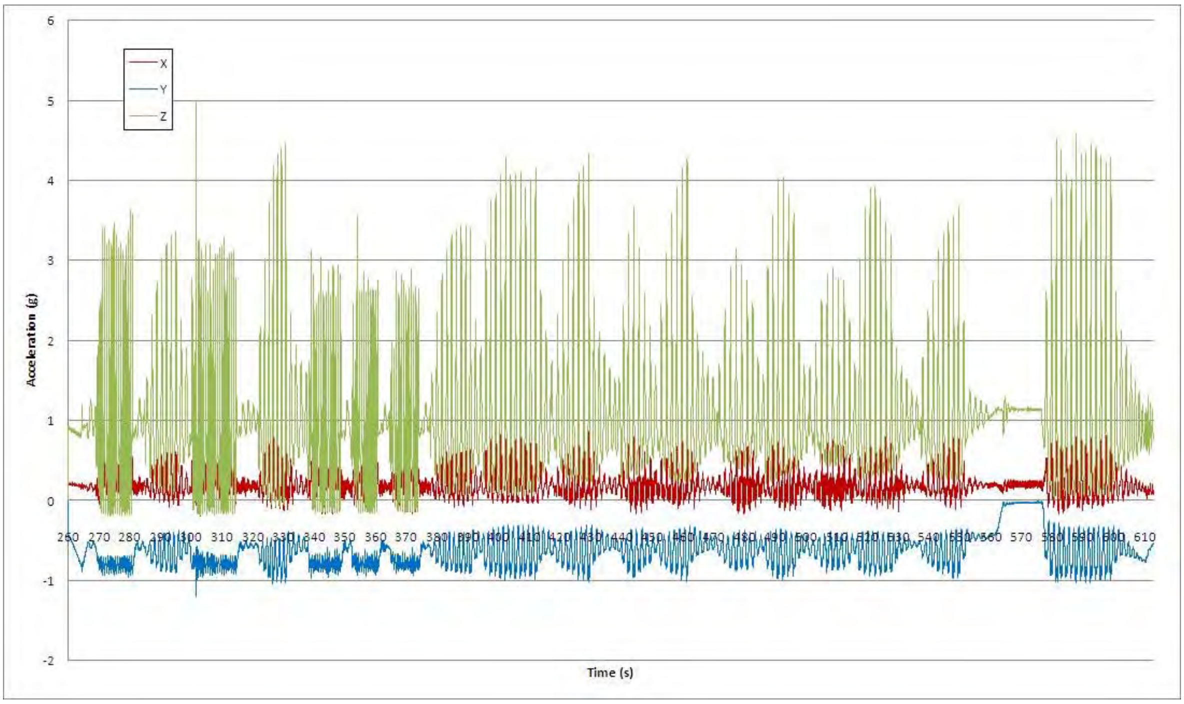

Figure 112 Test run 19 Full

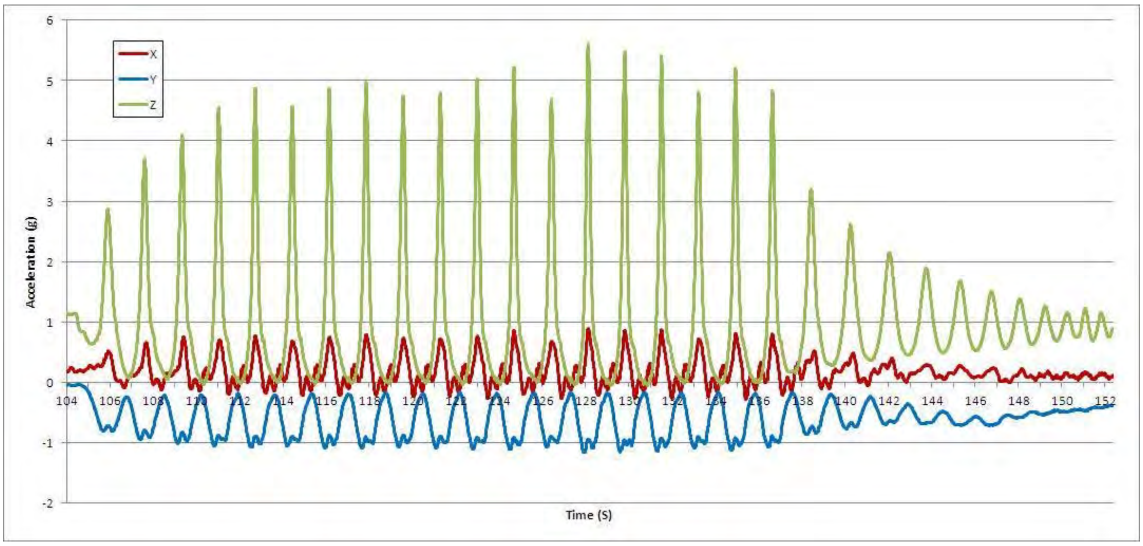

Figure 113 Test run 19, Program 1

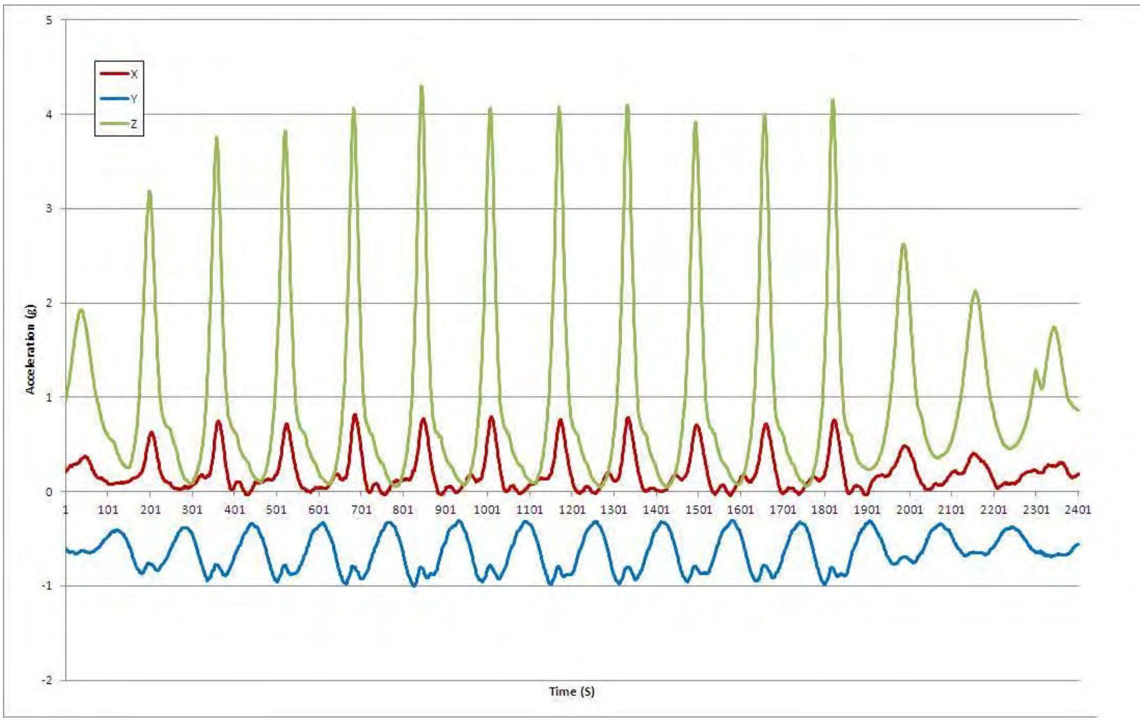

Figure 114 Test run 19, Program 1, Foot pedal

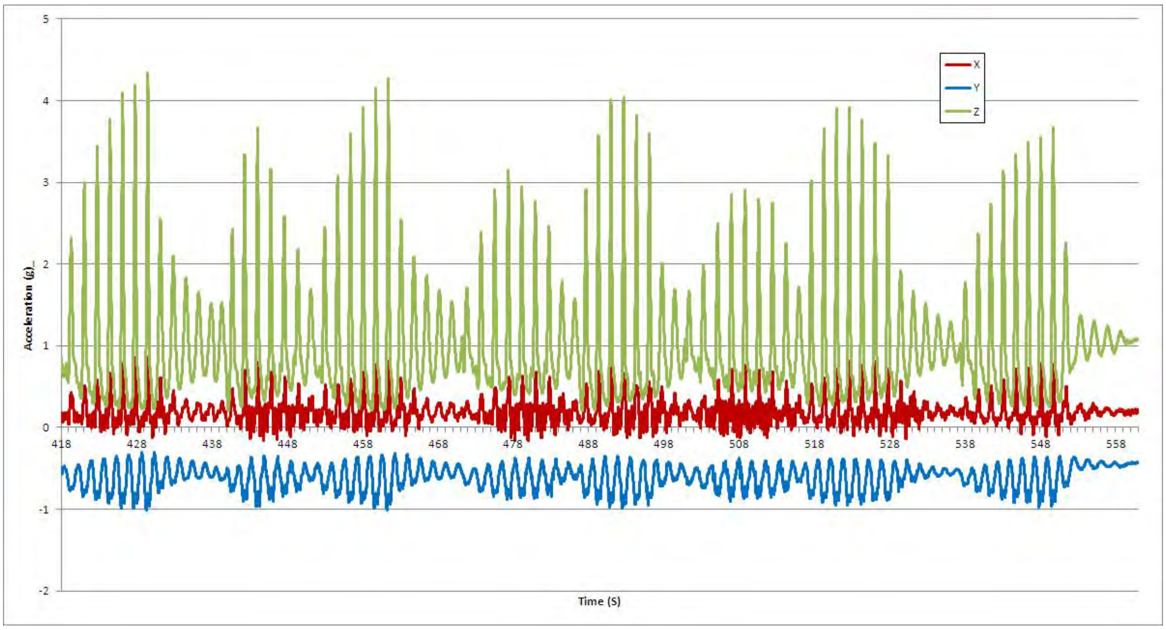

Figure 115 Test run 19, Program 2

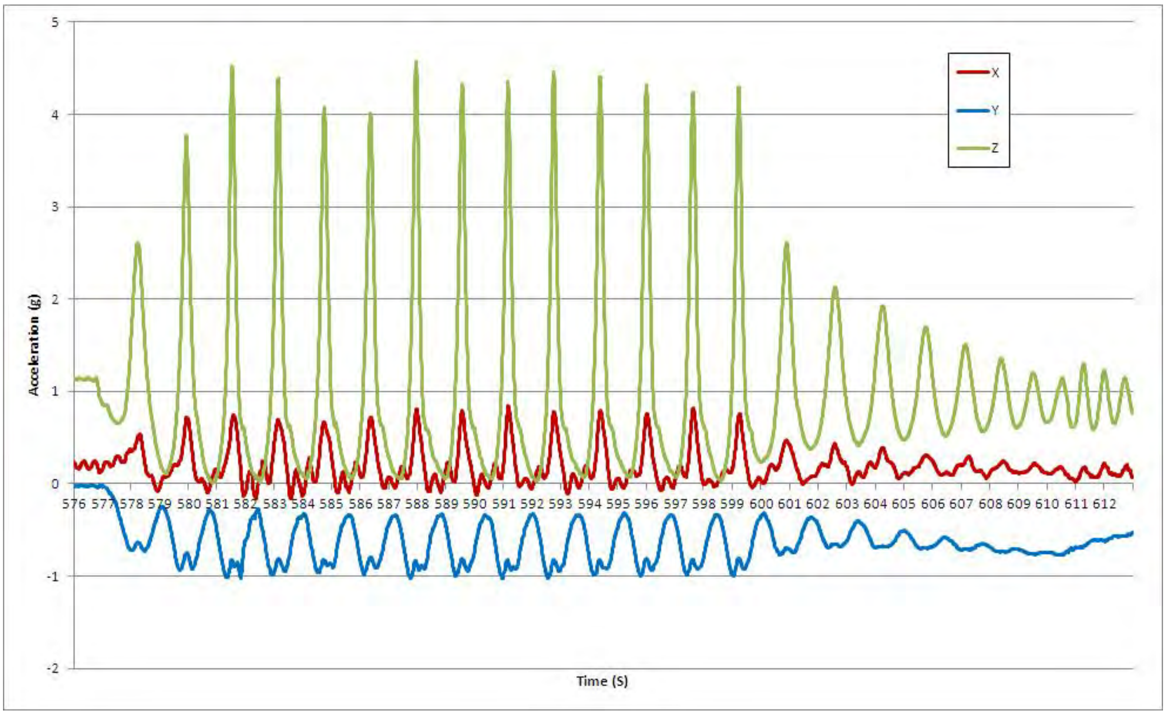

Figure 116 Test run 19, Program 2, Foot Pedal

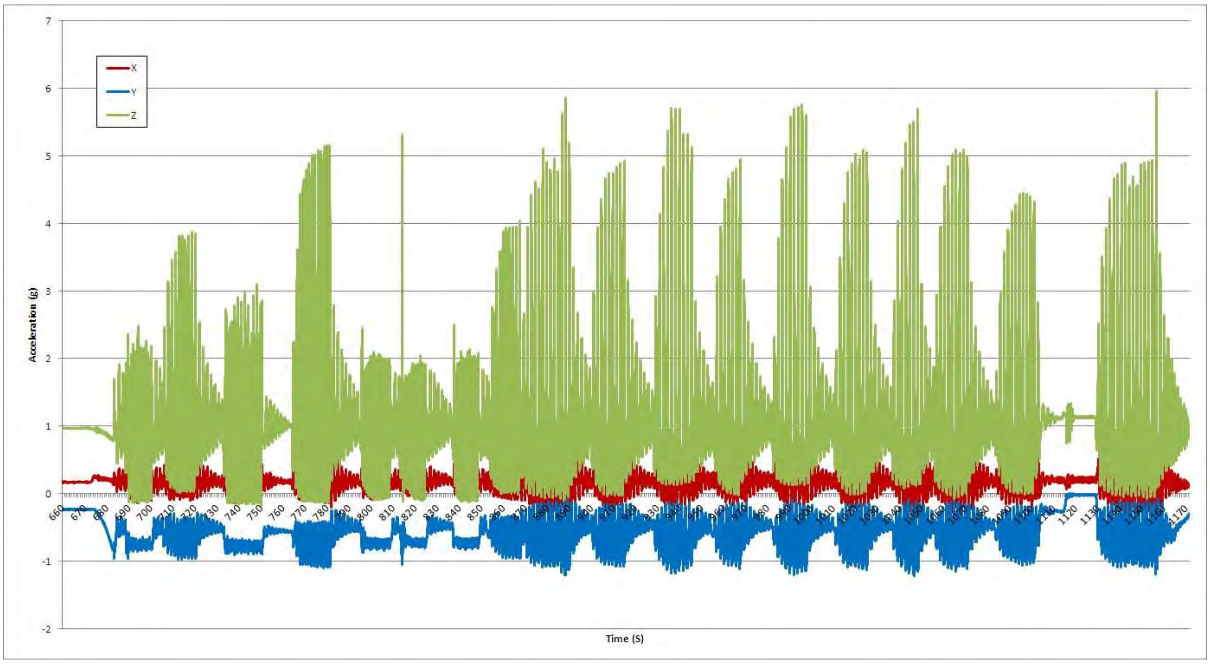

Figure 117 Test run 20 full

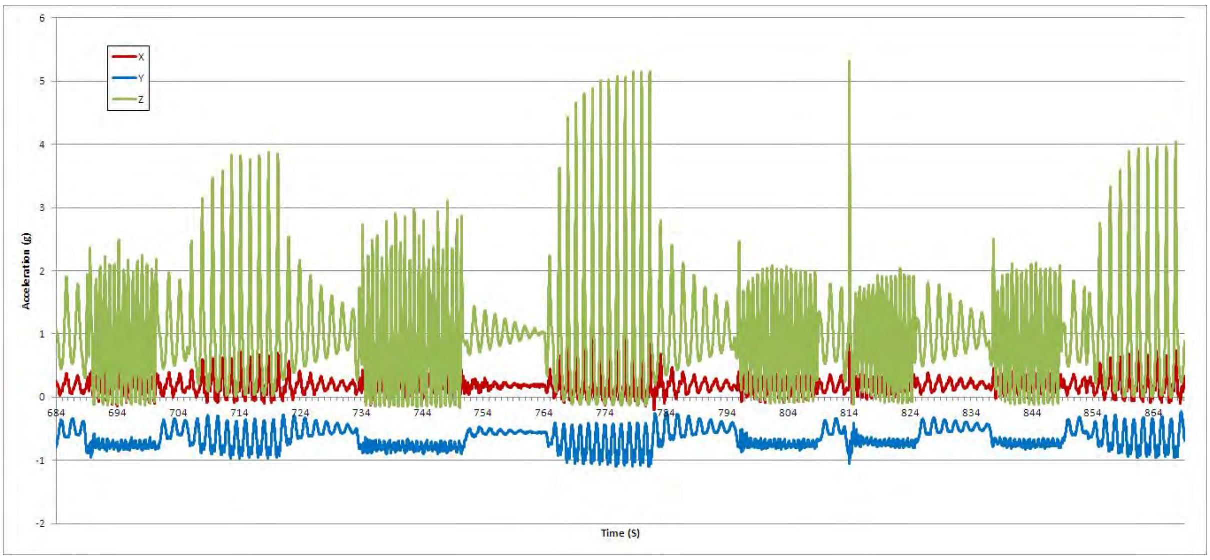

Figure 118 Test run 20, Program 1

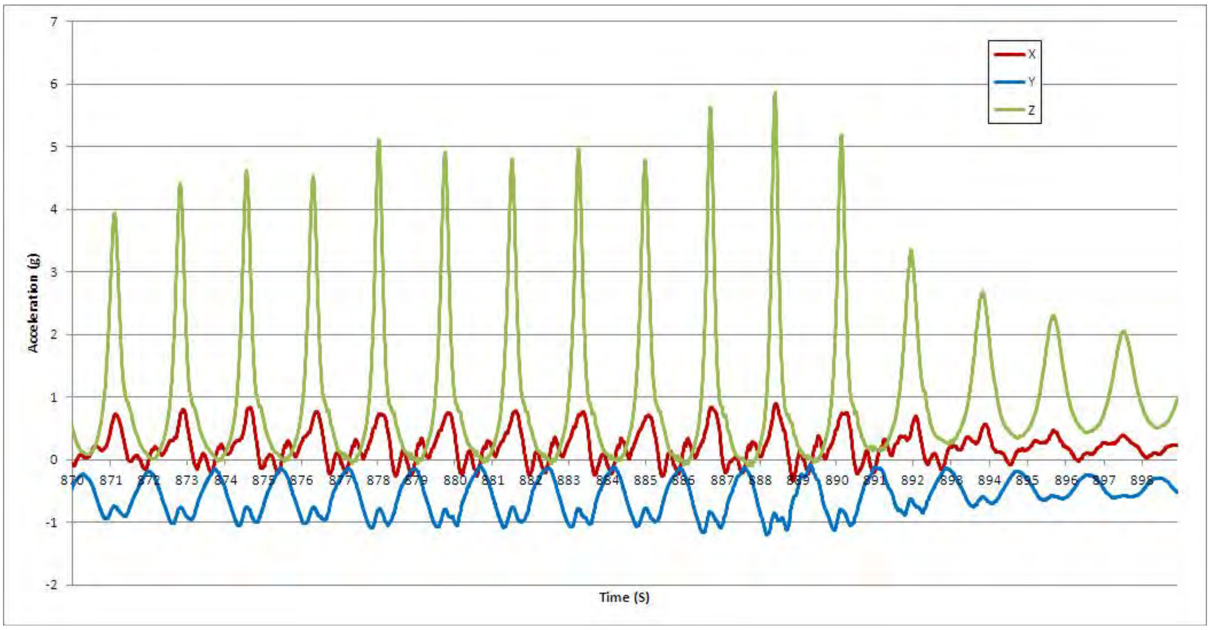

Figure 119 Test run 20, Program 1, Foot pedal

Figure 120 Test run 20, Program 2

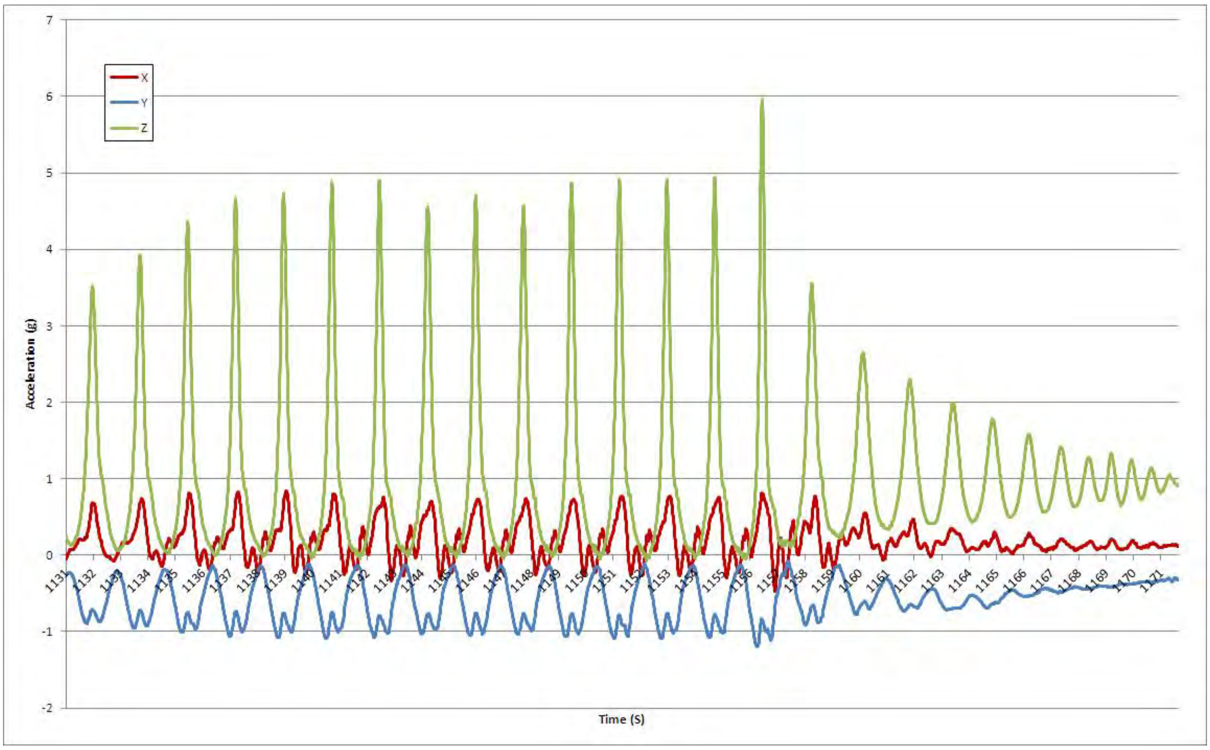

Figure 121 Test run 20, Program 2, Foot pedal

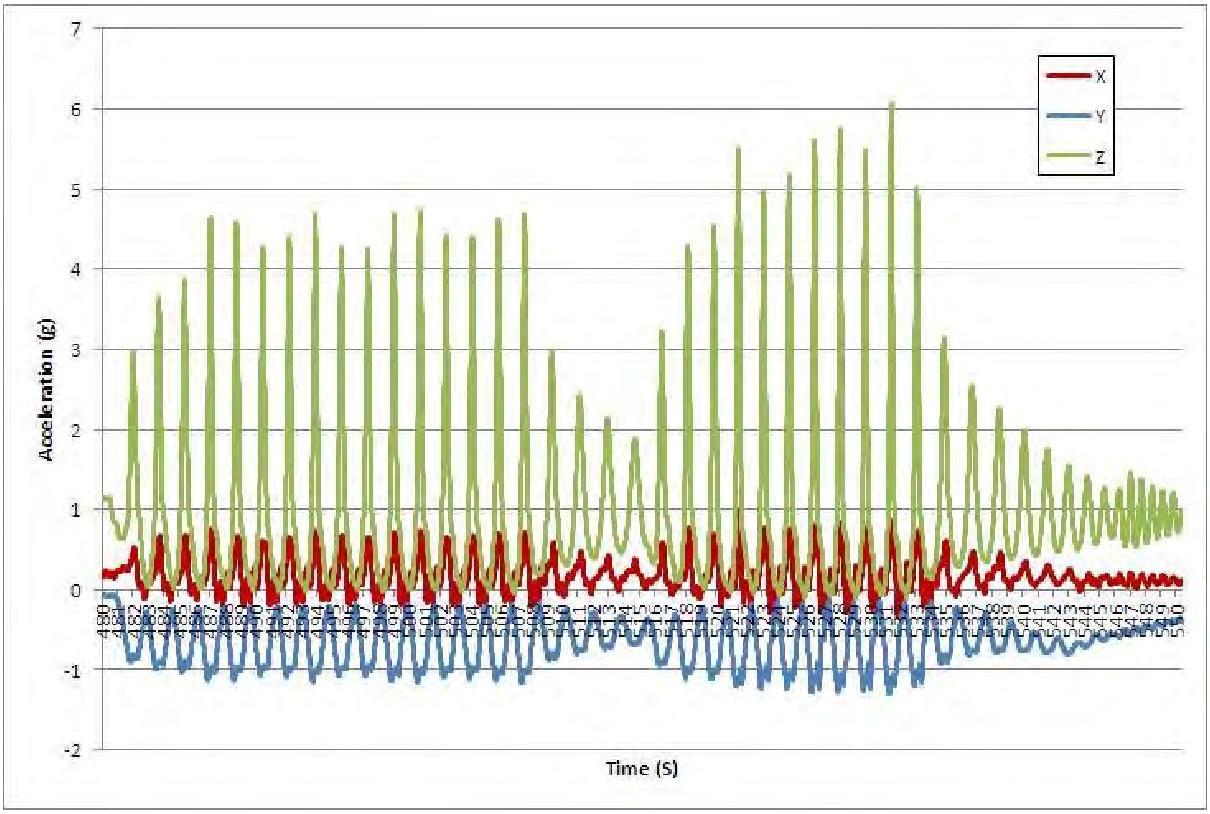

Figure 122 Test run 21 Part 1

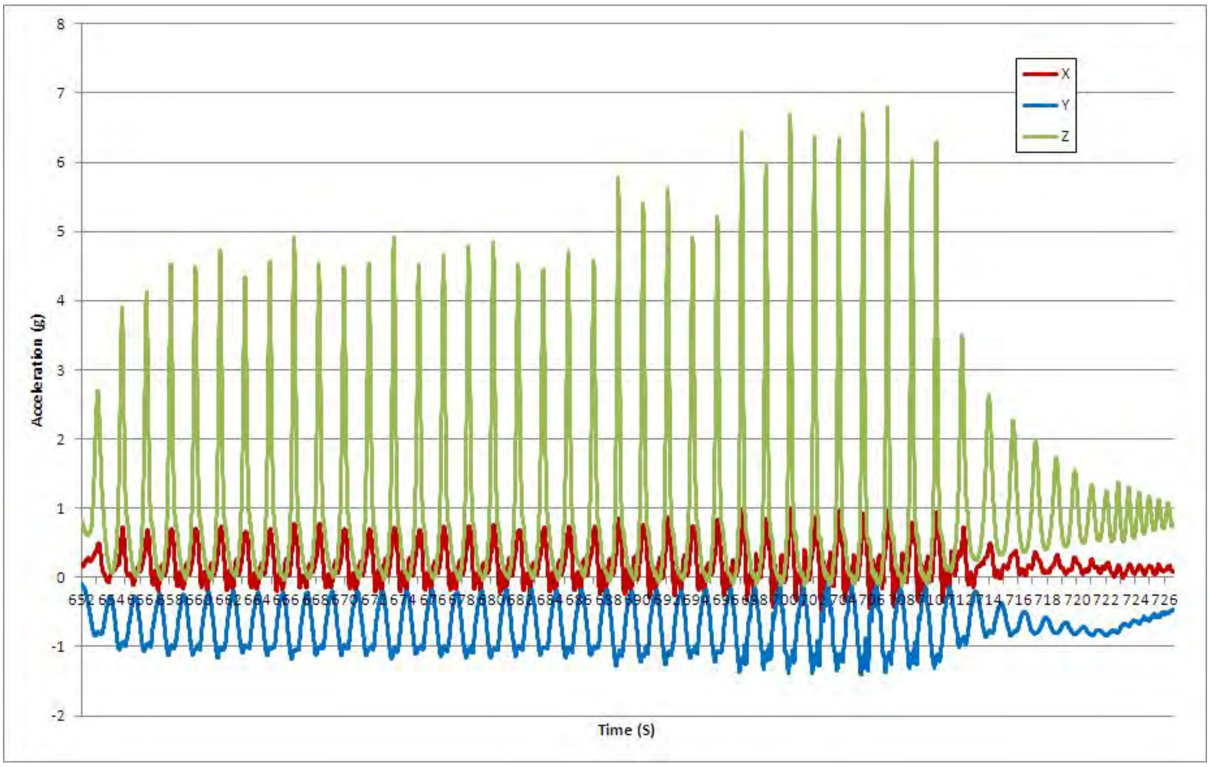

Figure 123 Test run 21 Part 2

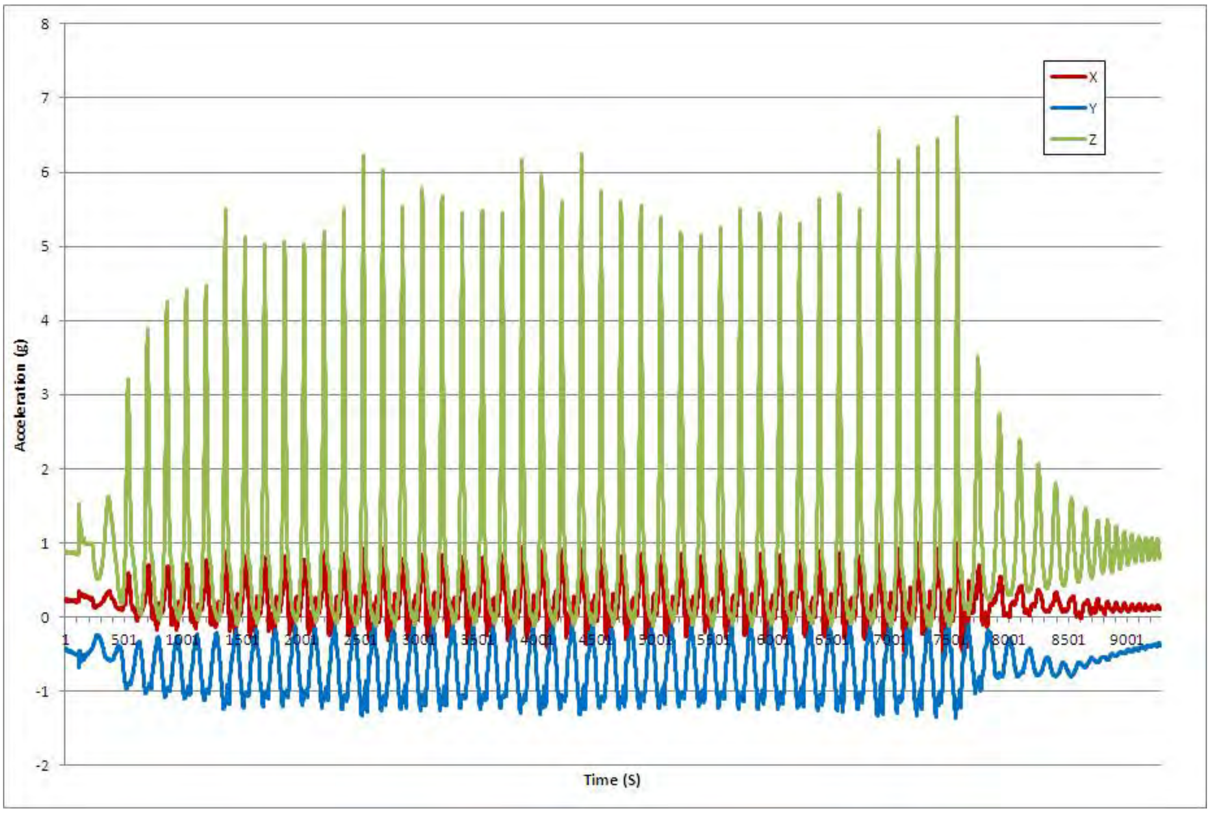

Figure 124 Test run 21, Part 3

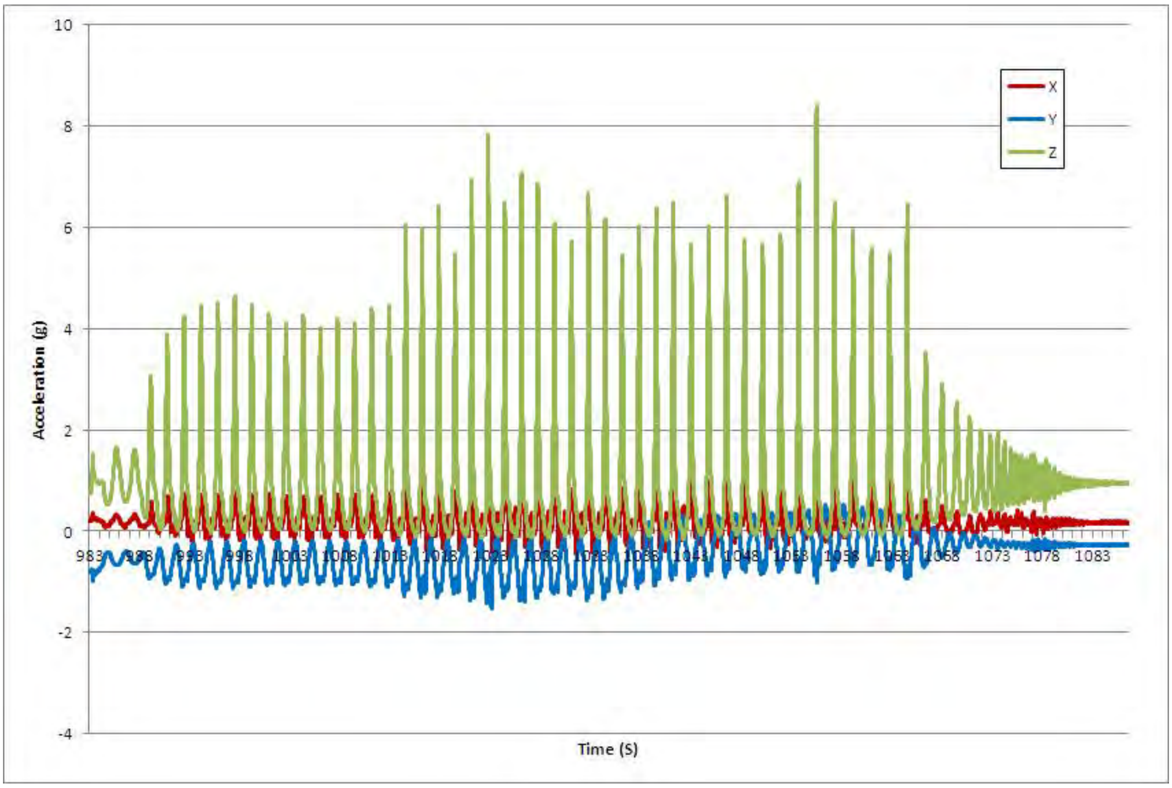

Figure 125 Test run 21, Part 4

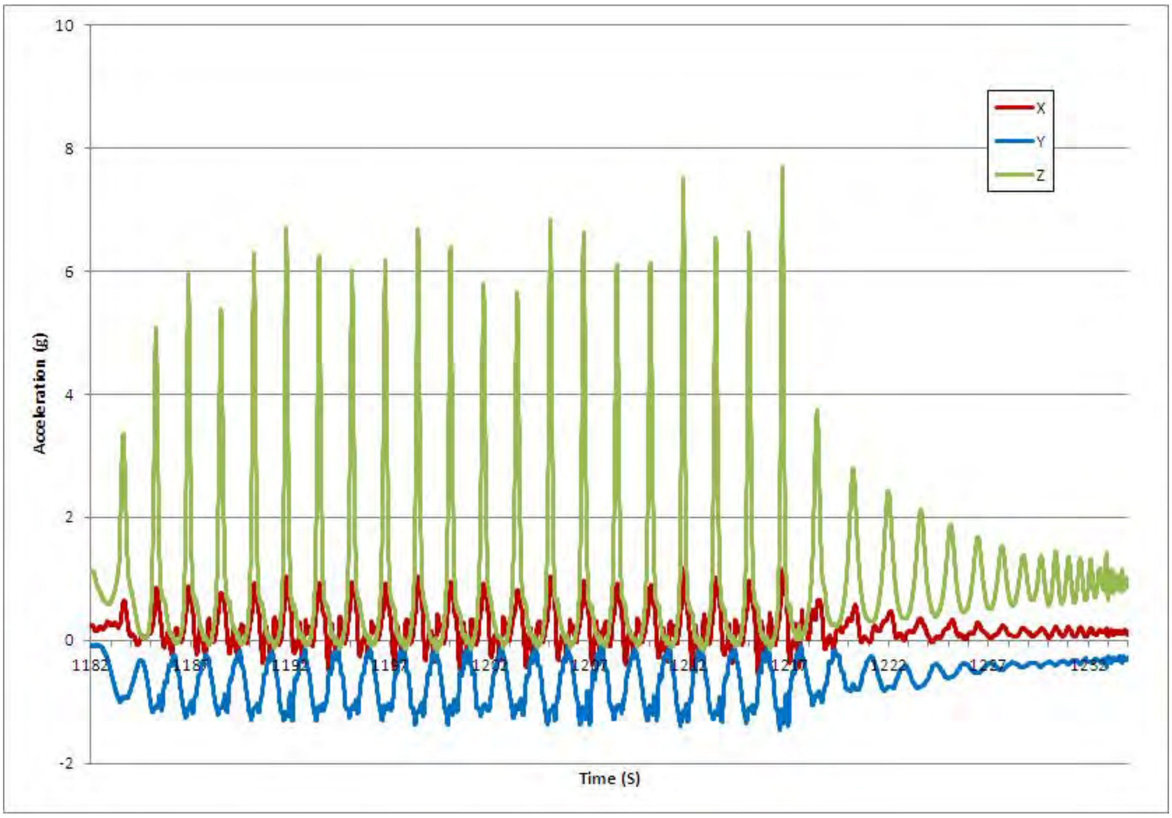

Figure 126 Test run 21, Part 5

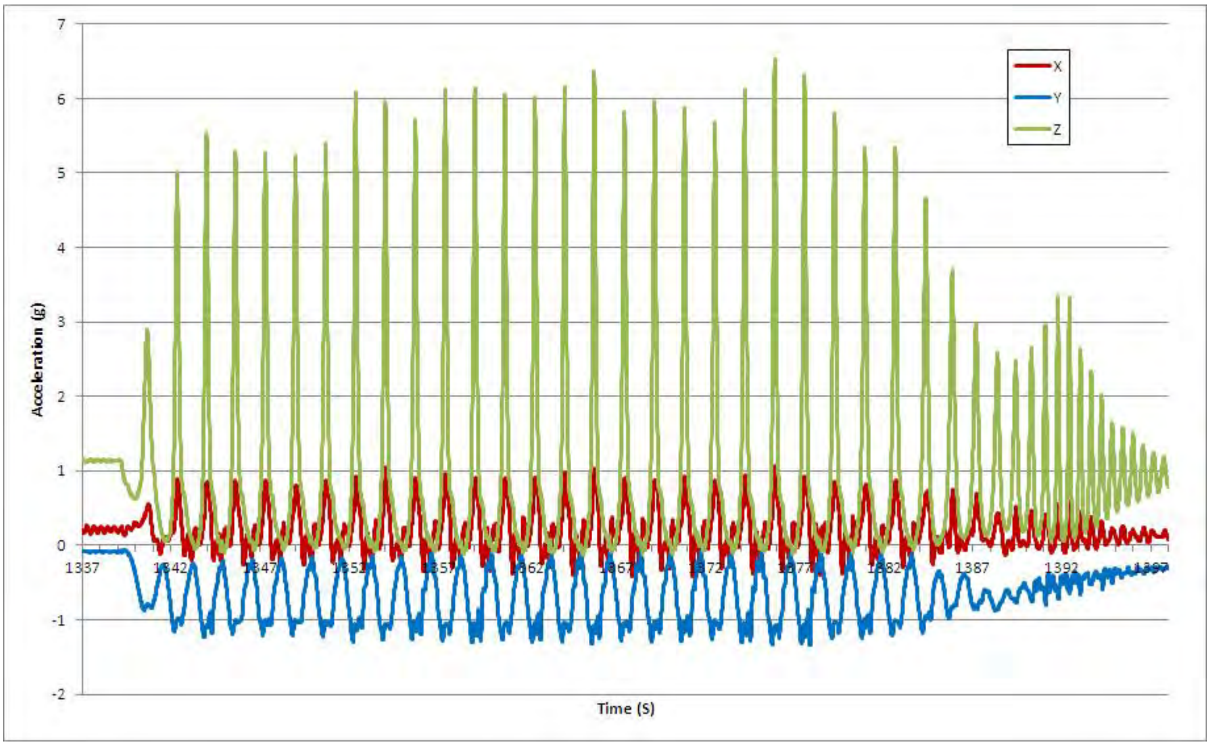

Figure 127 Test run 21, Part 6

6.4 ANTHROPOMETRY

Age	3 year olds						8 years olds					
Percentile	5th		th		95th		th		50th		95th	
Measurement / Gender	Boy	Girl	Boy	Girl	Boy	Girl	Boy	Girl	Boy	Girl	Boy	Girl
Upper thigh depth (standing, US boy/girl, Snyder, 1977)	69		85		99		96		119		141	
Thigh depth (maximum sitting, Belgian, PeopleSize Pro 2008)	69	50 65	81	77	96	5 95	93	95	111	109	133	135
Hip breadth (seated, UK, Pheasant, 1986)	175	175	195	195	250	215	200	205	235	245	270	285
Hip breadth (sitting, Belgian, PeopleSize Pro 2008)	173	175	188	190	205	209	210	115	237	145	267	184
Abdominal depth (seated, UK, Pheasant 1986)	135	135	150	150	145	165	135	140	170	180	205	220
Abdominal depth (sitting, Belgian, PeopleSize Pro 2008)	134	136	144	146	157	161	146	150	170	178	201	220
Chest depth (standing, UK, Pheasant 1986)	105	105	125	120	145	140	115	120	150	150	185	180
Popliteal length (UK, PeopleSize Pro 2008)	195	200	230	230	325	260	295	295	325	330	355	365
Buttock – Popliteal length (UK, PeopleSize Pro 2008)	225	215	250	260	330	305	305	310	340	355	375	400